Monthly Scientific-Technical and Production Journal

The Paton WELDING JOURNAL

December 2002 # 12

English translation of the monthly «Avtomaticheskaya Svarka» journal published in Russian since 1948

Founders: *The E.O. Paton Electric Welding Institute of the NAS of Ukraine, International Association «Welding»*
Publisher: *International Association «Welding»*

Editorial and advertising offices:
E.O. Paton Electric Welding Institute,
International Association «Welding»,
11, Bozhenko str., 03680, Kyiv, Ukraine
Tel.: (38044) 227 67 57
Fax: (38044) 268 04 86
E-mail: journal@paton.kiev.ua
http://www.nas.gov.ua/pwj

State Registration Certificate
KV 4790 of 09.01.2001

Subscriptions:
$460, 12 issues per year,
postage and packaging included.
Back issues available

CONTENTS

SCIENTIFIC AND TECHNICAL

Paton B.E., Bulatsev A.R., Gavrish S.S., Zagrebelny A.A., Pavlova S.V. and **Shulym V.F.** Welding technologies under extreme conditions. Part 2. Degree of risk and possibilities for risk mitigation 2

Markashova L.I., Dobrushin L.D. and **Arsenyuk V.V.** Improvement of weldability of high-strength aluminium alloys in explosion cladding 12

Korotynsky A.E., Makhlin N.M. and **Bogdanovsky V.A.** About design of electronic controllers of welding current for multistation welding systems 16

40th ANNIVERSARY OF THE PWI DEPARTAMENT FOR PHYSICAL-METALLURGICAL PROCESSES OF WELDING LIGHT METALS AND ALLOYS

Ishchenko A.Ya. Investigation and development of the technology of light alloy welding at the PWI 25

Dovbishchenko I.V. and **Steblovsky B.A.** Development of methods for arc welding of aluminium and its alloys 27

Voropaj N.M. Distribution of rate and pressure of plasma flows in welding arcs 31

Ishchenko A.Ya., Dovbishchenko I.V., Mashin V.S. and **Pashulya M.P.** Features of consumable-electrode arc welding of aluminium alloys in neon and its mixtures with helium and argon 35

Poklyatsky A.G., Lozovskaya A.V. and **Grinyuk A.A.** Prevention of formation of oxide films in welds on Li-containing aluminium alloys 39

Skorina N.V. and **Mashin V.S.** Coated electrodes of UANA grade for welding and surfacing aluminium and its alloys 43

Voropaj N.M. and **Mishenkov V.A.** Combined method for plasma and arc welding using different-polarity current pulses (Hidra-process) 46

BRIEF INFORMATION

Tararychkin I.A. Method of determination of corrective actions in statistical control of welding processes 48

Khorunov V.F., Sabadash O.M., Maksimova S.V. and **Stefaniv B.V.** Dispersion-strengthened heat-resistant solder 50

Index of articles for TPWJ'2002, No. 1–12 53

List of authors 59

WELDING TECHNOLOGIES UNDER EXTREME CONDITIONS
Part 2. Degree of risk and possibilities for risk mitigation

B.E. PATON, A.R. BULATSEV, S.S. GAVRISH, A.A. ZAGREBELNY, S.V. PAVLOVA and **V.F. SHULYM**
The E.O. Paton Electric Welding Institute, NASU, Kyiv, Ukraine

Results of basic tests conducted to verify and establish safety of the «Universal» hardware in performing welding operations under the open space conditions and the possibilities of reducing the degree of risk are considered.

Key words: *electron beam, radioactive radiation, light and infrared radiation, high voltage, electrostatic discharge, metal spatter, testing, risk mitigation*

First experimental work with the electron beam hand tool was performed more than 25 years ago [1, 2]. Since experiment performance envisaged a direct involvement of the operator, experimental program included analysis of potential hazards, as well as human capabilities during welding performance. Flight welding experiments with versatile hand tool (VHT) unit (1984, 1986) and ground-based testing of «Universal» hardware as part of International Space Welding Experiment (ISWE) and «Flagman» Programs, performed at the end of 1990s, using more advanced testing and training facilities, were the basis to conduct comprehensive investigations of the safety of manual electron beam technologies and outline future directions for their improvement.

Construction of International Space Station (ISS) is in progress now, and the start of its scientific operation is scheduled for the middle of the current decade. Creation of ISS made the participants of this unique project standardise practically all the issues of its construction and operation. ISWE performance preceded the «Flagman» Program, so that all the most urgent design and research problems on preparation of the space welding experiments, using the electron beam tool of the new generation — «Universal», were optimised under this program by the specialists of the E.O. Paton Electric Welding Institute and NASA G. Marshall Space Flight Center (MSFC). During preparation of «Flagman» experiment together with specialists of the S.P. Korolyov Rocket Space Corporation (RSC) «Energiya», Company «Zvezda» and Yu.A. Gagarin Cosmonaut's Training Center, Russia, check testing of the greatest «bottle neck» aspects in terms of experiment safety was further conducted and the required cycle of operator training under the conditions, simulating those of space, was retrofitted.

This introduction was made by us in order to explain why most of the materials, presented in this article, were obtained during performance of studies in one of USA's best space centers — MSFC.

Possibility of electron beam injury. When processing operations are performed with the electron beam in space, one of the main sources of hazard is the damaging ability of the beam. The working tool uses a short-focus gun, in which the specific power of the beam becomes smaller by a quadratic dependence with the increase of the distance to the exposed object. In addition, accidental switching on of the electron beam is practically impossible, as this requires deliberately performing several successive operations with the tool, aimed into the working zone. This improves the safety of using the electron beam hand tool, although a certain degree of risk still remains. In view of the above-said, the main object of studies has always been the impact of the electron beam on the materials of the spacesuit and protective clothing of the cosmonaut-welder.

The PWI has many times conducted such research, which confirmed the damaging ability of the electron beam. However, the US experts repeated this research in preparation for ISWE. They decided to check the assumption that electron beam hitting an insulated section of the material of astronauts' clothing will lead to accumulation of the charge and, as a result, interlocking of the electron beam gun (EBG).

When experiments were performed (Figure 1), the electron beam was aimed from the distance of 25 mm at a fragment of the spacesuit, which is a multi-layered package of materials, mounted in a metal frame, which is insulated from the vacuum chamber and connected to the measuring instruments. No appearance of the beam was observed, although all of the hardware and cathode filament were switched on, and no charge was registered on the sample of the spacesuit material. When the tool was moved to the metal frame, the beam appeared, and when it was moved back to the spacesuit material, the beam immediately disappeared. And although the charge of the sample material was not registered, partial melting of the material in the frame corner was found during examination. A similar situation was also observed on a new sample of material after its more reliable insulation. With increase of the distance between the tool and sample up to 100 mm and its exposure to an operating

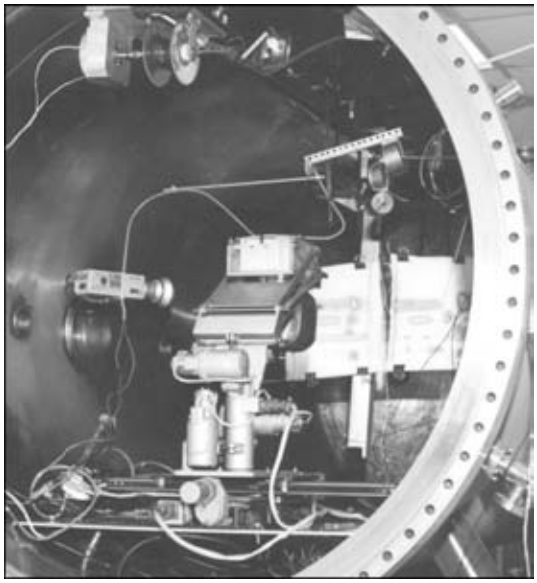

Figure 1. Equipment lay out during performance of experiments on electron beam impact on spacesuit materials

gun, partial melting of the material upper layer was found, which was followed by disappearance of the beam. Beam re-appearance was accompanied by a burn-through of the next layer, and beam switching-off, i.e. material destruction was a cyclic process: electron beam appeared with an interval of about 3 to 4 s for ≈ 1 s. However, no charge accumulation was found in this case, either. A similar pattern was also observed with an increase of the distance between the tool and the sample up to 175 mm.

The occurring processes may be explained as follows. At a small distance from EBG to the sample charge accumulation on its surface (even though it was not registered) occurs, which leads to EBG interlocking. Heating of the sample material from the hot cathode is observed at the same time, which is sufficient for evolution of highly volatile elements from it. The latter, penetrating into the gun zone, cause break-downs to trigger off the protection system (electron beam does not appear). At 100 mm and greater distance to the sample, a pulsed switching on of the beam is observed, which results from the fact, that because of the large distance to the sample, the charge accumulated on it, has enough time to flow down, and the highly volatile substances are removed from the gun zone by pumping down means. There is no doubt that the electron beam destroys operator clothing. This was confirmed by subsequent experiments, made with different materials of the operator protective clothing and elements of the cargo bay interior (teflon, nextil, kevlar, betacloth) from 100 mm distance, including a fragment of spacesuit glove from 500 mm distance. In all the cases, with the gun switching on vacuum deterioration in the chamber from $1 \cdot 10^{-2}$ to $6 \cdot 10^{-2}$–$1 \cdot 10^{-1}$ Pa was observed, depending on sample material.

Thus, the results of the performed experiments confirmed that protection from the possible accidental damage of the operator clothing, when working with

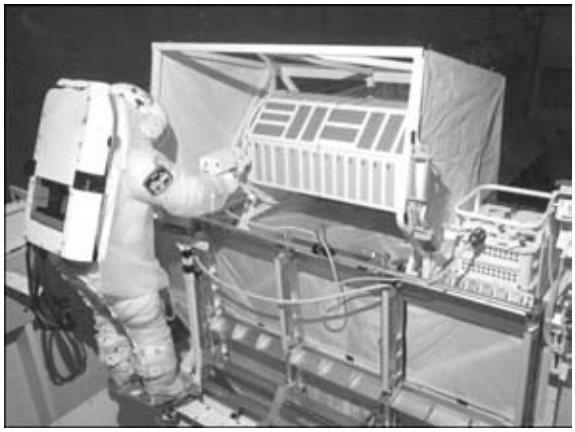

Figure 2. Work place of cosmonaut-welder (special protective clothing is worn over the spacesuit)

the electron beam hand tool is the most important factor of its safety. Performance of an experiment on welding in space also requires thorough organising of the operator work place. This was given special attention during ISWE preparation (Figure 2).

Alongside with the operator mobile work station, mounting of samples on a rotating sample holder and of working electron beam tools in special seats, a mechanical device was also used. It was developed and manufactured to fit into the working platform of the Shuttle Orbiter, and limited the possible motion of the operator's arm with the working tool beyond the zone of welding operations performance (Figure 3).

The PWI specialists carry on development of devices to improve the safety of using the electron beam hand tools [3–5]. A method to monitor the tool position in space with contactless orientation sensors, used in computer systems, has been tested. This method allows assigning any rectangular region within an area of 50×50 cm and tracing the tool position. When it left this zone, its functioning automatically stopped. A computer with special software is the base of the system, which is used to «correlate» the current position of the tool with an assigned configuration of the working zone, as well as to determine the presence of a situation of «leaving the working

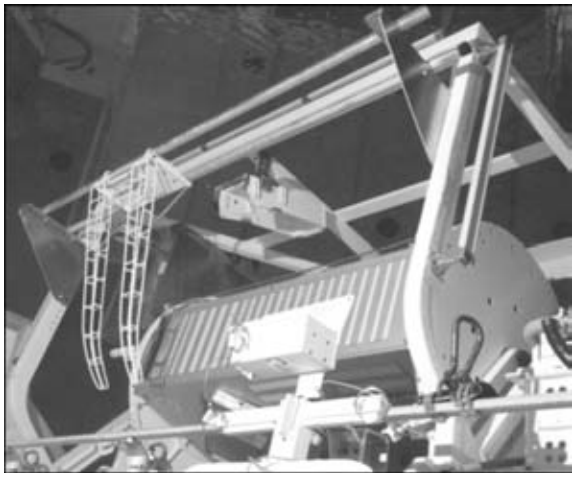

Figure 3. A device, limiting the possible movement of the operator arm with the tool beyond the working zone

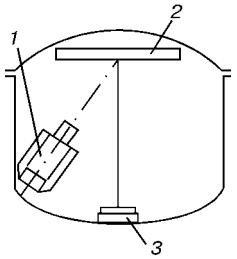

Figure 4. Schematic of measurement of radioactive radiation in operation of «Universal» hardware, using SLP-04160 sensor: *1* — «Universal» hand tool; *2* — target; *3* — sensor

zone». The described mock-up of the system was tested in a vacuum chamber as part of «Universal» unit with positive results. The advantages of the above system are quick response, easy mastering by the operator of the techniques of assigning the working zone and monitoring fulfilment of the main requirements, namely tool switching off, when leaving the working zone.

It should be noted that, in addition to the general goals of risk mitigation, when using the electron beam hand tool, the problem of improvement of the safety level should be solved for the specific conditions of work performance.

Theoretically it is possible to create devices, which will completely eliminate the possibility of electron beam accidentally hitting the operator or surrounding objects. However, as noted above, working with the hand tool under the open space conditions requires the operator to have certain skills. Therefore, development of safety systems is not a goal in itself. It should be an integral component of the package of design and logistic measures, facilitating performance of complex processing operations for the operator.

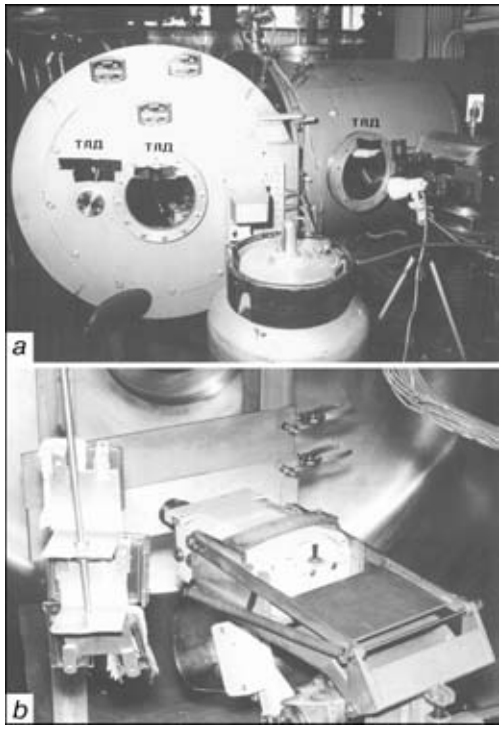

Figure 5. Arrangement of TLS on the outer surface (*a*) and inside (*b*) vacuum chamber during performance of radiation tests at MSFC

Measurement of radioactive radiation in operation of «Universal» hardware. During development and testing of «Universal» hardware X-ray radiation field and exposure dose in its operation were determined, considering the higher (up to $U = 8$ kV, $U_{o.-c} = 10$ kV) accelerating voltage, compared to VHT. These tests were conducted in 1989 together with representatives of the Institute of Nuclear Physics of the NAS of Ukraine, using X-ray spectrometer, based on SLP-04160 sensor, located in the vacuum chamber, and Ortec analyser of 5604 type. Pressure in the vacuum chamber was maintained at the level of $5 \cdot 10^{-2}$ Pa, and a stainless steel plate 20 mm thick was used as target (Figure 4).

EBG of the hand tool of «Universal» hardware was repeatedly switched on for a short time (3 min operation, 3 min pause). The electron beam had the following parameters: $U = 8$ kV and $I = 52$ mA. In order to record 200 pulses (by the conditions of taking measurements with this instrumentation) EBG was required to operate for 18708 s. As a result of processing the obtained data, the total radiation field was $7 \cdot 10^{-5}$ Gy/h.

By the data of [6], for gamma and X-ray radiation at Q-factor equal to a unity, the exposure dose should not exceed $1 \cdot 10^{-4}$ J/(kg·h) for this circuit and working materials. The measurements taken led to the conclusion that during performance of processing operations with «Universal» hardware, the operator can work for 5 to 10 h without any special protection means.

As part of ISWE the US experts also measured the field of radiation from weld pool inside and outside the vacuum chamber during performance of welding operations, using «Universal» hardware. This was done, first of all, to check the degree of protection of ground service personnel by the vacuum chamber walls and material of its viewing windows, secondly to determine the radiation dose, to which an operator in a spacesuit may be exposed during performance of welding operations in space. Weld pool radiation was measured by thermoluminescent sensors (TLS), used for personal monitoring of experts, exposed to ionising radiation. Sensor location on the outer surface of vacuum chamber during performance of one of radiation tests is shown in Figure 5, *a*. Inside the chamber the sensors (Figure 5, *b*) were mounted at the same distance from the weld pool (450 mm), and to immobilize the weld pool, not the tool, but the sample being processed, was moved.

Part of the sensors was covered by samples of materials of the spacesuit, pressure helmet glass and protective welding clothing, which allowed evaluation of the actual impact of weld pool radiation on the operator in the spacesuit, and one sensor was mounted under the guard on the tool handle. When welding operations were performed, the beam current was varied in the range of 55 to 76 mA.

All together 22 samples of stainless steel 304SS, aluminium alloy 2219Al and titanium alloy Ti–6Al–

4V were processed. Total time of the tool operation was 63 min 10 s. When the second radiation test was performed, this time was shortened to 30 min, as such time was determined as duration of welding operations by the last scenario of experiment performance in space. In this case the target was alloy 2219Al, and the sensors were covered only by samples of spacesuit material.

Analysis of sensor readings after testing was conducted in the US Army Center of Ionizing Radiation Monitoring with the participation of specialists from the US National Institute of Standards and Technologies (NIST). Low-energy X-ray radiation, generated by «Universal» hardware, did not fall under the existing algorithm of conversion of the radiation dose equivalent. Therefore, additional information was required, concerning TLS functioning in the photon energy region. Data, generated by NIST, enabled maximum accurate determination of the doses, picked-up by the sensors.

Sensors, mounted on the outer surface of vacuum chamber and its viewing windows, remained «clean» and those, mounted inside the chamber and completely unprotected, went off scale, as the irradiation doses were so high, that the analyzing systems could not determine them. Data, obtained, using the sensors with different degrees of protection (all the data are reduced to 30-minute duration of welding operations performance), is given in Table 1.

As is seen from the Table, application of protective welder outfit (easily removable teflon clothing) reduces the level of operator exposure 1.7 times. Thus, increase of the number of clothing material layers provides the required degree of operator protection. However, the report [7], submitted by US experts, does not give the exposure doses, admissible by US norms, nor does it have information on measurement results, which would indicate exceeding such norms. Safety Commission, involved in ISWE preparation, and considering all the aspects of safety, never raised the issue of radiation protection of the operator. The authors just confined themselves to stating the obtained results and let the experts in this field draw their own conclusions. It should be noted that measurement of the intensity of radioactive radiation from low-energy sources is not a simple task, either in our country, or in the USA, which is indicated by the results of the conducted tests. Therefore, in preparation of the welding experiment on board orbital station (OS) «Mir» by «Flagman» Program, the authors used the norms, given in [6] as guidelines.

Measurement of the intensity of light and infrared radiation of the weld pool. These tests were conducted in September, 1996 at MSFC. Their purpose was to provide a reply to the question of the Safety Commission on the adverse impact on operator sight of the visible and infrared radiation of the molten metal pool during performance of welding operations in space. Testing had the following objectives: measurement of the intensity of radiation from the weld pool during welding of all the candidate materials, using «Universal» hardware in the range of wave lengths of λ = 300–1100 nm with subsequent interpolation of the obtained results up to λ = 3000 nm (using the theory of black body radiation); determination of sufficiency of the protective light filter of the astronaut-welder pressure helmet, as a reliable eye protection; identifying materials, which required eye protection.

Table 1. Readings of TLS, mounted inside the vacuum chamber

Protective means (material)	*Exposure dose* $\times 10^{-2}$, *Gy*
Guard on tool handle (stainless steel 0.127 cm thick)	0.158
Spacesuit with protective welding clothing (one layer of teflon)	4.900
Spacesuit without protective welding clothing	8.200
Pressure helmet glass, protective and welding visor (lexan 0.5 cm thick)	2.750

Measurements were taken during partial melting of 2219Al alloy 6 mm thick, 5456Al alloy 6 mm thick, 304SS 2.5 mm thick, Ti–6Al–4V alloy 1.5 mm thick by electron beam hand tool of «Universal» hardware.

Spectral radiometer Optronics 740A was used, which measures the intensity of radiation as the function of wave length and material being welded. Weld pool temperature was determined, using a pyrometer with laser sight. Measurements were conducted through viewing windows of the vacuum chamber, and to allow for the error, introduced by the window glasses, their light transmission was determined before and after welding each material. Distance from radiometer lens to the weld pool was 63.5 cm.

Maximum permissible doses of light radiation to prevent eye injury because of excess impact of optical radiation, were established in the conference of State Industrial Hygienists of US Army.

The maximum admissible time of impact on the operator's eyes was determined, allowing for the following factors: ultraviolet radiation, causing photokeratitis; radiation, close to ultraviolet radiation (λ = = 320–400 nm), promoting development of the cataract, resulting from thermal burn; photochemical injury of the retina («blue light» injury), causing photoretinite; thermal injury of the retina; infrared radiation (λ = 770–3000 nm), causing thermal injury of the comea.

Calculated values of the radiation dose and corresponding maximum time of the impact on the eye, with the astronaut using the standard spacesuit sun filter and without it, are given in Table 2. As is seen from the Table, in the case of application of the sun filter and at up to 30 cm and greater distance from the welding zone, the level of weld pool radiation impact on the eyes for 2 h (anticipated duration of the space experiment) is below the maximum permissible values and, therefore, the radiation does not harm the astronauts' eyes.

Table 2. Exposure doses and maximum time of eye impact

Consequences of harmful impact	λ, *nm*	*Maximum permissible doses,* mW/cm^2	*With protection*		*Without protection*	
			Calculated radiation doses, mW/cm^2	*Maximum permissible time of impact, h*	*Calculated radiation doses,* mW/cm^2	*Maximum permissible time of impact, h*
Photokeratitis	180–400	3	$1.3 \cdot 10^{-9}$	> 8	$1.3 \cdot 10^{-9}$	> 8
Development of cataract as a result of thermal impact of ultraviolet radiation	320–400	1	$2.0 \cdot 10^{-8}$	> 8	$2.6 \cdot 10^{-5}$	> 8
Photoretinite, caused by «blue light»	400–700	10	$3.6 \cdot 10^{-4}$	7.8	$2.2 \cdot 10^{-3}$	1.25
Thermal injury of the retina	400–1400	5	$1.6 \cdot 10^{-3}$	> 8	$13.7 \cdot 10^{-3}$	> 8
Thermal injury of the comea with possible development of the cataract	770–3000	10	0.27	> 8	4.3	> 8

Without the sun filter in space the maximum time of exposure, which causes photochemical «blue light» injury is 1.25 h. Level of radiation, which leads to thermal injury of the comea and possible development of cataract, also reaches almost half of the admissible limits. Light intensity may make observation of the welding process difficult. Therefore, US experts Hongly Wu and Arnold Orsak in the NASA Report on Analysis of Adverse Impact on the Eyes of Welding in Space (September 13, 1996) recommend using the sun filter in welding stainless steel and titanium.

High voltage, possibility of initiation of corona and electrostatic discharges. High voltage (up to 10 kV), used in EBG operation, presents a potential hazard. This factor cannot be eliminated, as the high accelerating voltage is a mandatory condition of operation of the electron beam device. Therefore, we can only speak of the safe design of the working tool.

Electron beam forms between the cathode assembly and the anode, which is the EBG outer case.

In VHT and «Universal» systems the high-voltage transformer, its rectifier and filament transformer of the cathode assembly are combined in a monoblock with insulation of epoxy compound [8] and are located directly on the working tool. Low (up to 100 V) variable voltage at the input of the anode and filament transformers allows eliminating the high-voltage cable, which significantly improves the safety and reliability of the hand tool operation. High-voltage block is enclosed in a metal case, which, together with the anode, gun outer case and item being processed, is at the same electric potential. Thus, the high negative electric potential is localized and does not present a hazard for the operator. Reliable control of the strength of high-voltage insulation at the stage of unit manufacturing, as well as testing at extreme values of electric voltage, ambient temperature and pressure practically eliminates the possibility of electric breakdowns in the high-voltage block. As all its outer parts are at the same electric potential, even in case of an emergency, no shock to the operator will occur, just malfunction of the hand tool is probable.

Special attention should be given to reliable electrical connection of the cases of all the parts of the hardware system, item being processed and connecting cable screens. Resistance between these elements (particularly, anode–item) should not exceed 0.2 Ohm. This will permit eliminating accumulation of the electrostatic charge on the item being processed.

As regards the possible initiation of corona discharges, item 3.4.9 of the joint NASA/RSC Document SSP 50094 (edition A, March, 2000) states the following: «Electric and electronic subsystems, systems and equipment, which generate or use in steady-state or transient processes any electric voltages, equal to or greater than 123 V, including the input and output intermediate inner voltages, should be designed so as to prevent the appearance of the breaking or damaging corona in any environment at the ISS».

In the considered hardware system this is only possible inside the EBG between the cathode and anode at a considerable deterioration of vacuum (below $5 \cdot 10^{-1}$ Pa) in the working tool zone. This causes operation of the hardware protection system and beam switching off. Working pressure of the environment should be not less than $5 \cdot 10^{-2}$ Pa for normal operation of the hand tool. Initiation of an electric discharge between the hardware components, as well as between the hardware and parts of the space vehicle is impossible, as all these elements are at one electric potential, namely that of the case.

Nonetheless, during ISWE preparation testing was conducted to check the possibility of initiation of corona and arc discharges during performance of welding in open space. According to the data, derived during 39th mission of Shuttle Orbiter, the anticipated pressure in the spacesuit zone is in the range of $1 \cdot 10^{-4}$ with individual peaks of up to $1 \cdot 10^{-2}$ Pa. Conducted calculations showed that spacesuit leakage may reach $5 \cdot 10^{-3}$ Pa with individual peaks of up to $1 \cdot 10^{-2}$ Pa. Therefore, it was decided in the vacuum chamber at the pressure of $1 \cdot 10^{-2}$ Pa to obtain plasma at the pressure of plasma gas (argon) of $5 \cdot 10^{-3}$, $15 \cdot 10^{-3}$ and $1 \cdot 10^{-1}$ Pa, using a low-pressure plasma generator and needle leak valve, and in the case of initiation of corona or arc discharges to record them, using video recording devices. Despite the fact, that during testing argon pressure was much higher and was in the range of $(1–2) \cdot 10^{-1}$ Pa (as at lower pressures the process of plasma formation is unstable or is interrupted

Table 4. Quantity of particles, collected in welding butt joints of samples of different materials

Sample material	*Number of samples*	*Number of collected particles*
Aluminium alloy 2219	10	386
Aluminium alloy 5456	6	123
Titanium alloy Ti–6Al–4V	6	33
Stainless steel 304SS	4	0

completely), no corona or arc discharges were recorded during performance of welding. Therefore, the hardware was stated to be safe.

Evaluation of the impact of possible spatter of molten metal and other products, accompanying manual EBW, on the spacesuit material and interior elements. Electron beam technological processes are accompanied by evolution of the following products from the weld pool: molten metal spatter in the form of particles of up to 2 mm size; particles of the metal being welded or its components in the solid or liquid form, flying out of the weld pool and observed as sparks of 1–500 μm size; metal vapours, which are groups of atoms of less than 1 μm size. During ISWE preparation, theoretical analysis and calculations, performed by US experts, were complemented by a number of tests and investigations to determine the main characteristics of the above particles: change of particle velocity by analysing the video recordings, made by a high-speed camera; evaluation of their impact on samples of materials of the spacesuit and operator protective clothing; determination of the sizes and number of the particles. For this purpose during welding of each sample all the particles, flying out of the weld pool, were collected, and their dimensions were measured in a microscope, which was followed by construction of statistical distribution models.

Having analyzed the data of video recording of welding 223 samples, made of different materials, which were intended for use in the experiments, it was established that spark and spatter formation occurs mostly in welding alloys 2219 and 5456, and to much smaller extent in welding of alloy Ti–6Al–4V, and that it is practically absent in welding of steel 304SS. In this case the average velocity of the particles, determined by the results of high-speed video filming, was 10.5 m/s (maximum 17.9 m/s) for aluminium alloys, and 18.2 m/s (maximum 33.0 m/s) for the titanium alloy.

Table 3. Characteristics of samples of materials of the spacesuit and protective clothing

Sample material	*Thickness, mm*	*Temperature of melting (charring), °C*
Polyethylene	0.0375	113
Nylon 6 (kapron)	0.0500	224
Kapton	0.0625	310–670
Teflon	0.2425	320–610

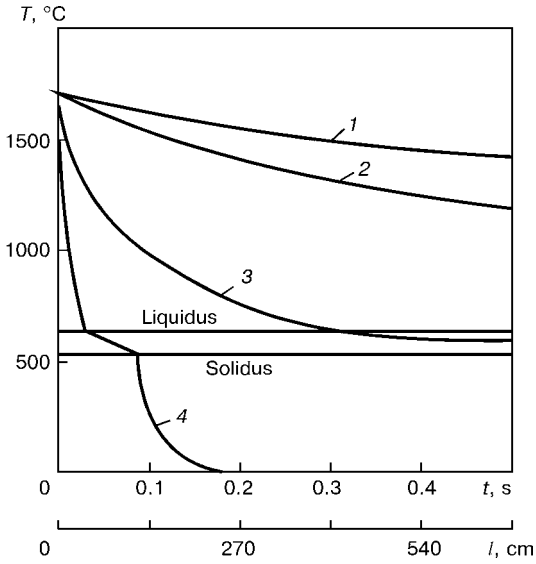

Figure 6. Dependence of particle temperature T and distance l from weld pool on time in welding of alloy 2219Al (particle velocity of 10.5 m/s): *1* — particle diameter of 250; *2* — 100; *3* — 10; *4* — 1 μm

Dependence of temperature of particles of alloy 2219Al on time, since the moment of their separation from the weld pool, derived by thermal calculations, is given in Figure 6. As is seen from the figure, particles of 10 μm and larger size, may hit the operator clothing at the temperature of 500 °C.

To assess the impact of particles on the materials of the spacesuit and protective clothing of the operator, samples of these materials were placed at the distance of 300 mm from the weld pool (Table 3).

During testing appearance of individual burns-through of polyethylene and kapron samples was observed in welding aluminium alloys 2219 and 5456, but not a single burn-through was found in welding of the titanium alloy.

To determine the quantity and sizes of particles during welding of each sample, the particles were collected, for which purpose they were separated and collected from EBG anode. A special trap was mounted on the anode, which allowed collecting most of the particles, flying out of the weld pool. Table 4 gives the total quantity of particles, collected in welding 26 samples of butt joints each 175 mm long.

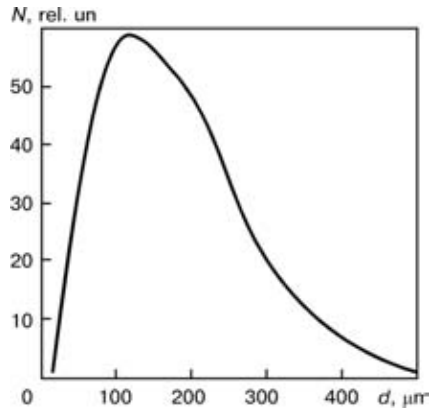

Figure 7. Dependence of the quantity of particles N of alloy 2219Al on their size d

Table 5. Maximum values of coating thickness and content of the main elements in the coatings

Sample material	*Coating thickness, μm*	*Weight fraction of elements, %*					
		Mg	*Si*	*Mn*	*Al*	*C*	*O*
Aluminium alloy 2219	–	–	35.9	–	–	7.1	57.0
Aluminium alloy 5456	0.80	38.8	–	–	–	13.6	47.5
Titanium alloy Ti–6Al–4V	0.27	–	–	–	30.8	8.5	55.7
Stainless steel 304SS	0.25	–	–	25.2	–	20.6	51.0

Particle sizes in welding of aluminium alloy 2219, determined in a microscope, are shown in Figure 7.

The performed research revealed the following:

- EBW of samples is accompanied by different levels of particle evolution from the weld pool. Particles evolution is completely absent in welding stainless steel and reaches 126 particles per sample in welding of aluminium alloy 2219;
- particle sizes in welding aluminium alloys are $d \leq 500$ μm, and in welding of the titanium alloy — $d \leq 140$ μm;
- particle temperature at 300 mm distance from the weld pool is ≤ 500 °C in welding of aluminium alloys and ≤ 1600 °C for the titanium alloy;
- rate of particles evolution in welding of the aluminium and titanium alloys is equal to $v \leq 18$ and 33 m/s, respectively.

In order to determine the quality and composition of products, evaporating from the weld pool, witness-samples were used, which were located at different distances from it. Data on maximal values of coating thickness and content of the main elements in them is given in Table 5.

Thus, no coarse drops of molten metal in the form of particles of 1–2 mm size were recorded during testing. Welding of titanium and, particularly, aluminium alloys is accompanied by evolution of a large number of fine particles, having rather high velocity of motion and temperature. However, their dimensions are so small, that they cannot damage the standard operator clothing (spacesuit), the latter will just be contaminated. Therefore, special clothing, protecting the spacesuit, should be used in manual EBW. During performance of the space welding experiment first on board the US Shuttle Orbiter and then of the Russian OS «Mir», it was intended to apply the operator protective clothing. For US astronauts it should have been an easily-removable teflon clothing (coat and pants) and a replaceable visor of lexan (plexiglass) over the light filter, and for Russian cosmonauts an apron of arimide cloth (TU 17-04-08/3-457–94) and replaceable shielding of fluoroplastic film F10 (TU-2245-062-00203-521–2000) for the pressure helmet. Mock-up samples of this clothing have been tested in the water tank in the US and in the space simulation test chamber at Company «Zvezda», Russia. Testing results confirmed the serviceability and effectiveness of the clothing.

Table 6. Dependence of the time of contact of the operator's gloved hand on temperature of structural elements

Temperature of structural element, °C	*Time of contact, min*
130	≥ 1
100	≥ 2
75	≥ 4
50	> 30
–50	≥ 6
–75	≥ 4
–100	≥ 2
–130	≥ 1

Hot zones. During performance of processing operations, involving heating and melting of metals, which include welding and allied processes, the hot zones of the items being welded, as well as the working tools, heated during functioning, present a great hazard for the operator.

Determination of dangerous zones in performance of such work, evaluation of their temperature characteristics and development of safety recommendations, were performed during testing in the space simulation test chambers, both in the automatic mode, and with the participation of the operator. Certain temperature limitations should be imposed to ensure safe performance of the operator, wearing a spacesuit. As required by the US standards, which were used as guidelines, when preparing for ISWE, during extravehicular activity of the operator, the temperature of the surface, which the spacesuit glove may touch, is limited by the range of –120–+113 °C and time of 0.5 min (Standard NASA-STD-300/vol. 1/rev.). According to Protocol 057-25/73-00, for the Russian «Orlan-M» spacesuit, a certain time should be ensured for contact of the gloved hand with structural elements, depending on the structural element temperature, during operator working on ISS outer surface.

The outer layer of the spacesuit skin tolerates short-time contact with surfaces of the temperature of ± 150 °C (Table 6).

Maximum temperature during performance of welding operations rises up to or even a little higher than the melting temperature of the metals being welded. Therefore, organizing the operator's work place requires taking a range of design and procedural measures, which allow prevention of the operator accidentally touching the sample or the item being welded with limited mobility.

Since during performance of ISWE on board of both the Shuttle Orbiter and OS «Mir» it was intended to mount the samples to be welded on the panels of the rotating sample holder, made of aluminium alloys and having a high heat conductivity and heat capacity, the temperature of panel surfaces, which the operator may touch, remained low. During operator training in the space simulation test chamber in preparation for the welding experiment on board «Mir», 6 sensors with maximum measurement temperature of 300 °C were mounted on the panels of the rotating sample holder and tool guard, the sensors monitoring the heating of panels during performance of welding operations. As is seen from Figure 8, their maximum temperature did not exceed 70 °C (curve *1*), and near the handles, which the operator used to rotate the holder, it was 30 °C.

Functioning of the electron beam tool proper is also accompanied by its heating due to internal heat evolution of the transformers, incorporated in it and radiation of the weld pool, which is at a short distance from the tool, because a short-focused gun is used. The gun case (anode) is heated to a maximum temperature, due to radiation from the emitting surface of the cathode assembly (emitter temperature is above 1550 °C), as well as scattering of the peripheral part of the electron flow and their braking on the gun case. Therefore, the anode temperature may reach 150–200 °C. In the tool for coating application the temperature may be equal to 350–400 °C, due to heat transfer from the crucible, despite the system of heat-insulating shields. In this connection, all the electron beam hand tools were fitted with special protective shields, which eliminated the possibility of the operator accidentally touching the tool parts, heated up to such high temperatures (Figure 9). As shown by measurements during testing in the space simulation test chamber, the temperature on such shields is not higher than 70–75 °C, and in the zones of direct long-term contact with the operator glove (handle, guard and tool lower part) — 40 °C (Figure 8, curve *2*).

Thus, the conducted testing and training in the space simulation test chamber confirmed that a cosmonaut-welder, wearing a spacesuit, can safely perform the processing operations of heating and melting of metals, using electron beam hand tools. This simply requires a thorough organising of the work place, taking a number of design and procedural measures and the appropriate level of operator training.

Electromagnetic compatibility and interference. One of the important kinds of testing the hardware, intended for participation in the space welding experiment, was evaluation of the electromagnetic interference, including assessment of the influence of hardware operation on the space vehicle systems, its payload, as well as evaluation of the influence of the space vehicle systems on the hardware functioning during experiment performance.

Limit requirements, made of the hardware, depend on the space vehicle, elements of its payload and the

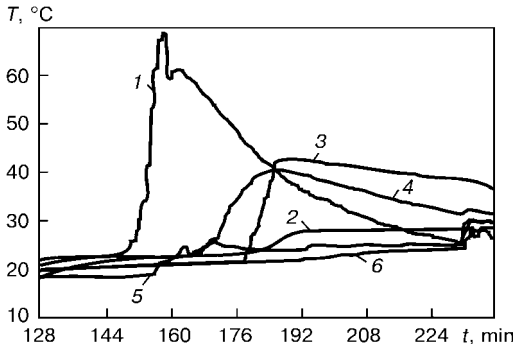

Figure 8. Change of the temperature of different parts of the electron beam hand tool during performance of testing in the space simulation test chamber: *1, 3, 4* — the sensors, located on panels of the rotating sample holder with samples for brazing, welding and cutting, respectively; *2, 5, 6* — the sensors, located on the guard from the inner and outer side and on tool handle, respectively

hardware being tested. Let us specifically consider «Universal» system during operation in the Shuttle Orbiter.

Hardware appearance during testing for electromagnetic compatibility is shown in Figure 10. «Universal» working tool and water-cooled copper target were located in a vacuum chamber, which was a glass cover of 420 mm diameter and 700 mm height. Main power and coolant supply to the chamber and chamber pumping down were performed through the base — aluminium plate 50 mm thick. Vacuum chamber was located in a shielded room, and was connected to the external pumping down unit by a piping of inner diameter of 150 mm and total length of about 2000 mm, as by the testing conditions it was prohibited to place the supporting equipment and instruments in the shielded room. Vacuum unit consisted of the roughing pump with the pumping speed of 5 l/s and turbomolecular pump with the speed of 470 l/s and limit vacuum of $1 \cdot 10^{-6}$ Pa. Vacuum level was monitored directly at the inlet of the pumping down unit, and during testing it was $1 \cdot 10^{-2}$–$1 \cdot 10^{-3}$ Pa.

All the requirements to testing and test procedures were taken from MSFC-SPEC-521B «Requirements to electromagnetic compatibility of the payload and subsystems», except for the narrow-band radiation section. Its values were taken from the last variant of ISD-2-10001 Document «Standard interfaces of

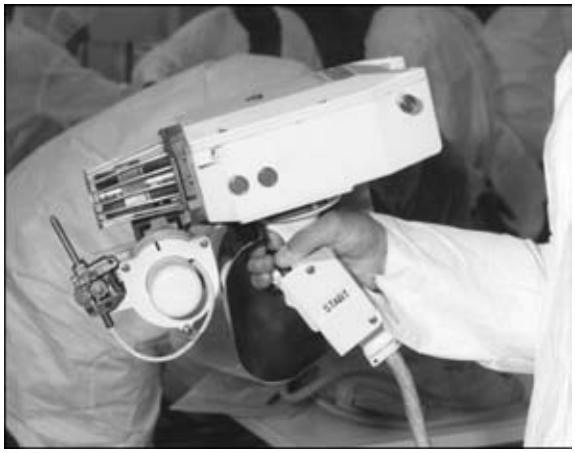

Figure 9. Protective shield of hand tool EBG

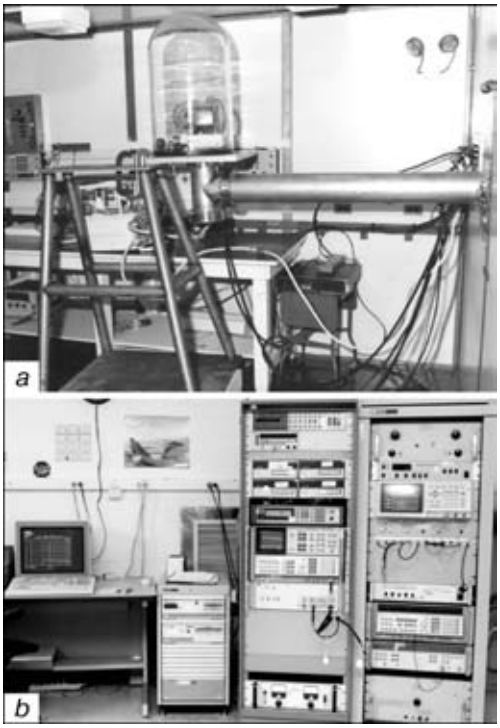

Figure 10. Appearance of the hardware during performance of testing for electromagnetic compatibility: *a* — vacuum chamber; *b* — instrumentation system

Shuttle Orbiter and payload». Before ISWE performance on board the Shuttle Orbiter, it was necessary to make sure that ISWE will not cause any electromagnetic interference with the flying vehicle, payloads, participating in the mission, or astronaut spacesuit. The following tests were conducted for this purpose.

Testing for conducting radiation. These tests were required to confirm that the ripple and transient processes by voltage, which ISWE would superpose on the power bus line of the Shuttle will not exceed the admissible values or cause electromagnetic interference between the vehicle systems and other payloads, connected to the same power bus line, including the following factors: voltage ripple in the DC power bus line by the positive and negative poles in the range from 0.03 to 20 kHz; the same for the positive and negative poles in the range from 20 to 50 MHz; transient processes in the DC power bus line at the hardware switching on and off.

Testing showed a certain overshooting of the maximum permissible values of the conducting radiation

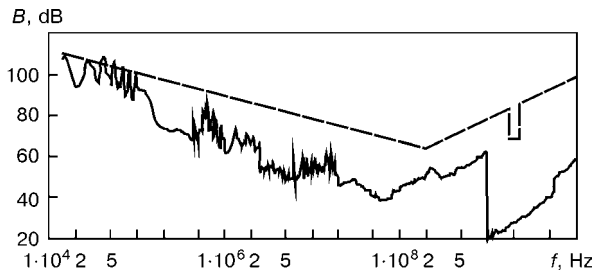

Figure 11. Dependence of the level of radiation *B* of «Universal» hardware on the frequency range *f* (dash line is the admissible level of radiation)

level. To eliminate these drawbacks, an electric interface device with a filter has been developed and successfully tested. In addition, it was noted that it is necessary to connect «Universal» hardware to a separate power bus line or switch off other payloads during ISWE.

Testing for RF emissions. These were conducted to check the influence of electric and magnetic fields of ISWE hardware on the electromagnetic environment of the Obiter, manned manoeuvring unit or other payloads, including the narrow and broad bands of electric field radio frequency emission at frequencies of $14 \cdot 10^3$–$1 \cdot 10^4$ hHz, as well as radio frequency emission of the magnetic field at the frequencies of 0.05–50 kHz.

Testing for conducting radiation susceptibility. These tests were required to check the resistance or reveal the susceptibility of ISWE hardware to voltage ripple or voltage transient processes, which may arise in the Orbiter power bus line, namely to voltage ripple of 4.2 V in the input power bus lines (positive and negative) in the range of frequencies of 0.03–50 kHz; to voltage ripple in the DC power bus line (positive and negative) of 0.2 V in the range of frequencies of 0.05–400 MHz. The hardware should not be sensitive at the test signal of ≤56 V amplitude of 10 μs duration. The transient process was applied both to the positive and to the negative bus lines. Repetition rate was 10 pulses of 1 s duration for 2 min.

Testing for susceptibility to radio emissions was conducted to reveal the susceptibility of ISWE hardware to electric fields, which may be part of electromagnetic environment of the Orbiter in the radio frequency sub-bands of 0.014–10^4 MHz at the electric field intensity of 2 V/m, 1.7–2.3 hHz at 10 V/m and 13–15 hHz at 12 V/m.

Testing demonstrated the following drawbacks of «Universal» hardware: insufficient screening of the cables of the technological block, working tools and motor of the filler wire feed unit (Figure 11).

The cables were improved by adding common screens, reliably connected from both sides to the hardware case, which essentially lowered the level of the emitted interference. A lot of attention was given to the working tools with the filler wire feed, as operation of their motors generated electromagnetic noise in the working frequencies of the radio receiver-transmitter of the astronaut spacesuit. In order to eliminate this drawback, additional screening of the motor power cable and the motor proper was made, pass filters were mounted and all the screens were reliably connected to the tool case.

These improvements, together with the measures, taken after the first type of testing, yielded positive results, and «Universal» hardware was accepted for conducting the space experiment. It should be noted, that the limit values of the conducted tests depend on the type of the Orbiter, payloads and point of hardware connection. Therefore, for the existing ISS

the NASA/RSC Document SSP 50094, item, 3.4 «Electromagnetic compatibility» (edition A, March 2000) should be used as guidelines.

CONCLUSION

Despite the application of a short-focused gun in the electron beam tools, the electron beam at up to 0.5 m distance has a damaging impact on all the materials of the spacesuit and protective clothing of the cosmonaut-welder at direct hitting. Therefore, in order ensure safe performance of the processing operations, it is necessary to take a number of design and procedural measures, eliminating the possibility of the beam hitting these materials, or the operator touching the items being welded.

When up to 10 kV accelerating voltage is used in the electron beam hand tools, the radioactive radiation does not exceed the established norm. A certain inconsistency of the obtained experimental data is attributable to use of various procedures and complexity of measurement of the intensity of radiation from low-energy sources.

It is anticipated that in the future application of manual welding will be required in case of emergencies, but the bulk of welding operations, most probably, will be performed by the operator, using flexible adaptive robotic systems. This will permit increasing EBG power and accelerating voltage, required to provide the quality of welded joints; however, monitoring the intensity of radioactive radiation will be required. If the operator is removed from the zone of performance of any extreme process to a rather short distance, i.e. to the zone of visibility and accessibility of the item being processed, the degree of total risk may be minimised.

Judging by the results of the conducted tests, the light and infrared radiation of the weld pool in manual EBW should not raise any particular concern. In welding of aluminium alloys, which in the future will be the main metals, welded in space, the operator does not have to use any additional protective means, and the few problems, arising in welding of stainless steel and titanium alloys, are completely solved with application of a standard sun filter by the cosmonaut-welder. In addition, there currently exist developments of sun filters of a variable density, based on composite liquid-crystal materials with very quick response [9, 10], which may be used by the operator for eye protection.

EBW process is much «quieter», compared to other welding processes, in terms of spattering [11]. Experience of ISWE preparation demonstrates that with appropriate technological preparation of welding operations, it is possible to practically completely eliminate spatter. As regards the processes of evolution from the weld pool of fine particles, leading to contamination of the operator spacesuit, we can only speak of its minimising. Therefore, in performance of manual EBW, use of protective welding clothing, put over the spacesuit, is a necessary safety measure.

Welding hardware, designed for application in space vehicles, should generate a minimum level of various interference (electromagnetic, in power circuits, etc.), not influencing the functioning of service systems, and should itself be protected from interference. Checking of its compatibility with these systems, as well as other possible payloads, is performed during integrated testing.

Results of the conducted testing of the new generation of manual EBW hardware — one of the standard and required tools for repair-restoration work in space, as well as special training of cosmonauts-welders of Russian crews in the space simulation test chamber, confirmed the possibility of realisation of experimental and applied welding tasks on the outer surface of the space vehicle.

1. Paton, B.E., Dudko, D.A., Bernadsky, V.N. et al. (1977) On the possibility of manual electron beam welding in space. In: *Space materials science and technology*. Moscow: Nauka.
2. Nikitsky, V.P., Lapchinsky, V.F., Zagrebelny, A.A. et al. (1985) Test of manual electron beam tool in open space. In: *Problems of space technology of metals*. Kyiv: Naukova Dumka.
3. Lankin, Yu.N., Gavrish, S.S. (2001) Device for provision of safe operation of manual electron beam tool in space. *The Paton Welding J.*, **4**, 36–38.
4. Bulatsev, K.A., Bulatsev, A.R. (2001) System of monitoring the position of manual electron beam tool. *Ibid.*, **4**, 39–41.
5. Tochin, V.V., Yushchenko, B.I., Rusinov, P.P. et al. (2001) Safety system of electron beam tool. *Ibid.*, **4**, 41–42.
6. *OSP-72–80*. Main sanitary regulations of operations with radioactive materials and other sources of ionizing radiations. Ministry of Health of the USSR. Moscow: Energoizdat.
7. Edwards, D.L., Russell, C.C., Carruth, M.R. et al. (1996) *Test report for the assessment of ground-based personnel and crew exposure to X-ray radiation during electron beam welding using the international space welding experiment*. MSFC, Nov. 18.
8. Lebedev, V.K., Zaruba, I.I., Shelyagin, V.D. et al. *Device for electron beam welding*. USSR author's cert. 206991, Int. Cl. B 23 K. Publ. 08.12.67.
9. Smorgon, S.L., Presnyakov, V.V., Zyryanov, V.Ya. et al. (1997) Device for polarization and modulation of light. *Pribory i Tekhnika Eksperimenta*, **1**, 164.
10. Crawford, G.P., Zumer, S. (1996) *Liquid crystals in complex geometries*. London: Taylor & Francis.
11. Mikhajlovskaya, E.S., Shulym, V.F., Zagrebelny, A.A. (2002) Results of experiments on manual EBW in a manned space simulation test chamber. *The Paton Welding J.*, **2**, 23–27.

IMPROVEMENT OF WELDABILITY OF HIGH-STRENGTH ALUMINIUM ALLOYS IN EXPLOSION CLADDING*

L.I. MARKASHOVA, L.D. DOBRUSHIN and **V.V. ARSENYUK**
The E.O. Paton Electric Welding Institute, NASU, Kyiv, Ukraine

Peculiarities of plastic deformation and process of hardening in the zone of the joints on commercially pure aluminium AD1 and annealed aluminium alloy 1201AM, explosion welded to high-strength aluminium alloy of the 1201AT type, are considered. To increase the safety factor for ductility of the deformed layers and improve weldability in cladding high-strength aluminium by the explosion welding method, it is recommended to soften the mating surfaces by preliminarily chemically cleaning them from hardening phases.

Key words: *explosion welding, aluminium alloys, weldability, plastic deformation, hardening phases, shear bands, chemical cleaning*

One of the imperative conditions for producing full-strength joints on metals and alloys in cladding by the explosion welding method is the possibility of achieving the sufficiently intensive plastic deformation of the mating surfaces in the collision zone [1–5]. A distinctive feature of high-strength aluminium alloys of the 1201 type is their susceptibility to solid-phase strain hardening, which is several times as high as the effect of other hardening processes (substructural, lattice friction, etc.) [6–8]. Phase precipitates in these alloys act as arresters which prevent movement of the crystalline lattice defects in slip systems during the deformation process, thus causing reduction of the volume of metal capable of participating in plastic deformation [9]. Ductile properties of metal in the welding zone and, hence, weldability deteriorate accordingly.

In the case of explosion welding the concept of improvement of weldability implies the possibility of increasing and/or ensuring the specified strength properties of the joints under the minimum collision conditions. It is known from the experience of application of explosion welding that high-strength aluminium alloys of the 1201 type are classed with hard-to-weld ones. Explosion welding of commercial-purity aluminium to such alloys involves no special difficulties, which is likely to result from increased ductile properties of aluminium, compensating to a certain degree for low ductility of a high-strength aluminium alloy. Therefore, alloys of this type are usually clad through thin ductile interlayers of commercial-purity aluminium.

The purpose of this study was to investigate physical-chemical processes occurring in the contact zone during explosion welding and reveal actual causes leading to deterioration of weldability in cladding high-strength aluminium alloys of the 1201 type in order to subsequently adjust the technological process to improve their weldability and produce quality welded joints.

Materials and experimental procedures. The experiments conducted included explosion welding of flyer (cladding) plates of commercial-purity aluminium of the AD1 type and annealed aluminium alloy of the 1201AM type to target plates of hardened aluminium alloy of the 1201AT type, the main hardening phase in the latter being $CuAl_2$ (copper content $\approx$ 7 %). Averaged values of tensile strength of the above materials were as follows: 73, 200 and 420 MPa, respectively. Prior to welding, for technological reasons the aluminium claddings on plates of both alloys was removed by machining and chemical etching (designations of alloys in the text are given in their original form).

Explosion welding was performed by the angular method using a high-speed thin-sheet explosive with a density of 1.56 g/cm^3 and detonation velocity of about 7600 m/s. The plan size of the plates welded and initial setting angle between them in all the experiments were 100×50 mm and 10°, respectively.

Controlled parameters of explosion welding of the AD1 + 1201AT joint were as follows:

- thickness of the flyer and target plates 3.0 mm,
- collision velocity during welding 690 m/s,
- welding speed — 2740 m/s.

Minimum parameters of explosion welding and strength of the 1201AM + 1201AT joints with different methods of preliminary preparation of surfaces for welding were as follows:

- thickness of the flyer and target plates 3.72 mm,
- collision velocity 560 m/s,
- welding speed 2260 m/s,
- strength of the joint without treatment 20–50 MPa,
- strength of the joint after chemical treatment 190–200 MPa,
- strength of the joint after electrochemical treatment 50–60 MPa.

The method of special etching using the arc discharge in a vacuum ion-etching unit (JEE-4C, Japan) was employed to estimate depth R of the intensive plastic deformation zone (region of the maximum thermomechanical effect exerted by welding) on the basis of variations in density of dislocations revealed by the etching pits. The content of the hardening phase

* The authors are grateful to Dr. M.I. Zotov for participation in the experiments and discussion of the results.

was estimated using the Cameca microanalyser on the basis of variations in the concentration of copper in the contact zone $2R$ wide.

The character of plastic deformation and the effect of hardening phase precipitates on ductility of metal in the welding zone were studied by optical microscopy, analytical scanning electron microscopy Philips SEM-515 microscope and transmission microdiffraction electron mocroscopy JEOL JEM-200CX microscope at an accelerating voltage of 200 kV.

Experiments and discussion of results. Special studies of the contact zone on the AD1 + 1201AT joint were first conducted to investigate in more detail the causes of decrease in ductility and find methods to increase it. Structure of aluminium alloy 1201AT, sizes and character of distribution of the hardening phases are shown in Figure 1, *a*. Mean sizes of the hardening phases in metal are ≈ 6 μm. With direct transmission examinations this structure in a welded joint (in the region adjoining base metal) looks like that shown in Figure 1, *b*.

It can be seen that the phase precipitates are different in size. Examination of distribution of etching pits on transverse sections showed that the intensive plastic deformation zone characterised by an increased density of structural defects, first of all dislocations, and their oriented distribution extended to a depth of about 150–200 μm (Figure 2, *a*). This zone can be clearly seen using an optical microscope at low magnifications.

More detailed studies of the contact zone by transmission microscopy yielded the following results. It was established that redistribution of phases under the effect of welding strains took place in the near-contact zone on the side of alloy 1201AT (200 μm deep). Firstly, it is «expanding» of the hardening phases (Figure 2, *c*) and, secondly, their refining to sizes of hundredths of a micron (≈ 0.07–0.01 μm) (Figure 2, *c, d*). The noted redistribution of phases is especially active in the local contact zone tens of microns deep (Figure 2, *b, c*). The process of redistribution of phases in this case is accompanied by an active mass transfer of copper within the regions adjacent to the phases, including the contact zone of the AD1 + 1201AT joint.

Transmission examinations of a fine structure of cross sections of the contact zone showed that plastic deformation occurred by different mechanisms in the near-contact zones of commercially pure and hardened aluminium (Figure 2, *b, d, f, g*). For example, plastic deformation in commercially pure aluminium occurs by the shear mechanism, which is evidenced by formation of a developed system of shear bands (Figure 2, *b, f*). As opposed to this, plastic deformation in the welding zone of hardened alloy 1201AT occurs by a discrete shear with a drastic reorientation of shear bands in the zone of collision with a hardening phase (Figure 2, *b, d, g*). In addition, the microdiffraction methods revealed structural elements indicative of turns (rotations) of different sizes of microregions of the hardened metal, which is the extreme form of plastic relief of internal stresses in the deformed metal. The character of variations of the types of structures formed on the side of each of the metals welded through depth of the welding zone is shown in Figure 3.

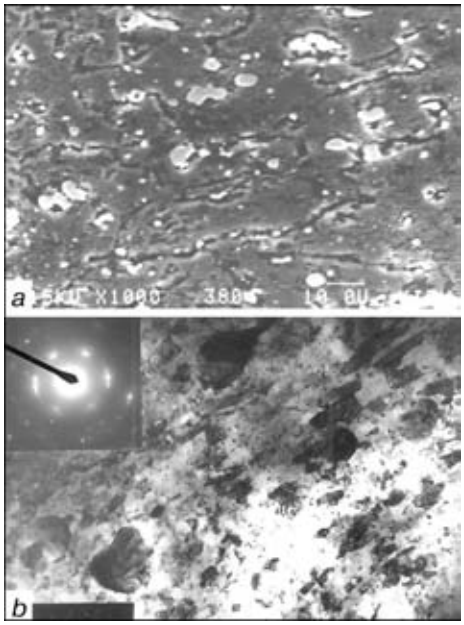

Figure 1. Structure of base metal (aluminium alloy 1201AT): *a* — surface with phase precipitates $CuAl_2$ (scanning electron microscopy) (×1000); *b* — fine structure and distribution of phase precipitates (transmission electron microscopy) (×15,000)

Therefore, while plastic deformation in the contact zone of commercially pure aluminium is characterised by a high intensity, having almost no obstacles to occur actively, in the contact zone on the side of hardened aluminium the situation is different.

Discreteness of the shear bands, drastic change in their orientation (Figure 2, *d, g*) and substantial increase in density of dislocations in locations where the shear bands collide with the hardening phase (Figure 2, *h*) are indicative not only of a retarded flow, but also of a considerable local hardening of aluminium alloy 1201AT in the welding zone (at a depth of about 150–200 μm from the contact surface). It is likely that considerable hardening of metal in the contact zone is associated not only with phase precipitates and drastic increase in the dislocation density, but also with increase in the concentration of copper leading to increase in the solid-solution component of metal hardening. In addition, deterioration in weldability and separation of such joints in explosion welding, which is often seen in practice, may be caused also by the «expanded» phases present in the contact zone (Figure 2, *c*), which are localised at a depth of about 3–5 μm from the contact surface.

Given that phase precipitates (partially redistributed, but still substantial in size) exert such an unfavourable effect on ductility in the welding zone, it was of interest to look for methods for cleaning the contact surfaces from the phases. Moreover, cleaning should be done to a certain depth associated with the depth of plastic deformation in explosion welding (in this case it is 150–200 μm). Two methods of preliminary treatment of surfaces for cleaning were tried out for this purpose: electrochemical and chemical etching. The choice of these methods was based on the fact that they allowed phase precipitates to be selectively removed [10]. In addition, dissolution of redundant phases (and, accordingly, weakening of boundaries between grains and phases as a result of selective treatment) will pro-

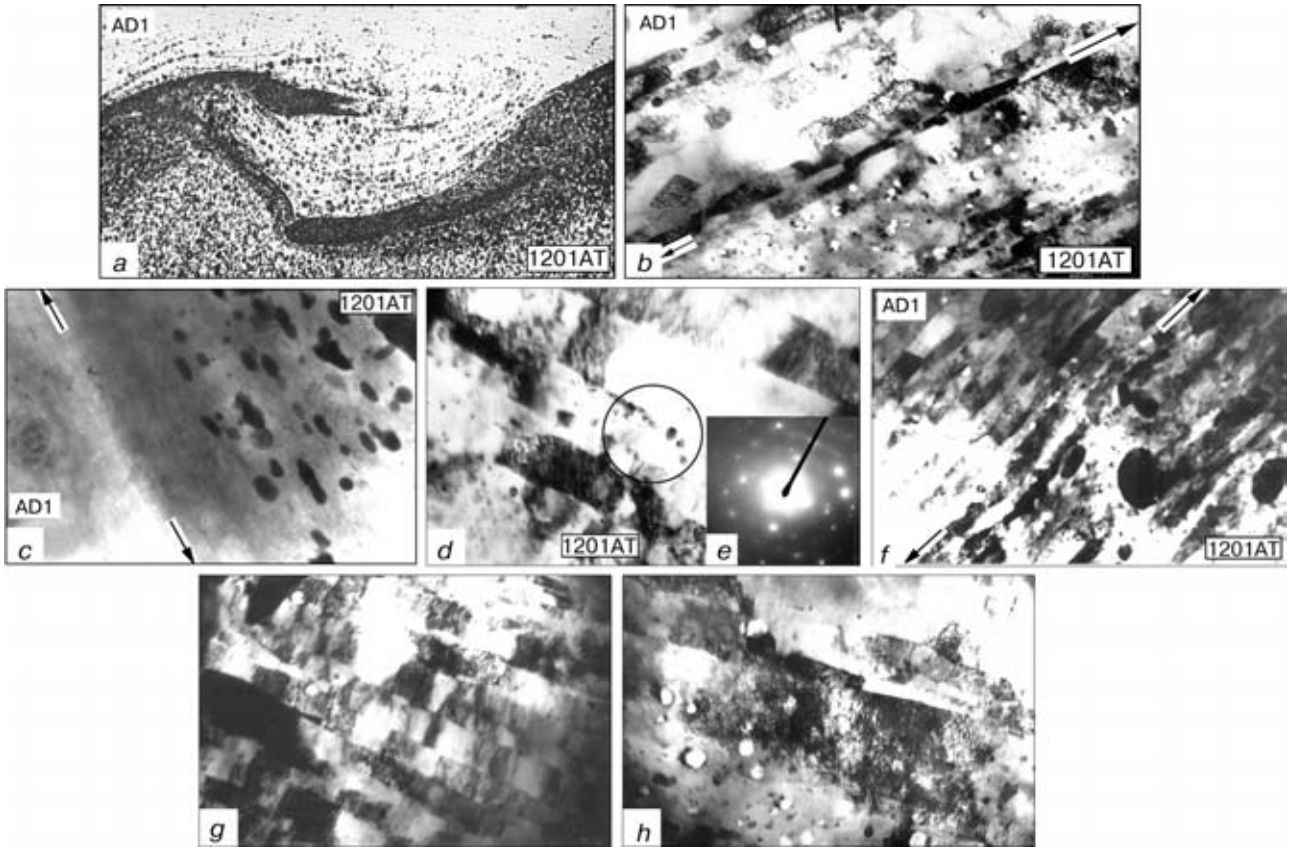

Figure 2. Contact zone of the AD1 + 1201AT joint and variation in morphology of hardening phase precipitates in alloy 1201AT in the welding zone (arrows show direction of the contact boundary of the joint): *a* — general view of the welded joint boundary (×100); *b* — fine structure of the AD1 + 1201AT contact zone exhibiting extended shear bands (AD1) and reorientation of the bands in the hardening phase locations (1201AT) (×10,000); *c* — hardening phase precipitates in the contact zone on the side of alloy 1201AT (×1000); *d*, *f* — reorientation of the bands in alloy 1201AT in the zone of collision with phases of different sizes (region with finely dispersed phases is marked by a circle) (×15,000); *e* — diffraction of the reorientation bands; *g*, *h* — local increase in dislocation density in the zone of reorientation of the shear bands on the side of alloy 1201AT (×30,000)

mote turns (rotations) of microvolumes of the deformed metal during the welding process. The latter should favour improvement in weldability, as the regular mechanisms of plastic deformation (dislocation, shear) can be supplemented in this case by an additional mechanism, i.e. rotational. Widening of the range of mechanisms by which plastic deformation may take place is especially important for such rigid deformation conditions which are formed during the explosion welding process.

The above premises were used as the basis for finding the possibility of minimising parameters of explosion welding of alloy 1201AM (almost 3 times as strong as alloy AD1) to hardened alloy 1201AT through a special preliminary preparation of the mating surfaces. Cladding with a stronger alloy allows the required thickness of the flyer plate and the pulse effect on structure in the cladding location to be decreased accordingly, which is extremely important for solving a number of practical problems. For technological reasons the preliminary treatment was done to the mating surface of only the flyer plate of alloy 1201AM. Electrochemical treatment was done at the anode and cathode polarisation, as well as at the corrosion potential of the $CuAl_2$ phase in the 5 % hydrochloric acid solution at a temperature of 20 °C. The time of treatment was 1 h. Chemical treatment was performed in the 10 % alkaline solution at a temperature of 80 ± ± 5 °C for 20 min, followed by treatment in the 25 % nitric acid solution. The depth of etching (Δ_c) and content of the hardening phase $CuAl_2$ were estimated in parallel with experiments on estimation of the effect of the preliminary treatment method and kinematic collision parameters on strength of the resulting 1201AM + 1201AT joints to separation of the cladding layer. The results obtained were compared with the similar data generated by using no preliminary treatment.

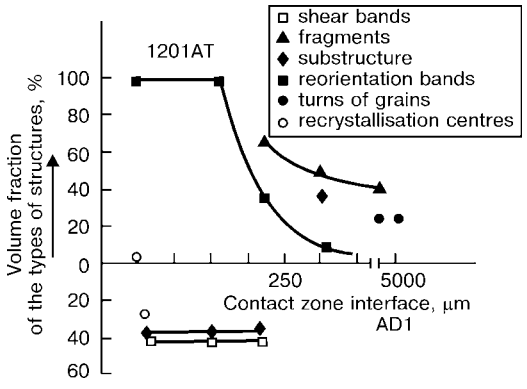

Figure 3. Character of variations in structures and their volume fraction through depth of the contact zone from the interface of the AD1 + 1201AT joint made by explosion welding

To ensure identical collision conditions, thinning of the flyer plates resulting from the preliminary treatment was compensated for by using cover plates. This was done to investigate the effect of total thickness of the flyer and cover plates on strength of the re-

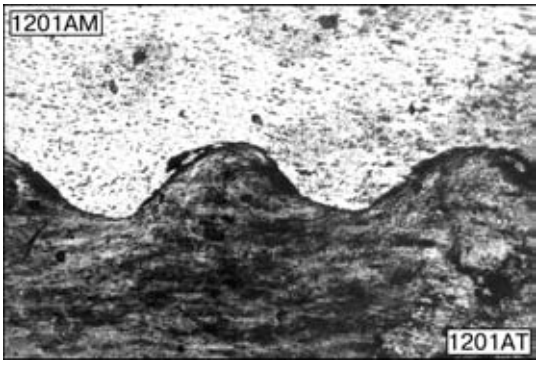

Figure 4. Typical microstructure of the zone of the 1201AM + 1201AT joint made with preliminary chemical treatment of the surface

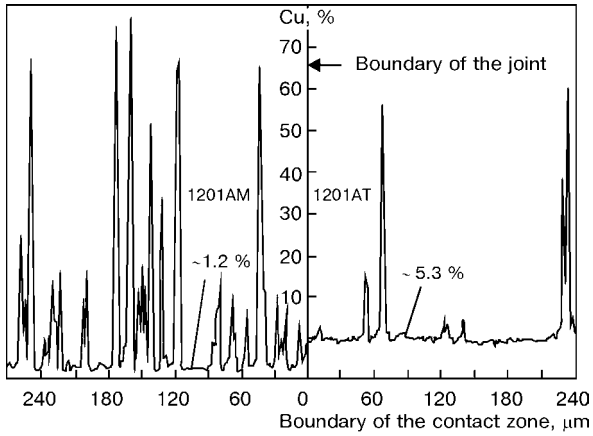

Figure 5. Distribution of the concentration of copper in the contact zone of the 1201AM + 1201AT joint made with preliminary treatment of the surface

sulting joints. The use of the cover plates provided the required time for formation of the joint through increasing the time of the effect of positive pressures in the contact zone during the process of collision of the plates. It was established that preliminary chemical treatment led to improvement of weldability: strength of the joint increased several times and amounted to that of the flyer plate of alloy 1201AM in the annealed state. Typical structure of the joint zone is shown in Figure 4. The attempts to produce the full-strength welded joint (with respect to alloy 1201AM) without preliminary chemical treatment of the flyer plates failed.

Analysis of distribution of copper in the joint zone (Figure 4) proved (Figure 5) that as a result of chemical treatment its concentration decreased both on the side of alloy 1201AM and on the side of alloy 1201AT (in the latter — by about 2 %). Precise determination of the concentration of copper is hampered by its levelling during the process of mass transfer through the contact boundary, occurring in combined plastic deformation of the mating surfaces, as well as by a partial removal of the treated layer as a result of the cumulation effect during explosion welding. Electrochemical treatment fails to provide the required degree of dissolution of phases, which does not favour weakening of intercrystalline bonds and does not improve weldability.

Generalisation of the results obtained allows the following parameters of explosion cladding of alloy 1201AT and preliminary treatment of alloy 1201AM to be recommended to solve problems associated with minimisation of the collision parameters for making the 1201AM + 1201AT joints. So, in the case of using a thin-sheet explosive with the above-mentioned parameters, the flyer plate should be approximately twice as thick as the explosive. With a smaller thickness it is necessary to apply the compensating cover plates. Otherwise there is the risk of separation of the joint due to the insufficient time of the effect of positive pressures in the contact zone during collision of the plates. To increase strength of the resulting joint, it is advisable to soften the mating surfaces by cleaning them from the hardening phases, which in this case is chemical etching of the surface of the flyer plate of alloy 1201AM in the 10 % alkaline solution, followed by treatment in the 25 % nitric acid solution.

The above developments were successfully utilised in elaborating technologies for repair of different damages in base metal of thin-walled shell metal structures of flying vehicles, including those made from heat-hardening aluminium alloys of the 1201AT type, by the explosion cladding method.

CONCLUSIONS

1. Plastic deformation under explosion welding conditions is localised at a certain depth R from the interface between the plates welded. This depth depends primarily upon the thickness of the flyer plate and parameters of its collision with the substrate being clad, and is a controllable parameter of the process.

2. Plastic deformation in the explosion welding zone occurs by different mechanisms, depending upon the type of metal welded. In metals which are pure with respect to their phase content (aluminium of the AD1 type) it occurs primarily by the shear mechanisms due to intensive shear bands. In metals containing hardening phases (aluminium of the 1201AT type) it is hampered and takes place by involving shear and reorientation, occurring in the zones of collision of the shear bands with the hardening phases.

3. It is recommended to soften the mating surfaces by removing brittle or low-ductility phases to increase the safety factor for ductility of the deformed layers and improve weldability in cladding aluminium alloy 1201AT by explosion welding. In this case softening can be done by chemical etching of the surface of the flyer plate of alloy 1201AM in the 10 % alkaline solution followed by treatment in the 25 % nitric acid solution.

1. Deribas, A.A. (1972) *Physics of explosion strengthening and welding*. Novosibirsk: Nauka.
2. Gelman, A.S., Chudkovsky, A.D., Tsemakhovich, B.D. et al. (1978) *Explosion cladding of steel*. Moscow: Mashinostroenie.
3. Epshtejn, G.N. (1988) *Structure of metals deformed by explosion*. Moscow: Metallurgiya.
4. Olson, G.B., Meskol, J.F., Azrin, M. (1984) *Shock waves and phenomena of high-rate deformation of metals*. Moscow: Metallurgiya.
5. Murr, L.E. (1984) *Shock waves and phenomena of high-rate deformation*. Moscow: Metallurgiya.
6. Gordienko, L.K. (1973) *Substructural strengthening of metals and alloys*. Moscow: Nauka.
7. Ivanova, V.S. (1965) *Role of dislocations in strengthening of metals*. Moscow: Nauka.
8. Goldshtejn, M.I., Litvinov, V.S., Bronfin, B.M. (1986) *Metal physics of high-strength alloys*. Moscow: Metallurgiya.
9. Orowan, E. (1954) *Dislocation in metals*. New York: AIME.
10. Akimov, G.V. (1945) *Theory and methods for examination of metal corrosion*. Moscow-Leningrad: AN SSSR.

ABOUT DESIGN OF ELECTRONIC CONTROLLERS OF WELDING CURRENT FOR MULTISTATION WELDING SYSTEMS

A.E. KOROTYNSKY, N.M. MAKHLIN and **V.A. BOGDANOVSKY**
The E.O. Paton Electric Welding Institute, NASU, Kyiv, Ukraine

It is shown that the main drawback of multistation systems based on ballast rheostats, consisting in increased energy consumption, can be prevented in their replacement by electronic controllers of welding current made on power transistor switches of the third and fourth generations. These schemes are based on welding current coverters using pulse-width modulators with wide functional capabilities of welding-technological properties.

Key words: *arc welding, multistation welding systems, energy-saving, converter, inverter, snubber, power transistor module*

Welding used in erection and repair of objects of power engineering, metallurgy, oil-gas chemical complex, pipeline transport, as well as in ship-building, heavy and transport machine-building and some other branches of industry is peculiar by the need to concentrate a large quantity of welding stations at a limited manufacturing area. In these cases it is rational to use systems of a centralized supply of welding stations with electric energy. These systems were named multistation welding systems (MWS) [1–4].

The MWS found the wide spreading in manual arc welding (MMA), mechanized welding in shielding gases (MIG/MAG) and non-consumable electrode welding in inert gases (TIG). They include a powerful power source with a rigid external volt-ampere characteristic (VAC), individual welding stations and branched electrical networks connecting them. Each welding station is connected to the power source through a ballast rheostat, made on linear and nonlinear resistors, with the help of which the control of welding conditions is realized [3, 5–8]. Similar MWS are characterized by some advantages, such as lower service expenses are required as compared with an equivalent number of single-station rectifiers; have higher characteristics of safety; there is no need in wiring of temporary networks of 380 or 220 V, creating an increased hazard in places of welding; service in the wide range of ambient temperatures is feasible. However, the MWS have also essential drawbacks: clearly expressed dependence of welding current on fluctuations of mains voltage and change in length of the arc gap; mutual effect of welding stations at their simultaneous operation; absence of possibility to maintain the preset technological conditions at a high accuracy, and also to program the welding cycle and to realize the welding conditions with a modulated current; frequent repairs of ballast rheostats [3].

The main drawback of MWS with ballast rheostats is the low efficiency factor, and, consequently, high energy consumption for welding jobs that is stipulated by large losses of power in ballast rheostats (50–80 % of power consumed by a welding station). The efficiency factor of welding station in MWS with ballast rheostats in accordance with [5] is determined as

$$\eta_{WS} = U_a / U_{rat},$$

where U_a is the arc voltage; U_{rat} is the rated operating voltage of power source (rectifier).

The total efficiency factor of MWS (without allowance for losses in busbars) has a form

$$\eta_{MWS} = \eta_{PS}\eta_{WS},$$

where η_{PS} is the efficiency factor of power source (rectifier).

It is seen from relations that at a sufficiently high efficiency factor of multistation rectifiers (90–92 %) the efficiency factor of MWS with ballast rheostats in the range of the most widely used and technologically-grounded welding conditions in case of MMA and MIG/MAG welding does not exceed 45, and in TIG — 23 %.

Therefore, almost simultaneously with the beginning of a wide application of MWS with ballast rheostats the attempts were made to design more economical MWS using electronic controllers of welding current [5, 9–12]. However, the practical solution of this problem was hindered by the lack of reliably-operated power semiconductor devices capable to commutate a high power at a high frequency (16 kHz and more).

Development and mastering over the recent 10–15 years of industrial manufacture of powerful field-effect transistors (MOSFET), insulated-gate bipolar transistors (IGBT) and other similar power devices, means of control of these devices, such as integral drivers, controllers of pulse-width modulation (PWM), and also quick-response power diodes and elements of snubber circuits gave an opportunity to create reliable pulsed high-frequency converters and highly-effective stationary and mobile MWS of the new generation on their base.

Among the variety of semiconductor pulsed DC converters, a single-action step-down converter has

found the widest spreading. It is characterized by a simple scheme of the power part, capability to function reliably at changes in wide ranges of supply voltage and load resistance, high efficiency factor, amounting usually to 80–90 %. The value of power factor of converter of this type is approaching unity. As the power semiconductor devices of the converter are included into the circuit of a lower voltage, the controllers of welding current made by the scheme of a step-down converter, are more reliable than the inverter power sources, and their properties as executive devices in systems of the automatic control are not worse than those of inverters [13, 14].

Class of DC converters has been studied comprehensively. At the same time, the use of a step-down converter as a controller of welding current has some specifics influencing both on the selection of parameters of power part elements and also on the design of the controller control system. These specific features include a comparatively high level of the commutating power (3–10 kW), dynamic nature of load changing in the process of welding at a high rate from open-circuit to short-circuit load resulting from the conditions of providing stability and steadiness of process of arc welding, necessity of converter operation in the conditions of continuous currents of an inductance choke, high heat power dissipating by semiconductor devices of a power part. The controller control system should provide formation of static and dynamic VAC in all the range of changing the load parameters.

Figure 1 gives schematic diagrams of welding current controllers for MMA, MIG/MAG and TIG welding.

Reliability and efficiency factor of these controllers depend greatly on type and parameters of active elements, on which the power part is based. MOSFET- and IGBT-modules, having high input resistance and, thus, consuming a negligible control power in a static condition, can be used as a power transistor switch *VT*. MOSFET-modules possess the best frequency properties among the advanced power semiconductor devices. They have high rates of switching and, consequently, low dynamic losses. At the same time, the conductivity losses in MOSFET-modules with drain–source voltage of more than 200 V are much higher than those of IGBT-modules. MOSFET-modules are much inferior to IGBT-modules both by characteristics of safety operation and also by switching capabilities (by voltage, current and dissipated power). Therefore, at load power of more than 3 kW and 16–30 kHz frequency of transformation, typical of welding current controllers, the use of IGBT-modules with the highest allowable collector–emitter voltage in a switched-on condition U_{CES}, being about 600 V, is most rational. As the power semiconductor devices, they have a number of unique properties [15, 16]. Typical values of parameters of IGBT-modules of the third generation with U_{CES} = 600 V in industrial series of companies «Mitsubishi Electric», «International Rectifier», «Semikron», «Siemens», «Hitachi» and others, which are leaders in the field of manufacture of these modules, are given below:

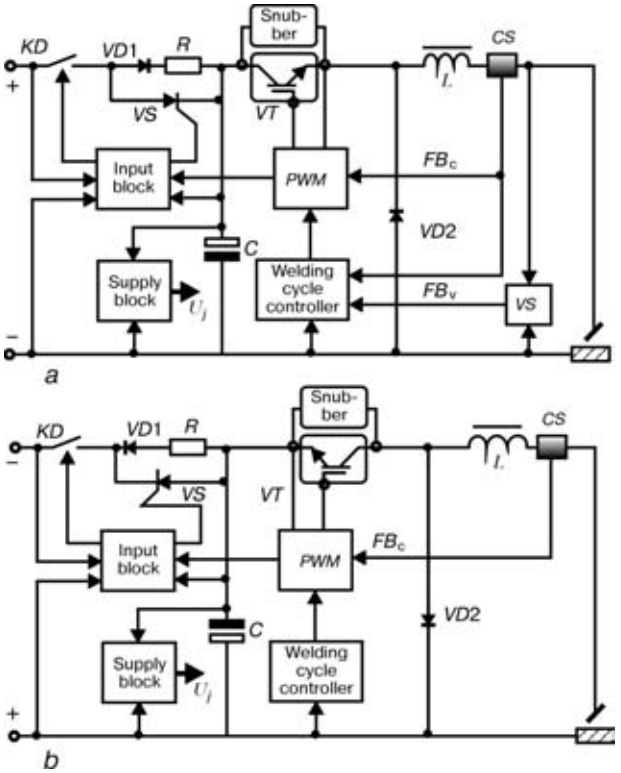

Figure 1. Structural-functional schemes of welding current controllers for MMA (*a*) and TIG (*b*) welding: FB_c and FB_v — current feedback and voltage feedback, respectively (the rest designations are given in the text)

Technical characteristic of IGBT-modules

Highest long-time direct current of collector, I_c, A	600
Collector–emitter saturation voltage (at I_c = 100–600 A), U_{CESAT}, V	1.5–2.8
Time of switch-on delay (at I_c = 100–600 A), $t_{d(on)}$, ns	85–350
Time of increment of collector current at switching on (at I_c = 100–600 A), t_r, ns	65–600
Time of switch-off delay (at I_c = 100–600 A), $t_{d(off)}$, ns	350–680
Time of collector current drop at switching off (at I_c = 100–600 A), t_f, ns	55–300
Losses of power (at I_c = 100–600 A), mW·s:	
in switching on, E_{on}	7–36
in switching off, E_{off}	5–42
Range of allowable temperatures of p–n transition, T_j, °C	–40 – +150
Range of allowable ambient temperatures (without current passing through the module), T_{STG}, °C	–40 – +125

Important characteristics, greatly influencing the reliability and efficiency factor of the controller, are quick-response and dynamic resistance of a reverse diode *VD2*. Time of a reverse recovery t_{RR} of diode *VD2* defines the switching current overloads of a power transistor switch *VT* of IGBT-module. In quick-response diode modules of such companies as IXYS, «International Rectifier», «Semikron», the direct current I_F is up to 600 A, direct voltage U_F = = 1.1–2.2 V, reverse voltage U_{REM} — up to 1200 V, time of reverse recovery t_{RR} = 150–300 ns. These

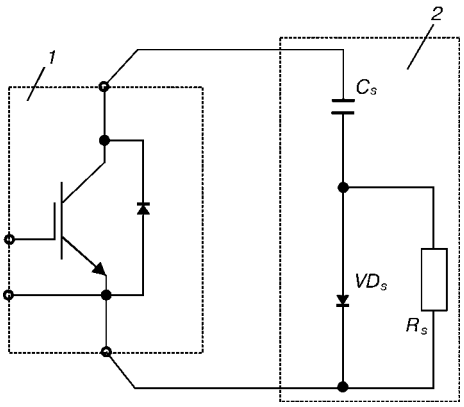

Figure 2. Scheme of a snubber circuit: *1* — transistor module; *2* — snubber

values of parameters of diode modules allow their use in a power part of the welding current controllers as a reverse diode.

The application of choppers, the integrated power devices, in which IGBT-transistor is combined with a reverse diode in a single diode-transistor or transistor-diode module, seems most rational for the design of a power part of the welding current controllers. In the range of current values up to 400 A the choppers are manufactured by companies «International Rectifier», «Semikron» and others. Parameters of IGBT-transistor and reverse diode of the choppers have almost the same values as the single IGBT-modules, equivalent by current, and quick-response diode modules.

Snubber (see Figure 1), a damping circuit for decreasing dynamic losses by correction of path of a working point in switching off of a power transistor switch, belongs to the obligatory elements of the controller power part. In case of IGBT the snubber, having the same configuration (Figure 2), is designed for limiting jumps of transition voltages at the transistor in its switching off, caused by parasitic inductances of, respectively, snubber L_s and busbar L_p of power circuit of IGBT-module, and also high values dI_c/dt, i.e. rates of change in collector current I_c in IGBT-module switching off. Figure 3 presents a diagram of voltage for IGBT-module at its switching off using the snubber. Voltage jump ΔU_1 was caused mainly by inductance L_s. Value ΔU_1 is determined from equation

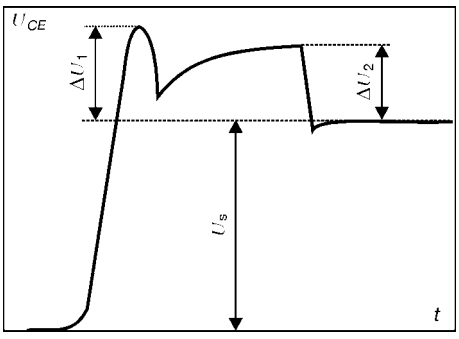

Figure 3. Diagram of collector–emitter voltage U_{CE} in switching on IGBT-module with use of a snubber

$$\Delta U_1 = L_s dI_c/dt.$$

As dI_c/dt can reach values 0.01–0.02 A/ns [16], the parasitic inductance of snubber L_s should not exceed 10.0–12.5 nH to limit values ΔU_1 (not more than 100 V). Fulfillment of this requirement is attained by use of quick-response diodes and film (for example, polypropylene) capacitors with a low inner inductance in the snubber and by the snubber location in the direct vicinity to the IGBT-module. «Jump» of voltage ΔU_2 depends on the capacity of the snubber capacitor C_s and parasitic inductance of busbar L_p. Amplitude of ΔU_2 is determined from expression

$$\Delta U_2 = I_c(L_p/C_s)^{0.5},$$

whence, at a preset maximum allowable value ΔU_2

$$C_s = L_p I_c^2/\Delta U_{2\,\max}^2 = L_p I_{\mathrm{w}\,\max}^2/\Delta U_{2\,\max}^2,$$

where $I_{\mathrm{w}\,\max}$ is the maximum value of welding current.

At $I_c = I_{\mathrm{w}\,\max} \le 400$ A in snubbers of welding current controllers the capacity of capacitor C_s is usually equal to 0.68–1.00 μF, that provides $\Delta U_2 < 100$ V at real design variants of power busbars. Losses in the snubber are determined by an active power generated in a resistor R_s (see Figure 2) in the process of discharge of capacitor C_s in switching on of IGBT-module and can be calculated by formula

$$P_{SSSB} = \frac{C_s U_s^2 f}{2}, \qquad (1)$$

where U_s is the supply voltage of controller; f is the frequency of voltage transformation.

The largest part of total losses in the welding current controller is the losses in a power transistor switch and reverse diode. For power transistor of any type the total losses in P_{SVT} represent a sum of losses of conductivity P_{SSVT} (static), losses in switchings P_{SWVT} (dynamic) and losses for control P_{SDVT}. In case of IGBT-module the losses for control can be neglected, as they are too small. Static losses are determined by voltage at power on transistor and effective value of the collector current. According to ratio, known for step-down converter [17], the effective value of collector current I_c in a power transistor of the welding current controller is

$$I_c = \left[\left(I_{\mathrm{w}}^2 + \frac{\Delta I_L^2}{12}\right)\gamma\right]^{0.5},$$

where $\Delta I_L = \Delta I_{\mathrm{w}}$ is the range of pulsations of welding current passing through choke L; $\gamma = U_{\mathrm{a}}/U_{\mathrm{s}}$ is the coefficient of pulse filling (relative duration of «on» state of IGBT-module).

As in the condition of continuous currents of choke L $\Delta I_L^2/12 << I_{\mathrm{w}}^2$, the expression for losses in IGBT-module can be presented in the form

$$P_{SVT} = P_{SSVT} + P_{SWVT} = \\ = U_{CESAT} I_w \left[\frac{U_a}{U_s}\right]^{0.5} + f (E_{SW(on)} + E_{SW(off)}), \quad (2)$$

where U_{CESAT} is the voltage of saturation of IGBT-module in «on» state; $E_{SW(on)}$ and $E_{SW(off)}$ are the energy losses, respectively, for switching on and off of IGBT-module, falling on one pulse.

It should be noted that in IGBT-module, the saturation voltage U_{CESAT} depends on some factors, such as current collector I_c, temperature of p–n transition T_j, gate voltage U_g, and energy of losses for switchings ($E_{SW(on)} + E_{SW(off)}$) depends on voltage U_{CES} at collector when IGBT-module is off, collector current I_c, resistance in gate circuit R_g [15, 16]. Figure 4 shows the dependence of static losses of conductivity P_{SSVT}, based on reference and experimental data, on welding current I_w at different values, γ ($\gamma = 0.2$ is typical of the range of TIG conditions, $\gamma = 0.45$ — for MMA and MIG/MAG welding) and temperature of p–n transition T_j for IGBT-module of CM400HA-12H («Mitsubishi Electric»). Dependence of dynamic losses P_{SWVT} of this module on I_w at different values f is shown in Figure 5.

Losses of reverse diode P_{SVD} include losses of conductivity P_{SSVD} and losses at reverse recovery P_{SWVD}

$$P_{SDV} = P_{SSVD} + P_{SWVD} = U_f I_f + E_{VD(off)} f = \\ = U_f I_w \left[1 - \frac{U_a}{U_s}\right]^{0.5} + U_s Q_{RR} f = \\ = U_f I_w \left[1 - \frac{U_a}{U_s}\right]^{0.5} + U_s \left(\frac{I_{RRM} t_{RR}}{2}\right) f, \quad (3)$$

where U_f is the drop of direct voltage on diode; I_f is the effective value of direct current passing through the diode; $E_{VD(off)}$ is the energy of losses at recovery falling on one pulse; Q_{RR} is the charge of diode recovery; I_{RRM} is the peak value of reverse current at recovery; t_{RR} is the time of reverse recovery.

The direct drop of voltage U_f depends on direct current I_f, maximum allowable value of reverse voltage U_{RRM} and temperature of p–n transition T_j; peak value of reverse current I_{RRM} depends on I_f, U_{RRM}, T_j and rate of drop of direct current di_f/dt at recovery, while in choppers it depends also on resistance R_g in gate circuit of IGBT-module. Time of reverse recovery t_{RR} is also a function of di_f/dt and T_j. Calculations showed that at frequency of transformation up to 30 kHz and application of quick-response diodes with $U_{RRM} \le 400$ V, $t_{RR} \le 200$ ns the losses at reverse recovery P_{SWVD} are very small as compared with losses of conductivity P_{SSVD} (not more than 2–5 %). Therefore, the expression (3) can be presented in the form

$$P_{SDV} \cong P_{SSVD} = U_f I_w [1 - U_a/U_s]^{0.5}. \quad (4)$$

Figure 6 gives the dependence of losses of conductivity on welding current at different values $(1 - \gamma)$

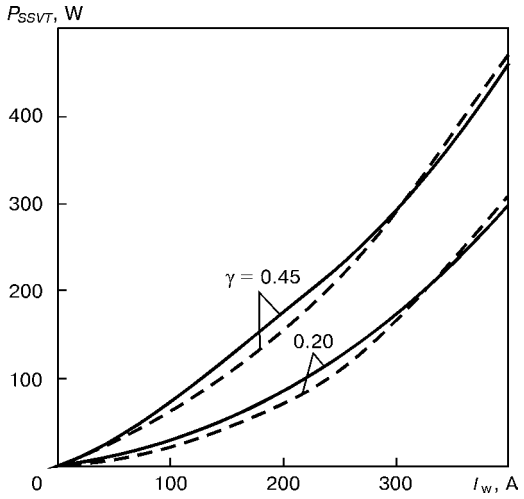

Figure 4. Dependence of static losses of conductivity P_{SSVT} in IGBT-module on welding current at $U_g = 15$ V (dash lines — T_j = = 125 °C; solid lines — $T_j = 80$ °C)

and temperature of p–n transition for module SKMD202E («Semikron»).

It should be noted that the values of parameters calculated by expressions (2)–(4) have an estimating nature and can be used for the approximate determination of losses to obtain the initial data for designing a system of cooling the modules of a power transistor switch and reverse diode or chopper and approximate calculation of thermal conditions of modules [16]. In most cases the real losses in IGBT-module are somewhat lower than calculated losses. This is explained by the fact that in calculation of dynamic losses dominating at $f > 10$ kHz (Figure 5) the regulated values of energy of losses $E_{SW(on)} + E_{SW(off)}$ are usually used, which refer to the maximum value of collector–emitter voltage U_{CES} of off IGBT-module. In welding current controllers $U_{CE\,max} < U_{CES}$ by 6–10 times, and, consequently, the values $E_{SW(on)}$ and $E_{SW(off)}$ are much lower than the regulated values. The real losses in reverse diode are also somewhat lower, as in the real conditions $25 < T_j < 125$ (°C), and regulated values U_f refer, as a rule, either to $T_j = 25$ °C or to

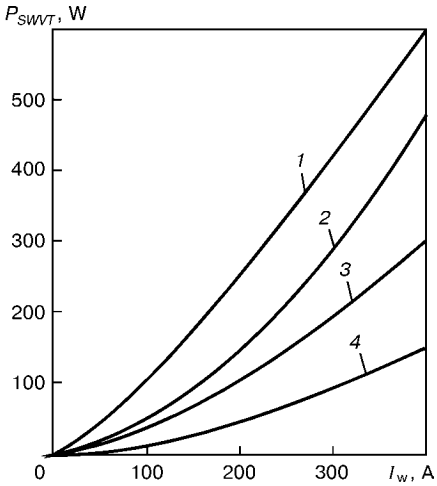

Figure 5. Dependence of dynamic losses P_{SWVT} in IGBT-module on welding current I_w and frequency of voltage transformation f at $U_g = 15$ V, $U_{CE} = 300$ V and $T_j = 125$ °C: *1* — $f = 20$; *2* — $f =$ 16; *3* — $f = 10$; *4* — $f = 5$ kHz

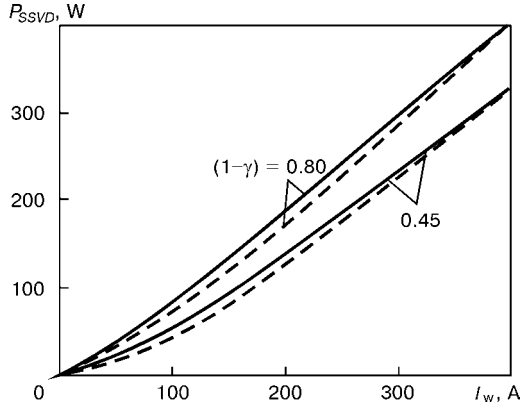

Figure 6. Dependence of power of losses of conductivity P_{SSVD} in reverse diode on welding current at U_{REM} = 300 V (the rest designation are given in Figure 4)

T_j = 125 °C. It is seen from expressions (2)–(4) that in the welding current controller the losses in a power transistor switch and reverse diode depend on arc voltage U_a, which is continuously changed in the process of welding, in particular in MMA and MIG/MAG welding, that makes the analytical determination of losses very difficult.

Losses in power modules can be determined more precisely by a direct measurement of temperatures T_c of casings (base plates) of modules. Values T_c are also important for estimation of conformity of energy conditions of operation of power modules to the criterion of reliability by a thermal condition, i.e. maximum admissible value of temperature $T_{j\,\max}$ (usually $T_{j\,\max}$ = 125 °C) of chips (of p–n structures) of modules. Temperature of p–n structures T_j and temperature of module casing T_c are linked with a known equation

$$T_j = T_c + P_s R_{th(j\text{-}c)},$$

where $R_{th(j\text{-}c)}$ is the regulated value of thermal resistance of p–n transition–casing.

Pulsation of welding current, which is determined by the choke inductance L, influences greatly the ranges of welding current control, stability and elasticity of arc, stability of weld formation. To provide the condition of continuous current through the choke of a step-down converter it is necessary to fulfil the condition [17]

$$L_b \le R_{l\,\max}(1 - \gamma_{\min})/2f,$$

where L_b is the boundary value of choke inductance at which the condition of current continuity is provided; $R_{l\,\max}$ is the highest value of resistance of converter load; $\gamma_{\min}$ is the least value of coefficient of pulse filling.

As regards to welding current controller the condition of current continuity through the choke in a more convenient form can be expressed as

$$L_b \ge U_{a\,\max}(1 - U_{a\,\min}/U_{s\,\max})/2f\, I_{w\,\min}, \qquad (5)$$

where $U_{a\,\max}$ and $U_{a\,\min}$ are the highest and least arc voltage, respectively; $I_{w\,\min}$ is the least value of welding current in the range of its control.

The condition of current continuity should be also fulfilled at short circuits of arc gap, taking place, naturally, both at the stage of arc exciting and also in the process of welding, especially in MMA and MIG/MAG welding. Here, $U_{a\,\min}$ is tended to zero, and $(1 - U_{a\,\min}/U_{s\,\max})$ in expression (5) — to unity. Taking this into account L_b can be presented in the form

$$L_b > U_{a\,\max}/2fI_{w\,\min}. \qquad (6)$$

In real controllers of welding current the inductance of choke L exceeds the calculated value L_b by not less than 2–4 times. This is explained by the tendency to optimize the welding current pulsation $\Delta I_w = \Delta I_L = (1 - \gamma)U_a/L_f$, to limit the maximum values of collector current of IGBT-module, direct current of reverse diode and current of a buffer capacitor, and also to decrease losses in a choke core.

Current I_L, passing through the winding of choke of the welding current controller, has constant and variable components, as also in smoothing chokes of inverter power sources. In these chokes the criterion of selection of a core magnetic material is the value of saturation induction B_s, here the mass and quality of choke do not depend almost on specific losses of the magnetic material [17–19], therefore, the electrical steels are used, as a rule, in the cores of smoothing chokes and chokes of the welding current controllers at frequencies of pulsation $I_L \cong 30$ kHz. In comparison with cores from other magnetic materials (for example, permalloy, ferrite) the cores from electrical steels are most operational and economic. In addition, they provide high stability of choke inductance within the wide range of temperatures (from –60 to +120 °C).

The total losses in choke P_{SL} represent a sum of losses in its magnetic core P_m and Joule losses in winding P_{wind}. In turn, the losses P_m in the electrical steel core are the result from the sum of losses for hysteresis and losses for eddy currents P_e. As the change in magnetic induction in the choke core occurs along the narrow separate loops of hysteresis, then the losses for hysteresis are so small that they may be neglected [18, 19]. Losses for eddy currents P_e can be determined by the method of design of chokes, given in [19], according to which

$$P_e = V_{core}(b_{st}U_L)^2/12\rho_{st}(wS_{core})^2,$$

where V_{core} is the volume of core; b_{st} is the thickness of electrical steel; U_L is the effective voltage at choke; ρ_{st} is the specific electric resistance of electrical steel; w is the number of turns of choke winding; S_{core} is the active area of core cross-section.

In step-down convertor of type $U_L = (U_s - U_a)\gamma = U_a(1 - \gamma)$ the expression for determination of P_e can be as follows:

$$P_e = V_{core}[b_{st}U_a(1 - \gamma)]^2/12\rho_{st}\&(wS_{core})^2 = V_{core}[b_{st}U_a(1 - U_a/U_s)]^2/12\rho_{st}(wS_{core})^2. \qquad (7)$$

Calculations made by the method [19] taking into account (7), show that when the welding current controllers typical of chokes are used, $L \le 250$ μH, $V_{core} \le 2.8 \cdot 10^{-4}$ m^3, $S_{core} \le 1.6 \cdot 10^{-3}$ m^2, $w = 18–20$ turns, the losses for eddy current P_e do not exceed 1.4 W at $b_{st} = 0.35$ mm and 3 W at $b_{st} = 0.5$ mm. This gives an opportunity to use the sheets from cold-rolled anisotropic electrical steel (for example, of 3411, 3412, 3413, 3414 grades) having a low cost, for the choke cores.

Joule losses in winding are determined using expression

$$P_{wind} = I_L^2 R_{wind} = I_w^2 R_{wind}, \quad (8)$$

where R_{wind} is the active resistance of choke winding which is calculated by formula

$$R_{wind} = \rho_{wind} w l_{ALT} / S_{wire} = \rho_{wind} w l_{ALT} j_d / I_w,$$

where ρ_{wind} is the specific electric resistance of winding wire; I_{ALT} is the average length of winding turn; S_{wire} is the area of cross-section of winding wire; j_d is the density of current in winding wire.

The current density is calculated by known methods [17, 18], an allowable overheating being here the calculation criterion. In the most cases $j_d = 2.5–5.0$ A/mm^2 (depending on upper value of the range of welding current control), while the Joule losses $P_{wind} = 50–120$ W. Taking into account that $P_{wind} >> P_e$, the losses in choke can be considered $P_{SL} \cong P_{wind}$.

Losses in the power part of the controller include also losses in elements of input circuit, i.e. in a buffer capacitor C and thyristor VS (see Figure 1). The buffer capacitor C combines functions of a smoothing filter and energy accumulator. The necessity in the smoothing filter is stipulated mainly by an inductive nature of impedance of the controller supply circuit, that is available in MWS, and also in the secondary circuits of single-station welding rectifiers. But the requirements to the allowable level of pulsations are not strict, i.e. their level is limited only by the amplitude of a variable component of voltage allowable for the selected capacitor [20]. In addition, in multistation rectifiers (as in most industrial single-station welding rectifiers) a three-phase bridge or six-phase (binary three-phase with an equalizing reactor, circular, etc.) rectifying circuits are used, providing pulsations, even without a smoothing filter, with a maximum range of not more than 12 % of an average value of the rectified voltage. Nevertheless, the selection of capacitor for its use as a buffer capacitor, has its peculiar features coming from the specifics of its operation as an energy accumulator, that requires the use of electrolytic (aluminium, as a rule) capacitors of a high capacity. Parameters of electrolytic capacitors depend mainly on frequency and temperature. The allowable load of the electrolytic capacitors is determined by their heating and limited by the temperature of the most heated point of the capacitor T_h, determined by relation [21]

$$T_h = T_a + P_{SBC} R_{th} = T_a + (I_{BC}^2 R_{ESR}) R_{th},$$

where T_a is the temperature of ambient medium; P_{SBC} is the losses power dissipating in the capacitor; R_{th} is the generalized harmonic resistance of capacitor; I_{BC} is the effective value of capacitor current; R_{ESR} is the equivalent active resistance of capacitor in a series circuit of its replacement.

As in the step-down converter the relation $i_{BC} = i_L - I_{CA}$ (here i_{BC} — instantaneous value of current of a buffer capacitor; i_L — choke current; I_{CA} — current average value consumed by converter) for the interval of switched-on state of a power transistor switch), then the current value of buffer capacitor will be

$$I_{BC} = [1/T \int_0^{\gamma T} i_{BC}(t)^2 dt]^{0.5} = [1/T \int_0^{\gamma T} (i_{L_0} - I_{CA})^2 dt] = [\gamma(1-\gamma) I_w]^{0.5}, \quad (9)$$

and an average value of variable component of current of a buffer capacitor is equal to

$$I_{BC\,av} = 1/T \int_0^{\gamma T} i_{BC}(t) dt = \gamma(1-\gamma) I_w. \quad (10)$$

In arc welding, in most cases $0.18 \le \gamma \le 0.50$, due to which the component $(\gamma)^{0.5}(1-\gamma)$ in expression (9) can be assumed equal to 0.365 with a sufficient accuracy for practical calculations. This allows calculated value of the losses power dissipating in a buffer capacitor to be determined with an error of not more than 10 % by an approximated formula

$$P_{SBC} \approx 0.1332 I_w^2 R_{ESR}. \quad (11)$$

Change in voltage (range of pulsations) at a buffer capacitor ΔU_{BC} relative an average value of voltage at capacitor U_{s_0} can be determined from expression

$$\Delta U_{DC} = 2\Delta Q / C_b = 2[1/C_b \int_0^{\gamma T} i_{BC}(t) dt] = 2\gamma(1-\gamma) I_w / C_b f, \quad (12)$$

where ΔQ is the amount of electricity stored by a buffer capacitor in charge and equal to amount of electricity at its discharge; C_b is the capacity of a buffer capacitor.

Taking into account (12) the coefficient of voltage pulsations at the capacitor is

$$k_p = \Delta U_{BC} / U_{s_0} = 2\gamma(1-\gamma) I_w / C_b f U_{s_0} = 2\gamma^2(1-\gamma) I_w / C_b f U_a. \quad (13)$$

Analysis of expressions (12) and (13) and reference data for parameters of electrolytic capacitors showed that at $I_w \le 400$ A and $\gamma \le 0.5$ the capacity

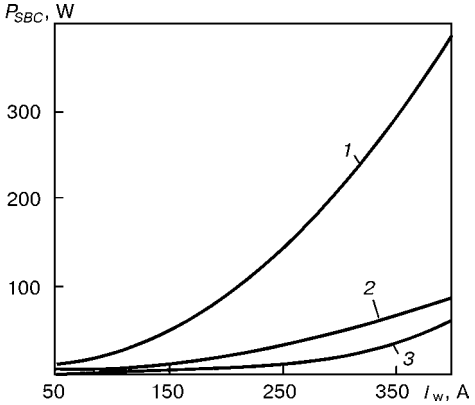

Figure 7. Dependence of power of active losses in buffer capacitor P_{SBC} on welding current at f = 16 kHz and R_{ESR} = 4 mOhm (at T = 20 °C): *1* — T_a = –20; *2* — T_a = 20; 3 — T_a = 50 °C

of a buffer capacitor of not more than $27 \cdot 10^3$ μF is sufficient to provide the level of voltage pulsations, not exceeding the allowable level. However, in real welding current controllers it is by 1.2–2.5 times higher that is caused by the necessity in fulfillment of requirements for maximum allowable values of long-passing current through the capacitor and temperature of the most heated point of the capacitor. The best combination of parameters is typical of capacitors manufactured by companies «Evox Rifa», «Philips», «BHC Aerovox», «Elekond» for their application as buffer capacitors.

Figure 7 shows curves of dependence of the losses power in capacitor PEH200PT533OM of $33 \cdot 10^3$ μF capacity on welding current and ambient temperature, obtained from data of «Evox Rifa» [22] with account for (11).

Limiting of charge current amplitude of a discharged buffer capacitor is realized by its «soft» charge using a circuit containing diode *VD1* and current-limiting resistor *R* (see Figure 1) which, after charge completion, is shunted by a thyristor *VS*. In a steady condition the thyristor *VS* plays a role of a cut-off diode whose presence almost eliminates the mutual effect of input circuits of controllers on each other during their simultaneous operation. Power loss at thyristor *VS* can be determined from expression

$$P_{SVS} = U_{FVS} I_{TVS} = U_{FVS} \gamma I_w = \\ = U_{FVS} (U_a / U_{s_0}) I_w, \qquad (14)$$

where U_{FVS} is the drop of direct voltage at thyristor; I_{TVS} is the direct current passing through thyristor.

Total losses in power P_{TOT} in the welding current controller represents a sum of losses in all its units. Taking into account (1), (2), (4), (8), (9) and (14)

$$P_{TOT} = f (0.5 C_s U_s^2 + E_{SW(on)} + E_{SW(off)}) + \\ + I_w [U_{CE} \gamma^{0.5} + U_f (1 - \gamma)^{0.5} + \gamma U_{FVS}] + \\ + I_w^2 [R_{wind} + \gamma (1 - \gamma)^2 R_{ESR}] + P_{CS}, \qquad (15)$$

where P_{CS} is the power consumed by the controller control system.

Hence, the expression for determination of the welding current controller efficiency factor η can be presented in the form

$$U_a I_w = \eta f (0.5 C_s U_s^2 + E_{SW(on)} + E_{SW(off)}) + \\ + \eta I_w \left[U_a + U_{CE} \left(\frac{U_a}{U_s} \right)^{0.5} + U_f \left(1 - \frac{U_a}{U_s} \right)^{0.5} + \frac{U_a}{U_s} U_{FVS} \right] + \\ + \eta I_w^2 \left[R_{wind} + \frac{U_a}{U_s} \left(1 - \frac{U_a}{U_s} \right)^2 R_{ESR} \right] + \eta P_{CS}. \qquad (16)$$

It is seen from (16) that one of factors influencing the controller efficiency factor is the frequency of transformation. In the range of 10–20 kHz the losses related to the frequency of transformation are 20–45 % of total losses in the controller. Taking this into account, in the welding current controllers made using IGBT-modules, f = 16–18 kHz, the real attainable values of the efficiency factor are 84–90 %, and the total efficiency factor of MWS (without account for losses in busbars) is 75–81 %.

Welding-technological properties of the welding current controllers are determined mainly by structure and characteristics of their control systems (CS).

The main part of CS is a control path, which includes (see Figure 1) a *PWM*, controller of welding cycle, welding current sensor (*CS*) and voltage sensor (*VS*). The latter is included into the control path mainly in case of MMA and MIG/MAG welding. As to the configuration, functional purpose of separate units and scheme the control path is similar to the main part of CS of inverter power sources in which *PWM* is used as a method of a pulsed control. The preference of use of this method in the welding current controllers is stipulated by the fact that in converters with a *PWM* the frequency of switching a power transistor switch and, consequently, the frequency of load current pulsations, is constant in the process of control, here the range of pulsations determined by the choke inductance can be of any small value [17, 23, 24]. This gives an opportunity not only to optimize the choke and buffer capacitor parameters, but also to provide premises both for the effective arc exciting at the initial stage of the welding process and also to maintain a stable arc discharge at low values of welding current, that is very important in case of TIG process.

The controller of welding cycle forms all the necessary time intervals and signals of presetting parameters of the controller VAC, corresponding to each stage of the welding process, and also the control signals of shielding gas feeding in cases of TIG and MIG/MAG welding.

In MMA and MIG/MAG welding (see Figure 1, *a*) signals, proportional to current and voltage of welding, enter the information inputs of the controller from *CS* and *VS*. As a result of processing and transformation of these signals and a signal of welding current setting in the controller, a signal of welding current presetting is generated, corresponding to a current stage of melting or electrode metal transfer. In a final form a signal of welding current presetting

is supplied from the controller output to the control input of a *PWM* whose information input is connected to a *CS*.

Vertical («pin») VAC in the controllers for TIG welding are provided by using a deep negative current feedback (see Figure 1, *b*). In this case a signal, proportional to the signal of welding current setting, enters a control input of a *PWM* from a controller output, and a FB_c signal enters an information input.

Except units of control path the CS of controllers includes an input block and supply block. The input block controls the process of a «soft» charge of a buffer capacitor *C*, forms pulses for thyristor *VS* control and provides protection of the controller from disturbance of polarity of input voltage and inadmissible its values. In addition, the input block includes executive elements of the CS units, providing controller protection from current overloads in welding circuit, overheating of power semiconductor devices, and in MMA and MIG/MAG welding protects also from short circuits in load, whose duration exceeds the preset values. In operation of executive elements of protection, the power part of the controller is deenergized with the help of an input commutating device *KD*, for example, contactor.

Functional units of CS, in particular a welding cycle controller and *PWM*, can be manufactured on analog or digital base, including also the use of microprocessors [25]. The detailed description of CS and its units will be not given in this article. Analysis and scheme of CS in high-frequency converters were presented in some works, including reviews [12, 14]. It should be noted that the welding controllers with CS structures given in Figure 1 provide the following: high quick-response of control path; formation of optimized static and dynamic VAC within the range of welding current control; reliable arc exciting and its steady burning in all spatial positions and in all technologically-grounded range of arc length; favourable transfer of electrode metal (in MMA and MIG/MAG welding); realization of a preset welding cycle and its elements (smooth increment and smooth drop of welding current at the initial and final stages of the welding process in TIG, «hot» start in MMA welding and so on); stability of preset welding condition parameters at external disturbances; feasibility of realization of welding condition with a modulated current.

Welding current controllers RDG-166U3.1 (for TIG welding) and RDE-206U3.1 (for MMA welding), developed at the PWI, possess most of abovementioned welding-technological properties, that is confirmed by the experience of their industrial service, in particular on objects of nuclear power engineering. The application of controller RDG-166U3.1 could increase significantly the quality of weld formation, especially root welds, in welding with and without the filler wire (mainly with use of modulated-current conditions) of position welds with V- and U-shaped edge preparation of pipelines and fittings of main equipment of power units of NPS, almost eliminate the formation of «shrinkage cavities» in welding of pipelines from austenitic steels, decrease the heat input into the parent metal. In MMA welding with use of RDE-206U3.1 controllers a spray transfer of electrode metal, quality weld formation in welding with a short and limiting too short arc using electrodes with any type of coating are provided. The welding with austenitic electrodes and electrodes designed for welding dissimilar steels becomes easier. In MMA welding with modulated current the welding efficiency in positions, different from flat, is increased by 25–40 %, the primary grain of weld metal is refined, mechanical properties of welded joints are improved, welding of root weld becomes easier, including in welding with a large gap, and, as a result, a quality formation of a back bead is attained.

Realization of advantages of MWS with electronic controllers of welding current can be realized in two ways. One of them includes the optimizing of power and operating voltage of the multistation rectifier, and also section of line (radial) busbars depending on the preset number of welding stations, while another way is the improvement of effectiveness of use of multistation rectifiers being in service.

The Table gives comparative characteristics of load capacity of the most widely used multistation rectifiers with use of the ballast rheostats and electronic controllers of welding current, here the welding current is taken equal to 200 A, duty cycle is 60 % and the coefficient of simultaneous operation of stations $K_s = 0.65$.

Equipping of operating MWS with electronic controllers of welding current makes it possible not only to increase the number of operating welding stations, but also to decrease significantly (by 1.8–2.7 times) the section of wires connecting each welding station to a line busbar. The noticeable advantage in mass of

Comparative characteristics of load capacities of multistation rectifiers

Parameter	*VDM-1001*	*VDM-1601*	*VMG-5000*
Rated welding current of rectifier, A	1000	1600	5000
Rated operating voltage, V	60	60	60
Primary power, kV·A	74	120	317
Number of MMA/TIG welding stations:			
in variant of ballast rheostats	10/10	16/16	50/50
in variant of electron controllers of welding current	18/27	28/44	90/140

connecting wires can be obtained when a radial scheme of MWS is used.

CONCLUSIONS

1. As to indices of energy consumption and material-content the MWS with electronic controllers meet the modern requirements for the welding equipment concerning energy- and resources-saving.

2. Multistation welding systems with electronic controllers are characterized by the same welding-technological characteristics as the high-quality single-station power sources of inverter type.

3. The wide industrial application of MWS with electronic controllers of welding current will improve greatly the technical-economical indices of welding manufacturing in different branches of industry.

1. Lebedev, V.K., Medvedenko, N.P., Zaruba, I.I. (1967) Analysis of multistation power supply system for CO_2 welding. *Avtomatich. Svarka*, **10**, 40–44.
2. Lebedev, V.K., Zaruba, I.I., Andreev, V.V. (1973) Centralised power supply of CO_2 welding sets. *Ibid.*, **3**, 62–64.
3. Bunkin, P.Ya., Donskoj, A.V. (1985) *Multistation welding systems*. Leningrad: Sudostroenie.
4. Koshkarev, B.T., Milovanov, K.A., Losev, V.G. et al. (1974) Cost efficiency of multistation CO_2 welding. *Svarochn. Proizvodstvo*, **2**, 38–40.
5. (1986) *Arc welding equipment*. Refer. Book. Ed. by V.V. Smirnov. Leningrad: Energoatomizdat.
6. Lebedev, V.K., Zaruba, I.I., Medvedenko, N.P. et al. *Multistation power supply system for electric arc welding*. USSR author's cert. 274280, Int. Cl. B 23 K 9/00. Publ. 24.06.70.
7. Andreev, V.V., Zaruba, I.I., Zislin, G.S. (1987) Selection of open-circuit voltage of multistation systems. *Avtomatich. Svarka*, **10**, 61–64.
8. Zaruba, I.I., Sidorenko, M.N., Bargamen, V.P. et al. (1983) Non-linear control of CO_2 welding conditions in multistation power supply system. *Ibid.*, **3**, 66–69.
9. Oseledko, V.G., Kagansky, B.A. *Welding current control device*. USSR author's cert. 206777, Int. Cl. B 23 K 9/00. Publ. 08.12.67.
10. Drabovich, Yu.I., Lebedev, A.V., Krachenko, V.V. et al. (1987) Control of mechanised CO_2 welding conditions using multistation current supplies. *Avtomatich. Svarka*, **10**, 70–71.
11. Paton, B.E., Lebedev, A.V. (1988) Control of fusion and electrode metal transfer in CO_2 welding. *Ibid.*, **11**, 1–5.
12. Gladkov, E.A., Fetisov, G.P., Sinelnikov, N.G. (1984) Improvement of arc welding processes on the base of high-frequency energy converters (Review). *Svarochn. Proizvodstvo*, **3**, 13–16.
13. Artyomenko, M.E., Krishtafovich, I.A., Sinitsina, I.Z. (1991) *Current methods of analysis of energy processes in transistorised voltage converters*. Kyiv: Institute of Electrodynamics.
14. Vereshchago, E.N., Kvasnitsky, V.F., Miroshnichenko, L.N. et al. (2000) *Circuit technique of inverter power supplies for arc welding*. Refer. Book. Nikolaev: UMGTU.
15. (1995) *Power semiconductors*. Ed. by V.V. Tokarev. Voronezh: Elist.
16. (1997) *Manual on application of bipolar transistors with isolated gate (IGBT) and «intelligent» power modules (IPM) of third generation*. Ed. by V.A. Pavlovsky. Kyiv.
17. Moin, V.V., Laptev, N.N. (1972) *Stabilised transistor converters*. Moscow: Energiya.
18. Gorsky, A.N., Rusin, Yu.S., Ivanov, N.R. et al. (1988) *Calculation of electromagnetic elements of secondary power sources*. Moscow: Radio i Svyaz.
19. Pentegov, I.V., Meshcheryak, S.N., Turty, M.V. et al. (1997) Calculation procedure of input and output filter choke of welding inverter power sources using standard magnetic core. *Avtomatich. Svarka*, **4**, 34–39.
20. Bas, A.A., Milovzorov, V.P., Musolin, A.K. (1987) *Secondary power sources with transformer-less input*. Moscow: Radio i Svyaz.
21. Anufriev, Yu.A., Gusev, V.N., Smirnov, V.F. (1976) *Service characteristics and reliability of electric capacitors*. Moscow: Energiya.
22. (1999–2000) *Electrolytic capacitors: Production catalog*. Evox Rifa.
23. (1986) Power supplies. *Electronic Eng.*, **733**, 52–58.
24. Romash, E.M. (1981) *Secondary power supplies of radioelectronics*. Moscow: Radio i Svyaz.
25. (2000) *Welding equipment: Production catalog. Bester SA*. Bielan.

In connection with the 90th birth anniversary of a prominent scientist in the field of welding metallurgy of non-ferrous metals, Prof. Daniil M. Rabkin, Dr. of Sci. (Eng.), Honoured Scientist of the Ukr. SSR, winner of Evgeny Paton Prize and 40th anniversary of the Department for Physical-Metallurgical Processes of Welding Light Metals and Alloys, which was led by D. Rabkin from 1962 till 1987, the Editorial Board presents to the readers a subject-oriented selection of papers by the staff members of the Department, which is now headed by Prof. Anatoly Ya. Ishchenko, Dr. of Sci. (Eng.), Corresp.-Member of the NAS of Ukraine. These papers set forth the stages and state-of-the-art of investigation and development of the current problems of welding aluminium alloys. Results of experimental studies of physical and metallurgical phenomena, proceeding in arc and electron beam welding, procedural features of new processes of fusion welding, metals science issues, concerning the weldability of high-strength aluminium alloys are considered, as well as mechanical properties of welded joints of advanced aluminium alloys under different conditions of service.

Editorial Board

INVESTIGATION AND DEVELOPMENT OF THE TECHNOLOGY OF LIGHT ALLOY WELDING AT THE PWI

A.Ya. ISHCHENKO
The E.O. Paton Electric Welding Institute, NASU, Kyiv, Ukraine

Key words: *aluminium alloys, welding, directions of investigations, developed technologies*

Aluminium and complex alloys and composites on its base are extensively applied in modern mechanical engineering. They enable the progress in many sectors of industry, mainly vehicle construction, where high-strength light materials are used particularly effectively.

In Ukraine, as in other industrialised countries, it is intended to increase the volumes of output of aluminium and its high-strength alloys in the form of wrought semi-finished products, required to produce railway passenger cars, automobiles and lorries, buses, aircraft, products for aerospace, chemical, medical and food industry, as well as in construction.

Considerable difficulties, arising in fusion welding of high-strength aluminium alloys, should be noted, which are related to the high chemical activity of the components in the alloy composition. Interaction with oxygen and susceptibility to hydrogen absorption lead to coarse oxide films and porosity in welds. The strongest alloys are prone to hot cracking and softening in fusion welding. These features are clearly manifested, when using advanced high-performance Al–Li alloys, which, due to their low density and increased rigidity modulus, allow reducing the structure weight by 10 to 15 %, and increasing the tonnage of passenger and transport aircraft and other vehicle, respectively.

Requirements currently made of materials and technologies of their welding are increasing continuously. Therefore, the PWI directorship is constantly encouraging research and development of more effective technologies, equipment, welding consumables for fabrication of light alloy structures. Specialised Department for Physical-Metallurgical Processes of Welding Light Metals and Alloys, established at the PWI, has made a significant contribution over the 40 years of its activity to solving urgent problems of welding science and technology. In particular, characteristics of weldability of certain alloys have been improved, advanced welding consumables have been developed, including efficient filler wires, containing zirconium and scandium, rational designs of weldments have been created, and arc and electron beam welding technologies and the required equipment have been developed. All this provided the high quality of welded joints, reliability of their performance, and promoted a higher efficiency of welding and reduced metal content of the products.

The first Department Head in the period from 1962 to 1987 was Daniil M. Rabkin, Dr. of Sci. (Eng.), Professor, Honoured Scientist of the Ukr. SSR. The main directions of investigations, performed by the Department, included studying the weldability of aluminium and magnesium alloys, development of the technology of welding various-purpose structures, including development of specialised equipment and welding consumables. Scientific-engi-

neering developments of the Department have been extensively introduced in many mechanical engineering enterprises in fabrication of boilers, railway tank cars and stationary tanks, equipment for chemical production and food industry, metro cars, high-speed railway cars, lorries and dump trucks, aircraft and aerospace products, as well as in repair of agricultural machinery and motor vehicles.

At present highly-qualified experts in the field of metallurgy and metals science, technology of welding light alloys and metal composites are using up-to-date welding and research equipment to conduct research for solving such problems as:

- weldability of advanced structural materials, based on aluminium and magnesium, when using various processes; Al-matrix composites and dissimilar materials;
- nature of hot welding cracks and development of methods of their prevention in welding of advanced high-strength complex alloys, including aluminium and magnesium alloys, containing lithium;
- interaction of weld pool with gases, development of methods of degassing of molten metal and evaluation of the influence of porosity in welded joints on their performance;
- structural transformations in the weld and HAZ, their influence on joint properties;
- improvement of the characteristics of strength and reliability of welded joints under different conditions of service.

Among the main technological developments, the following most efficient welding processes and examples of their application in fabrication of structures for various purposes should be noted:

- non-consumable electrode impulse-arc welding of Al–Li and other high-strength light alloys of different alloying systems, as applied to manufacture of critical items. The technology improves weld quality and increases their strength by 10–15 %;
- consumable electrode impulse-arc welding of sheet structures (1–4 mm) for manufacture and repair of boats, launches, ship superstructures, equipment for food and chemical industry, tank-cars, pipelines, etc. Technology provides a high efficiency of the process, lower distortion of structures and cost of welding;
- electroslag welding of components of aluminium busbars and blanks of a large cross-section (50 to 200 mm thick) under stationary conditions and in site. Electric resistance in the joint zone does not exceed that of the base metal and is characterised by a high stability;
- electron beam welding and surfacing of aluminium alloys to manufacture large-sized shells and tanks, stringer panels for construction of ships, aircraft, rockets and space products, structures of heat exchange apparatuses, pistons with cooling cavities and strengthened ring groves, and household appliances. Technology provides a high quality and stability of mechanical properties of permanent joints 0.5 to 350 mm thick;
- joining by different processes the dissimilar metals (aluminium and its alloys to steels, copper and other metals), Al-matrix composite materials, reinforced by fibres (steel, silicon carbide, carbon and boron) and disperse particles (oxides, carbide, intermetallics). Technologies of welding and brazing such materials are used in shipbuilding, automotive, aerospace industry and electric engineering.

Work is being performed now to develop welding wires (fillers), containing highly effective modifiers (titanium, zirconium, scandium), which provide high processing and strength properties of aluminium alloy joints. Effective stick aluminium electrodes of UANA series have been developed for repair welding and surfacing of parts and structures of wrought and cast aluminium alloys. Composition of flux coatings and technology of manufacturing the developed electrodes give them the welding-processing properties on a par with the best foreign analogs.

The Department regularly provides consultations and argumented expert's opinions, performs expert analysis of the projects of welded structures in terms of their adaptability to fabrication, conducts training and probation of specialists, directly participates in setting up fabrication of light-alloy products in industrial enterprises.

The best original developments of the staff of the Department for Physical-Metallurgical Processes of Welding Light Metals and Alloys are being continuously realized in the form of contracts and competitive projects, have been rewarded with numerous author's certificates for invention (more than 200), and four State Prizes.

DEVELOPMENT OF METHODS FOR ARC WELDING OF ALUMINIUM AND ITS ALLOYS

I.V. DOVBISHCHENKO and **B.A. STEBLOVSKY**
The E.O. Paton Electric Welding Institute, NASU, Kyiv, Ukraine

History of development and upgrading of methods and technologies for arc welding of aluminium and its alloys by the Department for Physical-Metallurgical Processes of Welding Light Metals and Alloys at the E.O. Paton Electric Welding Institute is described. The role of the Institute in mastering the technologies for welding specific parts is noted.

Key words: *aluminium alloys, semi-submerged arc welding, inert gases, fluxes, covered electrodes, tungsten electrodes, welding equipment*

Research and development in the field of welding aluminium and its alloys were initiated at the PWI in 1951 under the leadership of Prof. Daniil M. Rabkin from the Laboratory for welding non-ferrous metals and alloys, which was transformed into a Department for Physical-Metallurgical Processes of Welding Light Metals and Alloys in 1962. It was the demand of the time to arrange within very short terms the flow-line production of 18–20 mm thick tanks of alloy AMts for transportation and storage of liquid oxygen used in rocket complexes.

In 1951–1952 Prof. Rabkin developed a new method for automatic semi-submerged single-arc welding (over the flux layer) and flux of the AN-A1 grade [1]. This method differed from the known method of SAW of steel in the application of a thin flux layer ahead of the arc. The involved welding equipment, i.e. tractor TS-17 and head ABS, was upgraded. In 1952–1953 the process was mastered by Uralvagonzavod Factory (Nizhny Tagil, Russia) [2], where it was in application for more than 30 years. This welding method provided not only the required quality of the weld metal and mechanical properties of the joints, but also a high productivity of the process. Butt joints were welded on two sides without groove preparation at a speed of 15–16 m/h.

The attempts made at that time by the Factory to use inert-gas welding failed to give positive results, because a joint in metal 18–20 mm thick had to be made in several passes into the groove, and a thorough preparation of surfaces of weld edges and wire was required (in contrast to semi-SAW). In addition, a high-purity argon and, moreover, helium were scarce and expensive. Imperfection of the equipment of that time also mattered.

Improvements in the semi-SAW method were done in 1956–1959. Participating in the efforts were M.L. Zvonkov, B.A. Steblovsky, I.V. Dovbishchenko and M.P. Poritsky. The technology for split-electrode welding with a common current conductor connected to both wires (two-electrode welding) [3] was developed for metal 12–22 mm thick, which enabled the first internal welds, i.e. longitudinal and girth ones, to be made on the flux backing, and then the external welds to be made without a backing. That made it unnecessary to locate heavy steel backings inside a boiler and reduced requirements for assembly operations.

In the second half of the 1950s–early in the 1960s the method of automatic semi-SAW over the layer of flux of the AN-A1 grade was taking the key position in mass production of stationary aluminium vessels with a capacity of 2 to 100 m^3 at the «Bolshevik» (Kyiv), «Krasny Oktyabr» (Fastov), Sumy Machine-Building and a number of other factories [4, 5], as well as tank-wagon boilers at the Mariupol Production Amalgamation «Azovmash» [6]. Boilers and vessels were intended for storage and transportation of food and chemical products, such as water, milk, nitric acid, rocket fuel, etc. This method was employed to make joints on aluminium busbars. The Kyznetsk Metalwork Factory manufactured a unique ventilation pipe from alloy AMts with a diameter of 6 mm and 100 m high [7]. The PWI developed specialised equipment, i.e. tractors TS-31, TS-33 and TS-36, as well as suspended device A-586, for automatic semi-SAW.

Flux of the AN-A4 grade and electrodes AN-A103 were developed for mechanised and manual arc welding of low-alloy Al–Mg alloys. The flux and electrodes provided joints on alloys AMg3 and AMg5 with strength not less than 85–90 % of that of the base metal [8].

On this basis the PWI has developed in the last years new electrodes of the UANA series [9], intended for welding and surfacing of parts and structures from a wide range of wrought and cast aluminium alloys. Composition of a covering and technology for the manufacture of electrodes provided their welding-technological properties at a level of the best foreign analogues.

In the 1960s–1970s aluminium alloys were finding an increasingly wide application in rocket-space engineering, ship, tank and car building, chemical engineering, construction and other industries.

The attempts to use semi-SAW for high-alloyed aluminium alloys failed to yield positive results, as the required quality of the welds and necessary properties of the joints could not be achieved in this case. Welding metal more than 18–20 mm thick led to an increased risk of formation of slag inclusions in the welds and more stringent requirements for adherence to the specified sanitary-hygienic labour conditions. These circumstances intensified the development and improvement activities in the field of efficient meth-

ods and technologies for inert gas and electron beam welding. The efforts in these areas were performed in parallel, which allowed a flexible selection of different variants of technologies, depending upon the requirements to parts, their manufacture and service conditions.

TIG welding in argon atmosphere at the alternating current of the sinusoidal waveform took the leading position at the end of the 1950s–early 1960s among other methods of inert-gas welding of aluminium alloys. It provided better quality of the weld metal and higher mechanical properties of welded joints, compared with MIG welding. However, the penetrating power of the arc was limited by an insufficient life of thoriated tungsten electrodes. Automatic welding of metal 8–10 mm thick had to be performed with bevelled edges in several passes.

Collaborative research with the Moscow Plant for Electric Vacuum Devices, carried out from the beginning of the 1960s by D.M. Rabkin and O.N. Ivanova, resulted in production of the radiation-safe activated tungsten electrodes with an addition of up to 1.5–2.0 % lanthanum oxide (EVL) and up to 3.5 % yttrium oxide (EVI) [10]. The electrodes were made in compliance with GOST 23949–80. Later investigations conducted with participation of B.A. Steblovsky and V.P. Budnik made it possible to identify permissible values of the direct and alternating currents depending upon the grade and diameter of an electrode. The positive effect exerted by an activated addition is more pronounced in welding at the DCRP and at the AC with a bias to straight polarity [11].

The EVL electrodes are not inferior to the thoriated ones in consumption and acceptable density of the current, and they are widely applied for manual and automatic AC and DC welding. Electrodes with the yttrium oxide addition enabled the power density in the arc to be increased by a factor of 1.5–2 without a risk to overheat the electrodes, and provided a substantial rise in the efficiency of melting of metal welded. The electrodes with the yttrium oxide addition, 10 mm in diameter, made it possible to weld aluminium alloys 18–20 mm thick in single pass using the one-phase high-amperage arc (up to 900–1000 A) and those 30–40 mm thick using the three-phase arc. The corresponding welding equipment was developed. The field of application of TIG welding was substantially widened. By the middle of the 1960s the technology for automatic high-amperage arc welding of AMg6 (Al-6.2Mg) carrier rocket casing parts had been mastered in association with the staff of the Kujbyshev Factory «Progress», Assembly-Testing Complex in Bajkonur, Dnepropetrovsk Yuzhy Machine-Building Plant, etc.

Commercial experience in the fabrication of critical-application structures from alloy AMg6 showed that welds might have inadmissible oxide film inclusions, despite strict adherence to specifications for metal preparation and TIG welding technology. The idea of intensified stirring of the weld pool metal to refine oxide inclusions and, at the same time, to degas the weld pool was realised in TIG pulsed-arc welding. The work in this area was initiated late in the 1960s by D.M. Rabkin, N.M. Voropaj and V.A. Mishenkov [12, 13]. Experimental asymmetric-current sources of the OARS type were built.

Further investigations into the process of the pulsed force effect of the arc on the weld pool of aluminium alloys, conducted by A.Ya. Ishchenko, A.G. Chayun, R.V. Ilyushenko and A.G. Poklyatsky [14, 15], made it possible to identify the effective fields of its application and build specialised welding equipment (sources I-126 and I-160).

The relative length of oxide film inclusions in the welds on alloy AMg6 and the probability of formation of such extended inclusions in the welds on Li-containing aluminium alloys 1420 and 1460 were decreased 3 times as a result of variations in amplitude values of the straight- and reverse-polarity currents (asymmetric current). Large amplitude gradients during the pulse and pause periods (modulated current) provide decrease of 7–10 times in the total content of cavities in welded joints on alloys 1420 and 1460 [16].

The use of heat-hardening and cold-worked aluminium alloys required application of welding methods with the concentrated heat sources to ensure the sufficient penetration depth at a comparatively low heat input. Such arc welding methods include microplasma welding [17], AC plasma-arc welding, DC TIG welding in helium and MIG welding.

Studies conducted by I.V. Dovbishchenko, A.G. Poklyatsky, A.P. Zaparovany, et al. showed the efficiency of using the alternating asymmetric square-wave current for plasma-arc welding of aluminium alloys [18]. The time of the reverse-polarity current flow sufficient for cathodic cleaning of the metal surface is 25–30 % of the total cycle, which leads to decrease in load on the tungsten electrode. Deeper penetration of base metal is achieved during the straight polarity periods. This results in increase in the welding speed, decrease in heat input, weight and dimensions of the plasmatron. The possibility of formation of the weld back surface using no backing with through penetration by the arc provides escape of oxide films not destroyed by the arc to the back surface of the weld and removal of gases from molten metal. The experimental power supply I-196 and plasmatron PD-154 were developed.

Scientific and technological studies aimed at development of equipment, control devices and technology for TIG welding in helium atmosphere at the DCSP, i.e. helium-arc welding, date to the beginning of the 1970s (D.M. Rabkin, O.N. Ivanova, V.P. Budnik, B.A. Steblovsky).

The higher concentration of heat load in helium-arc welding, compared with AC TIG welding in argon atmosphere, leads to increase in the penetrating power of the arc, decrease of 1.5–2 times in heat input and a corresponding reduction in the HAZ of heat-treated alloys [19, 20].

These factors determined a wide commercial application of the process in aerospace engineering for the fabrication of structures from aluminium alloys AMg6 and 1201, including the «Energiya» complex components and the «Buran» orbital plane cabin (Figure 1). This technology is still in use.

Figure 1. Orbital plane «Buran»

MIG welding, in contrast to TIG welding, is less sensitive to sizes of the gap and over-thickness of the metals joined. Also, it provides a higher welding speed and an insignificant level of residual strains in the joints. Nevertheless, the inconsistent quality of the welds produced by stationary-arc welding in argon limited the application of this method to fillet and overlap joints, where it is convenient [21].

Development of pulsed-arc MIG welding [22] by the PWI was a major achievement in the field of fusion welding. Technological studies of the process of pulsed-arc welding using the pioneering pulsed current generators IIP-1 [23] and then other power supplies [24], conducted by such associates of the Department as B.A. Steblovsky, M.P. Pashulya, V.G. Ignatiev et al., allowed advantages of this process for welding aluminium alloys to be identified. In addition to increase in arc stability, the process provided an appreciable decrease in metal spattering and evaporation of volatile elements, as well as reduction in quantity and sizes of oxide inclusions and pores in the welds.

Owing to these advantages, pulsed-arc MIG welding found an increasing commercial application from the middle of the 1960s. It was employed for the fabrication of casing structures of rocket complexes at the Kujbyshev and Orenburg factories, casings of landing tanks at the Volgograd Factory, assemblies of railway coach cars [25] (Figure 2) and metro cars [26], dump truck platforms [27] (Figure 3), refrigerated trucks, ship superstructures, building structures and other items.

Figure 3. Dump truck MAZ-5551

High requirements imposed on welded joints in the AMtsS and commercial aluminium tanks 20–30 mm thick for storage and transportation of aggressive chemicals led to the development of a high-efficiency technology for MIG welding using the stationary arc and 3–4 mm diameter metal electrode in a mixture of inert gases, i.e. argon and helium (D.M. Rabkin, I.V. Dovbishchenko V.S. Bugaj and V.S. Mashin). The use of the helium-argon mixtures made it possible not only to decrease 2–8 times the amount of cavities in the deposited metal, improve mechanical properties and corrosion resistance of welded joints, but also raise the welding speed by 40–60 % [28, 29].

This technology was successfully applied for the fabrication of tanks from alloy AMtsS at the Balashikha Production Amalgamation «Kriogenmash» [30], mass production of aluminium tank-wagon boilers [31] (Figure 4) and casing elements of rockets from alloy AMg6 [32] at the Production Amalgamation «Azovmash». MIG welding using the 3 mm diameter metal electrode in argon was applied at the Kurgan Machine-Building Factory for the fabrication of armoured personnel carrier bodies from aluminium armour [33] (Figure 5).

Gas mixtures used in pulsed-arc MIG welding with the 1.0–1.6 mm diameter metal electrode made it possible to achieve a higher level of mechanical properties of the joints on Al–Li alloys, compared with pulsed-current TIG welding [34].

B.A. Steblovsky, V.I. Zaviryukha and Yu.A. Ryabets developed the technology of pulsed- and station-

Figure 2. Advance section of the high-speed electric train ER-200

Figure 4. Tank-wagon for transportation of aggressive chemicals

Figure 5. Armoured personnel carrier

ary-arc narrow-gap MIG welding in helium or its mixtures with argon for joining thick-walled structures (δ_{met} = 40–150 mm) from plates and shaped profiles of alloys AMg6 and 1201. This method allows the joints to be made in flat positions and on a vertical plane. Compared with welding into a wide X-shaped groove, narrow-gap MIG welding allows the number of passes to be reduced several times, the HAZ to be decreased from 4 to 6 times, the level of residual strains to be lowered and welding consumables and power to be saved [35]. The process found application for the experimental-commercial manufacture of assemblies of rocket casings at the «Progress» Factory and armoured personnel carrier bodies at the Kurgan Machine-Building Factory [33].

Costs of welding operations can be reduced through replacing helium as a shielding gas by finished helium-neon mixtures (3–25 % Ne) produced in Ukraine [36]. The price of 1 m^3 of such mixtures is 25 % lower on the average than that of pure helium.

The PWI developed the MIG welding equipment, such as suspended self-propelled devices A-1002, A-1431, automatic devices of the AD-238 series, welding tractors A-1012 and TS-56, unit UD-474 for welding the AMg6 alloy formed-welded roll structures for armoured personnel carriers, semi-automatic devices PSh-128, PSh-144, etc.

At present the Department is involved in research and development aimed at the combined use of two or more heat sources, including laser beam, to raise the process productivity and improve the quality of the joints.

1. Rabkin, D.M. (1953) New process for automatic welding of aluminium. *Avtomatich. Svarka*, **4**, 45–50.
2. Rabkin, D.M. (1955) Automatic welding of aluminium and its alloys. *Visnyk AN Ukr. SSR*, **7**, 41–44.
3. Rabkin, D.M., Zvonkov, M.L. (1958) Automatic double electrode welding of aluminium. *Avtomatich. Svarka*, **5**, 25–31.
4. Rabkin, D.M. (1958) Automatic welding of boilers from aluminium and its alloys. In: *Advanced sci.-techn. and industrial experience*, Issue 1.
5. Dovbishchenko, I.V., Sventsinsky, V.G. (1958) Experience in automatic welding of aluminium vessels with a capacity of 2 m^3. *Avtomatich. Svarka*, **8**, 89–92.
6. Antonets, D.P., Dovzhenko, A.F. (1965) Continuous production line for manufacture of aluminium tanks. *Ibid.*, **2**, 64–66.
7. Poritsky, M.P., Steblovsky, B.A., Narodnitsky, B.I. (1965) Experience in welding of aluminium ventilation pipe. *Ibid.*, **1**, 61–63.
8. Rabkin, D.M., Zvonkov, M.L., Verchenko, V.A. (1958) Experience of production of welded tanks from aluminium-magnesium alloys. *Ibid.*, **4**, 84–88.
9. Skorina, N.V., Mashin, V.S. (2000) Covered electrodes for manual arc welding of aluminium and its alloys. *Svarshchik*, **2**, 26.
10. Rabkin, D.M., Ivanova, O.N., Ipatova, S.I. et al. (1964) Influence of addition of oxides of some rare and rare-earth metals on properties of tungsten electrodes. *Avtomatich. Svarka*, **4**, 5–9.
11. Ivanova, O.N., Rabkin, D.M., Budnik, V.P. (1972) Admissible values of current in TIG welding. *Ibid.*, **11**, 38–40.
12. Rabkin, D.M., Voropaj, N.M., Mishenkov, V.A. (1968) Argon-arc welding of aluminium alloys with a square-wave alternating current. *Ibid.*, **7**, 74–75.
13. Rabkin, D.M., Voropaj, N.M., Mishchenko, V.A. (1978) Energy characteristics of welding process with asymmetric different-polarity current. *Ibid.*, **4**, 5–10.
14. Ishchenko, A.Ya., Chayun, A.G., Ilyushenko, R.V. (1985) Weldability and arc welding technology of aluminium-magnesium-lithium system alloy. *Ibid.*, **10**, 47–49.
15. Ishchenko, A.Ya., Poklyatsky, A.G., Yavorskaya, M.R. (1989) Prevention of oxide film inclusions in TIG welds on aluminium alloys. *Ibid.*, **6**, 38–41.
16. Poklyatsky, A.G., Grinyuk, A.A. (2001) Effect of parameters of asymmetric and modulated currents on quality of aluminium alloy welded joints. *The Paton Welding J.*, **7**, 33–36.
17. Voropaj, N.M., Gvozdetsky, V.S., Shcherbak, V.V. et al. (1969) Microplasma welding of light metals and alloys with cathode sputtering of oxide films. *Avtomatich. Svarka*, **7**, 5–10.
18. Brik, E.Yu., Dovbishchenko, I.V., Zaparovany, A.P. et al. (1992) AC plasma-arc welding of aluminium alloys. *Ibid.*, **4**, 53–54.
19. Rabkin, D.M., Ivanova, O.N., Steblovsky, B.A. et al. (1971) DCSP welding of aluminium alloys. *Ibid.*, **3**, 71–72.
20. Ivanova, O.N., Lozovskaya, A.V., Rabkin, D.M. et al. (1973) Properties of aluminium alloy welded joints made at a DCSP. *Ibid.*, **3**, 8–11.
21. Rabkin, D.M., Savich, I.M., Rozhdestvenskaya, T.S. (1962) Experience with production of all-metal aluminium passenger car. *Ibid.*, **2**, 60–65.
22. Paton, B.E., Potapievsky, A.G., Podola, A.V. (1964) CNC MIG pulsed-arc welding. *Ibid.*, **1**, 1–6.
23. Lapchinsky, V.F., Potapievsky, A.G., Steblovsky, B.A. et al. (1966) Pulsed-arc welding of aluminium alloys in argon atmosphere. *Ibid.*, **7**, 50–54.
24. Shejko, P.P., Slepchenko, N.N., Pashulya, M.P. et al. (1980) Experience of application of pulsed-arc MIG welding equipment and technology for manufacture of aluminium alloy products. In: *Proc. of 1st All-Union Conf. on Actual Problems of Welding of Non-Ferrous Metals*. Kyiv: Naukova Dumka.
25. Rabkin, D.M., Poritsky, M.P., Steblovsky, B.A. et al. (1975) Welding of body of the ER-200 electric train car. *Avtomatich. Svarka*, **9**, 48–51.
26. Ignatiev, V.G., Lobanov, L.M., Rabkin, D.M. et al. (1984) Structural-technological peculiarities of fabrication of welded metro car body from aluminium alloys. *Ibid.*, **2**, 51–53.
27. Rabkin, D.M., Poritsky, M.P., Steblovsky, B.A. et al. (1980) Aluminium platform of the BelAZ-7510 dump truck. *Ibid.*, **3**, 68–69.
28. Rabkin, D.M., Ryabov, V.R., Dovbishchenko, I.V. (1963) Application of helium and its mixture with argon for welding of aluminium alloys. *Ibid.*, **9**, 1–6.
29. Dovbishchenko, I.V., Ishchenko, A.Ya., Mashin, V.S. (1997) Application of helium for MIG welding of aluminium alloys. *Ibid.*, **2**, 14–15.
30. Dovbishchenko, I.V., Rabkin, D.M., Bugaj, V.S. et al. (1967) Welding of aluminium alloy vessels. *Ibid.*, **5**, 61–62.
31. Tsyplyukhin, A.V., Novikov, A.M., Borodenko, V.M. et al. (1986) TIG welding of aluminium boilers in helium-argon mixture atmosphere. *Ibid.*, **10**, 54–56.
32. Mashin, V.S., Slepchenko, N.N., Borodenko, V.M. et al. (1989) Comparison between technologies of MIG welding in helium-argon mixture atmosphere and with a three-phase argon arc for AMg6 alloy. In: *Transact. on Welding of Non-Ferrous Metals*. Kyiv: Naukova Dumka.
33. Paton, B.E., Gordonny, V.G. (2002) Works of the E.O. Paton Electric Welding Institute of the NAS of Ukraine in the field of millitary tank construction. *The Paton Welding J.*, **2**, 33–39.
34. Ishchenko, A.Ya., Lozovskaya, A.V., Poklyatsky, A.G. et al. (2002) Increase in strength of welds in arc welding of alloy 1420 using the Sc-containing fillers. *Ibid.*, **1**, 10–14.
35. Zaviryukha, V.I., Ryabets, Yu.A., Steblovsky, V.A. et al. (1985) Technological peculiarities of narrow-gap MIG welding of large-thickness aluminium alloys. In: *Pap. of 2nd All-Union Conf. on Actual Problems of Non-Ferrous Metals Welding*, Tashkent, October, 1982. Kyiv: Naukova Dumka.
36. Ishchenko, A.Ya., Budnik, V.P., Poklyatsky, A.G. et al. (2000) Effect of composition of shielding gases on technological characteristics of the arc during non-consumable electrode welding of aluminium alloys. *The Paton Welding J.*, **2**, 17–20.

DISTRIBUTION OF RATE AND PRESSURE OF PLASMA FLOWS IN WELDING ARCS

N.M. VOROPAJ
The E.O. Paton Electric Welding Institute, NASU, Kyiv, Ukraine

Radial and axial distribution of gas-dynamic characteristics of plasma flows in welding arcs has been studied. Arc column shape was approximated in the form of a truncated cone of a height, equal to arc length, and radii of upper and lower bases determined as corresponding sizes of a luminous region on the arc filming frames. Comparison of calculated data with available experimental data showed a satisfactory correlation of results obtained for the rate and pressure of plasma flows in definite welding arcs.

Key words: *welding arc, plasma flows, gas-dynamic pressure, magnetostatic pressure, arc constriction, asymmetric current, penetration shape, aluminium alloys, welding technology*

In welding arcs between the electrode of a relatively small diameter and parent metal with a developed surface the intensive flows of plasma are created by the axial forces caused by a gradient of a magnetic pressure [1–3]. Technological capabilities of processes of arc welding depend greatly on the rate and pressure of these flows. Due to a high temperature of welding arcs the direct change in rate and pressure of arc plasma flows is difficult that explains the rather limited number of works in this direction [2, 4]. The approximated procedure of calculations of parameters of plasma flows in welding arcs is described in [5]. To develop new methods of arc and plasma welding it is necessary to know the dependence of radial and axial distributions of gas-dynamic characteristics of plasma flows on arc parameters. The present article is devoted to the study of these problems.

According to [6, 7], the system of magneto-gas dynamic equations describing the arc plasma movement, taking into account the assumptions taken in [5], has a form

$$\frac{1}{r}\frac{\partial}{\partial r}(r\rho v_r)+\frac{\partial}{\partial z}(\rho v_z)=0; \quad \frac{\partial p}{\partial r}=-j_z B_\varphi;$$
$$\rho\left(v_r\frac{\partial v_z}{\partial r}+v_z\frac{\partial v_z}{\partial z}\right)=-\frac{\partial p}{\partial z}+j_r B_\varphi+\frac{1}{r}\frac{\partial}{\partial r}\left(r\eta\frac{\partial v_z}{\partial r}\right); \quad (1)$$
$$\frac{\partial B_\varphi}{\partial z}=-\mu j_r; \quad \frac{1}{r}\frac{\partial}{\partial r}(rB_\varphi)=\mu j_z,$$

where r is the arc column radius; ρ is the plasma density; v_r, v_z are the radial and axial components of plasma rate, respectively; p is the pressure; j_r, j_z are the radial and axial components of electric current density, respectively; B_φ is the azimuth component of magnetic induction vector; η is the coefficient of dynamic viscosity of plasma; μ is the magnetic permeability.

As regards to a cylindrical arc the equations (1) transform to equations of magnetostatics:

$$\frac{dp}{dr}=-j_z B_\varphi; \quad \frac{1}{r}\frac{\partial}{\partial r}(rB_\varphi)=\mu j_z. \quad (2)$$

To solve the given equations it is necessary to know the distribution of current density in arc column. According to [8], let us assume

$$j_z(r)=j_0\exp(-a^2r^2), \quad (3)$$

where a^2 is the coefficient of arc constriction characterizing the rate of diminishing $j_z(r)$ in increase of coordinate r. Substituting (3) in (2) at the condition of constancy of full current, we shall obtain

$$I_w=2\pi\int_0^\infty j_z(r)r\,dr. \quad (4)$$

We assume that the magnetic permeability of arc plasma does not depend on coordinates. Then, for the case of distribution of magnetostatic pressure in cylindrical arc column we shall find

$$p(r)=p_{at}+\mu\left(\frac{I_w}{2\pi}\right)^2 a^2\left[\mathrm{Ei}(-2a^2r^2)-\mathrm{Ei}(-a^2r^2)\right], \quad (5)$$

where p_{at} is the atmospheric pressure; $\mathrm{Ei}(-x)=\int_{-\infty}^{-x}\frac{e^t}{t}dt$ $(x>0)$ is the integral exponential function [9].

If the arc is not cylindrical, then the axial gradient of pressure is occurred, thus causing the arc plasma moving. In addition, the interaction of radial component of current density with a tangential magnetic field can influence this movement, i.e. term j_rB_φ in system (1). To define the rate of plasma flows, occurring in this case in the first approximation we neglect the inertia terms in the third equation of system (1) and consider that the electromagnetic force and gradient of pressure are equalized by the viscosity forces. Then the system of equations considered is transformed into the following system:

$$\frac{\partial p}{\partial r}=-j_zB_\varphi; \quad (6a)$$

Table 1. Change in function $\Phi(x)$ depending on values x

x	$\Phi(x)$	x	$\Phi(x)$	x	$\Phi(x)$
0.01	1.52	0.6	0.34	2.0	−0.70
0.05	1.36	0.7	0.23	2.5	−0.91
0.10	1.20	0.8	0.11	3.0	−1.09
0.15	1.08	0.9	0.03	5.0	−1.61
0.20	0.97	1.0	−0.07	10.0	−2.30
0.25	0.87	1.2	−0.23	15.0	−2.71
0.30	0.76	1.4	−0.38	20.0	−3.00
0.40	0.61	1.6	−0.50	50.0	−3.92
0.50	0.46	1.8	−0.59	100.0	−4.61

Note. $\lim \Phi(x) = c + 1$ (here $c \approx 0.577216$ — constant of Euler–Mascheroni).

$$\frac{\partial p}{\partial z} = j_r B_\varphi + \frac{1}{r}\frac{\partial}{\partial r}\left(r \eta \frac{\partial v_z}{\partial r}\right); \quad (6b)$$

$$\frac{\partial B_\varphi}{\partial z} = -\mu j_r; \quad (6c)$$

$$\frac{1}{r}\frac{\partial}{\partial r}(rB_\varphi) = \mu j_z. \quad (6d)$$

Distribution of axial component of current density taking into account of non-uniformity of system along z will be presented in the form

$$j_z(r, z) = j_0(z) \exp[-a^2(z)r^2] \quad (7)$$

or taking into account (4)

$$j_z(r, z) = (I_w/\pi)a^2(z) \exp[-a^2(z)r^2]. \quad (8)$$

Using (8), (6a) and (6d), similar to (5) we shall obtain

$$p(r, z) = p_{at} + \mu\left(\frac{I_w}{2\pi}\right)^2 a^2(z)\{\mathrm{Ei}[-2a^2(z)r^2] - \mathrm{Ei}[-a^2(z)r^2]\}. \quad (9)$$

Using (6c), term $j_r B_\varphi$ from equation (6b) will be presented in the form

$$j_r B_\varphi = -\frac{1}{2\mu}\frac{\partial}{\partial z} B_\varphi^2. \quad (10)$$

Thus, instead of system (6) we have

$$\mu\left(\frac{I_w}{2\pi}\right)^2 \frac{\partial a^2(z)}{\partial z}\{\mathrm{Ei}[-2a^2(z)r^2] - \mathrm{Ei}[-a^2(z)r^2]\} = \frac{1}{r}\frac{\partial}{\partial r}\left(r \eta \frac{\partial v_z}{\partial r}\right). \quad (11)$$

Equation (11) should be added with a boundary condition

$$v_z(r, z)\big|_{r=R_0} = u_0, \quad (12)$$

where R_0 is the radius of shielding gas nozzle; u_0 is the rate of shielding gas.

Let us assume that the viscosity of arc plasma does not depend on coordinates. Then, after some transformations, the solution of boundary-value problems (11), (12) will take a form

$$v_z(r, z) = u_0 + \frac{1}{8}\frac{\mu}{\eta}\left(\frac{I_w}{2\pi}\right)^2 \frac{1}{a^2(z)}\frac{\partial a^2(z)}{\partial z} \times \{2[\Phi(a^2(z)R_0^2) - \Phi(a^2(z)r^2)] - [\Phi(2a^2(z)R_0^2) - \Phi(2a^2(z)r^2)]\}. \quad (13)$$

Here

$$\Phi(x) = (x + 1)\mathrm{Ei}(-x) + \exp(-x) - \ln x. \quad (14)$$

Expression (13) describes the radial and axial distribution of rate of plasma flows as a function of welding current, coefficient of arc constriction (its dependence on coordinate z), rate of shielding gas and radius of a shielding gas nozzle. Function (14), calculated using [10], is given in Table 1.

Let us determine the gas-dynamic characteristics of plasma flows in a definite welding arc. In case of non-consumable electrode welding in argon the arc column shape can be approximated in the form of a truncated cone with a height equal to arc length l_a and radii R_1 and R_2, respectively, of upper and lower bases, determined as sizes of luminous region at arc (obtained with the help of filming). To determine the dependence of coefficient of conical arc on z, we shall use the relationship from [11] between a^2 and conditional radius of arc R (radius of circle, on the surface of which 95 % of arc current is passing):

$$a^2(z) = kR^{-2}(z), \quad (15)$$

where k is the dimensionless coefficient, used in calculations equal to 3.0–3.5.

Thus, for arc having the shape of a truncated cone

$$R^2(z) = (R_1 + [R_2 - R_1]\, z/l_a)^2 \quad (16)$$

we have

$$a^2(z) = \frac{k}{(R_1 + [R_2 - R_1]\, z/l_a)}. \quad (17)$$

It follows from (13) that the rate of plasma flows is proportional to the expression

$$\frac{1}{a^2(z)}\frac{\partial a^2(z)}{\partial z},$$

which with allowance for (17) can be written in the form

$$\frac{1}{a^2(z)}\frac{\partial a^2(z)}{\partial z} = \frac{2(R_2 - R_1)}{l_a(R_1 + [R_2 - R_1]\, z/l_a)}. \quad (18)$$

Near the anode surface ($z = l_a$)

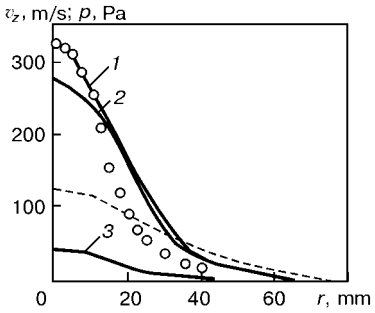

Figure 1. Radial distribution of rate of plasma flows v_z (dashed curve) and pressure p (solid curves) at anode of argon arc: *1* — full pressure; *2* — gas-dynamic pressure; *3* — magnetostatic pressure (points — the data of [2])

$$v_z - u_0 \sim \frac{1}{l_a}\left(1 - \frac{R_1}{R_2}\right). \qquad (19)$$

As an example, let us first consider the DC argon arc non-consumable electrode welding with the following parameters [2]: I_w = 100 A; l_a = 6 mm; R_1 = = 1.3 mm; R_2 = 4.2 mm; u_0 = 2.5 m/s; R_0 = 7.5 mm; ρ = 365 kg/m^3; $\eta = 2.5 \cdot 10^{-4}$ N·s/m.

Figure 1 shows a radial distribution of plasma rate, calculated by expression (13), magnetostatic (9) and gas-dynamic $p_g = \rho v_z^2/2$ pressures of plasma flow, and also full pressure equal to the sum of magnetostatic and gas-dynamic pressures. Comparison of obtained calculated data p_c with available experimental data p_{ex} shows a satisfactory coincidence of their results in central regions of the arc. Thus, on the anode axis at I_w = 100 A, p_c = 324 Pa and p_{ex} = 320 Pa. Similar coincidence is observed in the wide range of values of welding currents (Figure 2). In periphery regions of the arc there is some discrepancy in calculated and experimental data. The latter is, probably, explained by the fact that in the given procedure of calculation a radial spreading of plasma flow near the anode surface, which can lead to a faster pressure drop in the radial direction, is not taken into consideration.

Analysis of given data shows that the magnetostatic pressure p_m is much lower than the gas-dynamic pressure of the plasma flow p_g. In the center of arc anode at I_w = 100 A, p_m = 44 Pa and p_g = 280 Pa, i.e. almost 7 times lower. Approximately the same ratio of pressure values is observed also at other values of currents (see Figure 2). So, in conical arcs the main role in the process of forcing the weld pool molten

Table 2. Initial parameters of welding arc of asymmetric current taken for calculation of rate and pressure of plasma flows

τ, ms	$R_1 \cdot 10^3$, m	$R_2 \cdot 10^3$, m	R_1/R_2	$a^2 \cdot 10^{-5}$, m^{-2}	I_w, A	v_z, m/s	p_{max}, Pa
2.5	1.8	8.3	0.22	0.51	81	403	297
5.0	2.0	11.6	0.17	0.26	112	580	612
7.5	1.8	9.5	0.19	0.39	81	409	305
10.0	1.3	3.7	0.35	2.56	182	98	18
12.5	2.0	6.3	0.32	0.88	273	156	45
15.0	1.3	4.3	0.30	1.89	182	106	20

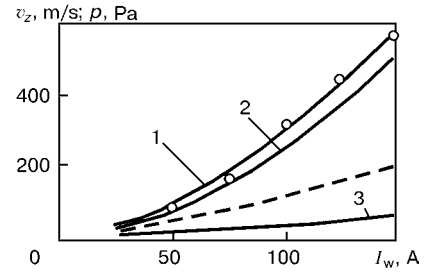

Figure 2. Dependence of rate of plasma flows (dashed curve) and pressure (solid curves) of plasma flows at the anode axis on welding current at l_a = 6 mm (*1–3* — the same as in Figure 1)

metal and in penetration of the parent metal is played by the plasma flows. As is seen from (19), it is necessary to try to decrease the arc length and to reduce the ratio R_1/R_2, i.e. to use small-diameter electrodes, to increase the rates of plasma flows (increase in penetration depth). To avoid the formation of defects of through penetrations type, caused by a mechanical action of arc weld pool, the welding of metal of small thickness is more preferable by the arc being narrowed to the direction of workpiece («needle-like» microplasma).

Coming from arc column sizes obtained by a high-speed filming of the process of argon arc welding of aluminium alloys with asymmetric alternating current [12], the rates and maximum pressure p_{max} of plasma flows in the central part of arc at the moments of current rising and drop for the cathodic and anodic parts of the period at the coefficient of current asymmetry K_{as} = 0.8 (Figure 3 and Table 2), were calculated using equations (13) and (14). At amplitude values of welding current the rate of plasma flows reaches 580 m/s. Figure 4 shows abrupt changes in rate and pressure of plasma flows in transition from the positive to negative part of the asymmetric current period. Consequently, one of the effective ways of control of depth of penetration and weld shape is the arc supply with the asymmetric variable-polarity current. This scheme of supply leads to a periodic change of a force action of plasma flows on weld pool metal, promotes more intensive its stirring and degassing, and also refining of microstructure and dispersion of oxide inclusions in the weld metal.

It is very important that with increase in coefficient of asymmetry of a variable-polarity current the

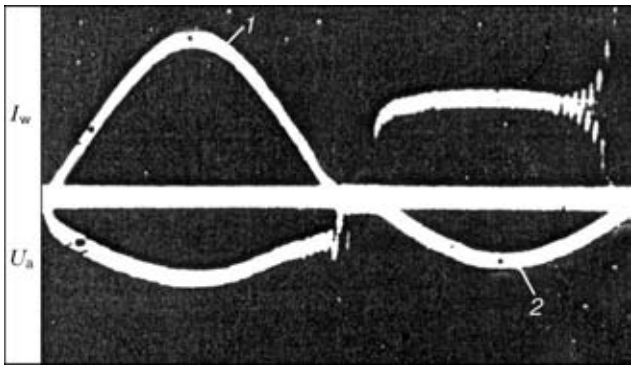

Figure 3. Oscillograms of asymmetric alternating current I_w and voltage at argon arc U_a: *1* — half-period of current at straight polarity; *2* — the same at reverse polarity

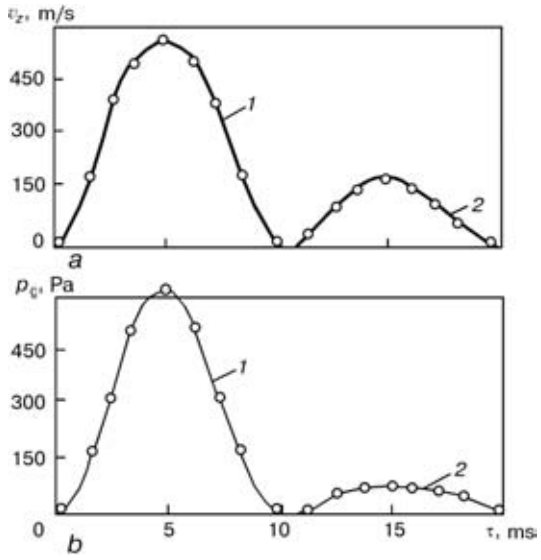

Figure 4. Change in gas-dynamic characteristics of plasma flows of arc of asymmetric alternating current with K_{as} = 0.8: *a* — rate of plasma points v_z; *b* — gas-dynamic pressure p_g; *1*, *2* — half-period of current at straight and reverse polarity, respectively

redistribution of arc power is occurred at straight and reverse polarity with an increase in a share of heat dissipating into the parent metal and with a decrease in a share of heat used for the electrode heating. Allowable current loads to the tungsten electrodes at K_{as} = 0.6–0.8 are 1.5–2 and 4–6 times higher than in welding, respectively, at a balanced alternating current and DCRP.

Processes of twin-arc welding with a combined non-consumable and consumable electrodes [13] and pulsed welding with two consumable electrodes [14] are another effective procedure of control of gas-dynamic characteristics of plasma flows and shape of penetration of the parent metal. In these cases it is possible to use the electrodes of a relatively small diameter due to separate feeding of current pulses for each electrode, that leads to a significant decrease in R_1/R_2 ratio of upper and lower bases of column of welding arcs and appropriate increase in depth of the parent metal penetration.

Acknowledgments. *The author expresses sincere thanks to Dr. I.V. Krivtsun for assistance in the solution of the system of magneto-gas dynamic equations, valuable advices and comments on the materials of the present article.*

1. Khrenov, K.K. (1949) *Electric welding arc*. Moscow-Kyiv: Mashgiz.
2. Shoek, P.A. (1966) Study of energy balance on anode of high-current arcs burning in argon atmosphere. In: *Current problems of heat exchange*. Moscow-Leningrad: Energiya.
3. Zaruba, I.I. (1968) Plasma flows in welding arcs. *Avtomatich. Svarka*, **10**, 1–5.
4. Kovalev, I.M., Akulov, A.I., Martinson, L.K. et al. (1971) Rate and thermal characteristics of arc flows. *Fizika i Khimiya Obrab. Materialov*, **5**, 27–34.
5. Voropaj, N.M., Krivtsun, I.V. (1978) Gas-dynamic characteristics of plasma flows in welding arcs. *Magnitnaya Gidrodinamika*, **1**, 132–136.
6. (1972) *Physics and chemistry of low-temperature plasma*. Ed. by S.V. Dresvin. Moscow: Atomizdat.
7. Engelsht, V.S., Gurovich, V.Ts., Desyatkov, G.A. et al. (1990) *Low-temperature plasma.* Vol. 1. Theory of electric arc column. Novosibirsk: Nauka.
8. Gvozdetsky, V.S. (1974) Constriction of electric arc column. *Avtomatich. Svarka*, **2**, 1–4.
9. Lebedev, N.N. (1953) *Special functions and their applications*. Moscow: Gostekhteorizdat.
10. (1954) *Tables of integral exponential function*. Ed. by V.A. Ditkin. Moscow: AN SSSR.
11. Gvozdetsky, V.S. (1973) About function of current density distribution in anode spot of arc. *Avtomatich. Svarka*, **12**, 20–24.
12. Rabkin, D.M., Voropaj, N.M., Mishenkov, V.A. (1978) Energy characteristics of welding process with asymmetric variable polarity current. *Ibid.*, **4**, 5–10.
13. Voropaj, N.M., Lesnykh, V.V., Mishenkov, V.A. (1994) Combined process of arc welding and surfacing with non-consumable and consumable electrodes. *Ibid.*, **4**, 56–57.
14. Voropaj, N.M., Protsenko, P.P. (2000) Features of welds and HAZ formation in gas-shielded pulsed twin-arc welding in high-strength low-alloyed steels. *The Paton Welding J.*, **8**, 40–46.

FEATURES OF CONSUMABLE-ELECTRODE ARC WELDING OF ALUMINIUM ALLOYS IN NEON AND ITS MIXTURES WITH HELIUM AND ARGON

A.Ya. ISHCHENKO, I.V. DOVBISHCHENKO, V.S. MASHIN and **M.P. PASHULYA**
The E.O. Paton Electric Welding Institute, NASU, Kyiv, Ukraine

Volt-ampere characteristics of the steady and impulse arc in mixtures of different inert gases and features of weld formation and geometry are analyzed. A fundamental possibility and cost-effectiveness of application of helium-neon mixtures for protection of the welding zone is demonstrated.

Key words: *arc welding, aluminium alloys, consumable electrode, inert gases, gas mixtures, volt-ampere characteristics, weld parameters, defects*

MIG welding is widely applied for fabrication and repair of large-sized structures of aluminium alloys. Unlike TIG welding, this process provides a higher efficiency of welding, reduction of the HAZ and lowering of the level of residual deformations of weldments (particularly of sheet material) [1]. Argon, helium and their mixtures are used as shielding gases in consumable electrode welding of aluminium alloys [1–6]. A disadvantage of argon-arc welding is a pronounced convexity of the weld, specific shape of penetration with a marked narrowing in the weld root, considerable loss of some alloying elements from the electrode metal, and increased porosity of welds. This results in relatively low mechanical and corrosion properties of welds. Application of helium alone is limited by its high cost, high flow rate in welding plate metal, unstable arc and increased metal spatter. Therefore, it is recommended to apply He + Ar mixtures as shielding gases. Helium content in such mixtures is between 50 to 75 %. Amount of argon and helium in the mixture depends on the composition of the alloy being welded, its thickness and requirements, made of weld metal quality [4, 5]. Cost of the process of welding in He + Ar mixtures remains to be high, compared to welding in argon alone. A mixture of helium and neon (3–25 % Ne) forms in the oxygen, nitrogen and argon processing line at a certain stage of air separation. Possibility of effectively using this comparatively inexpensive (compared to pure helium) mixture in TIG welding of aluminium alloys is shown in [7].

In this connection it is important to determine the influence of neon and its mixtures with argon and helium on the quality of welds in MIG welding of aluminium alloys by a steady and impulse arc, establish the influence of different compositions of shielding gases on volt-ampere characteristics (VAC) of the arc, stability of arcing, quality of formation and geometrical parameters of welds.

Investigations were performed, using Al-5Mg alloy (AMg5, GOST 4784–74) 18 mm thick and welding wires Sv-AMg5 (GOST 7871–75) of 1.6 and 2.0 mm diameter. Shielding gases were the highest grade argon (GOST 10157–79), A grade helium (TU 51-940–80), neon (TU-U-14299304-001–96), ready He + Ne mixture (85 % He + 15 % Ne) and two- and three-component mixtures, prepared from them. Physical characteristics of inert gases by the data of [8] are given in Table 1, and their composition in Table 2. By its characteristics neon takes up an intermediate position between helium and argon. Value of its ionization potential is closer to that of helium, and the coefficient of heat conductivity (specific heat conductivity) is close to that of argon. Such properties of neon, compared to argon, lead, first of all, to a noticeable increase of arc voltage (due to a relatively high potential of ionization compared to argon) and greater width of penetration (in view of a higher coefficient of heat conductivity compared to argon). In welding in neon (similar to welding in helium), apparently, the voltage drop on the anode and cathode is redistributed, arc column is constricted and energy density is increased.

Mixtures of inert gases were prepared by continuous mixing at a dosed flow rate of each component. Flow rate was determined by the readings of rotameters, calibrated for argon. In order to use them for neon, helium and mixtures, the calibration scales were

Table 1. Physical characteristics of inert gases

Parameter	*Helium*	*Neon*	*Argon*
Atomic mass	4.003	20.183	39.944
Density, kg/m^3	0.1785	0.8990	1.7840
Ionization potential, eV	24.58	21.56	15.76
Coefficient of heat conductivity, W/(m·K)	0.1430	0.0468	0.0167
Specific heat conductivity, J/(kg·°C)	5190	1030	520

Table 2. Composition of inert gas mixtures

Gas	Impurity content (≤ vol.%·10⁴)							
	Ar	*Ne*	*He*	N_2	O_2	H_2	H_2O	$CO_2 + CH_4$
Argon	Base	–	–	50	7	1	10	5
Neon	–	Base	35	3	1	1	2	1
Helium	1	40	Base	5	1	1	5	3
Helium (base) + 15 % neon	40	Base	Same	10	2	1	6	4

recalculated. The actual flow rate of gases was calculated by the following formulas:

$$Q = Q_{Ar}K, \quad K = \sqrt{\frac{\gamma_{Ar}}{\gamma_{gas}}},$$

$$\gamma_{gas} = (\gamma_{Ar} P_{Ar} + \gamma_{Ne} P_{Ne} + \gamma_{He} P_{He})/100,$$

where Q is the gas flow rate, l/min; K is the correction coefficient (for all rotameters of RS and RM type); γ is the gas density, kg/m^3; P is the gas content in the mixture, %. Correction coefficients K to determine the actual flow rate of He + Ne and He + Ar mixtures are shown in Figure 1.

Base metal surface was cleaned by chemical etching using a regular procedure [2]. Prior to welding the surface of the metal in the welding zone was scraped (0.05 mm). VDU-506, Fronius TPS-450 power sources and Fronius Pull MIG PM-502Z torches were used for single-pass consumable electrode welding (surfacing) by a stable arc (SA-MIG) and impulse arc (IA-MIG). Weld root was formed on a removable backing of stainless steel with a groove. Parameters of SA-MIG modes in argon, neon, helium and their mixtures were as follows: d_{wire} = 2.0 mm, $I_{w.av}$ = 220–380 A, $U_{a.av}$ = 24–36 V, v_f = 260–480 m/h, v_w = 15–40 m/h, l_a = 3–5 mm, Q = 30–60 l/min. Parameters of IA-MIG were: d_{wire} = = 1.6 mm, $I_{w.av}$ = 120–320 A, $U_{a.av}$ = 18–38 V, v_f = = 280–530 m/h, v_w = 20 m/h, l_a = 2–18 mm, I_p = = 460–540 A, f_p = 90–210 Hz, t_p = 3.1–3.8 ms, Q = = 40 l/min.

Geometrical parameters of welds (base metal penetration depth h, weld width from the face side B, its convexity height l) were determined, using MMI-2 microscope on transverse macrosections with the accuracy of up to ± 0.1 mm.

Analysis of VAC of an impulse arc, running in argon, neon, helium and He + Ne mixture (15 % Ne), at different electrode wire feed rates (l_a = 2–18 mm) showed, that at the same welding current the voltage of the arc, running in neon, is by 4 to 8 V higher than in argon (Figure 2). At the same rates of wire feed, v_f, the arc voltage is by 0.5 to 1.5 V lower in the He + Ne mixture than in pure helium (Figure 3). The higher the average welding current, the smaller is the difference in the VAC of the arc, running in helium and in He + Ne mixture. Addition of neon to argon right up to 100 % (at v_f = const) leads to shortening of the arc, greater spatter of electrode metal and lowering of average welding current by 20–30 A (Figure 4, *a*). In order to restore the stability of the welding process, it is necessary to increase the arc voltage by 2–8 V, depending on the content of neon in the mixture and value of current (Figure 4, *b*). The depth of metal penetration and weld width increase by 0.7–1.1 and 1.9–2.3 mm, respectively. The influence of neon on the electric parameters of the arc and geometrical shape of the welds is the most pronounced at its content in the mixture above 40 %.

Dependence of the geometrical parameters of SA-MIG welds on the shielding gas composition and welding speed is shown in Figures 5 and 6. Similar to

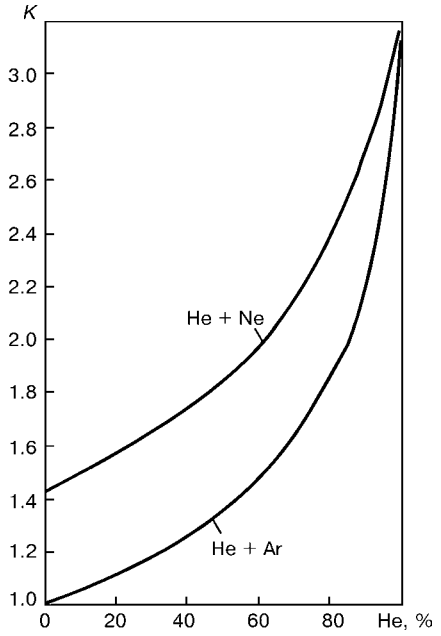

Figure 1. Correction coefficients K for determination of the actual flow rate of He + Ne and He + Ar mixtures using rotameters, calibrated for argon

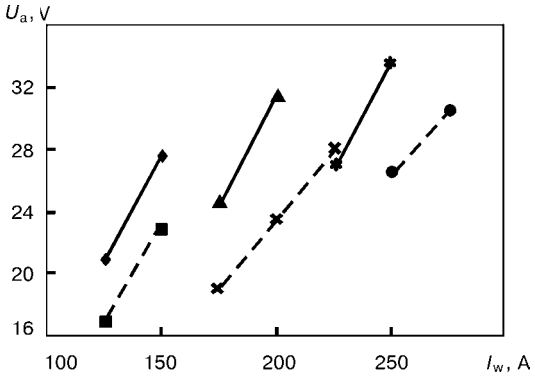

Figure 2. Volt-ampere characteristics of an arc, running in neon (solid curve) and argon (dashed curve), in IA-MIG, depending on the wire feed rate: ■, ◆ – 300; ▲, × – 400; ✻, ● – 500 m/h

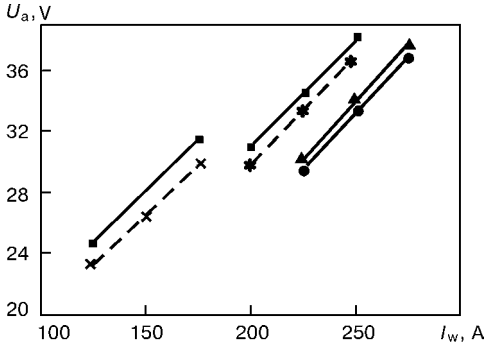

Figure 3. VAC of an arc, running in helium (solid curve) and He + Ne mixture, containing 15 % Ne (dashed), in IA-MIG welding, depending on the wire feed rate: ◆, × — 300; ■, ✻ — 400; ▲, ● — 500 m/h

IA-MIG welding, argon replacement by neon (0 % He) leads to a greater penetration depth, weld width and reduction of weld convexity. Helium addition to neon (at constant values of I_w and l_a) promotes still greater depth and width of the weld, particularly at the increase of helium content from 30 to 65 % (Figure 5). In this case, stability of the arc and weld formation and width of the cathode cleaning zone correspond to the indices, obtained in He + Ar mixtures (at the same content of helium).

Thus, at any proportions of neon and helium, irrespective of welding processes and modes, the width and depth of base metal penetration are greater than with the same proportions of argon and helium. Geometrical parameters of welds, made in helium and He + Ne mixtures (He ≥ 85 %, I_w = 250–350 A, v_w = = 15–20 m/h), have practically the same values (Figure 6). In the case of application of a mixture of gases with more than 92–95 % He, neon additives do not have any influence on weld dimensions.

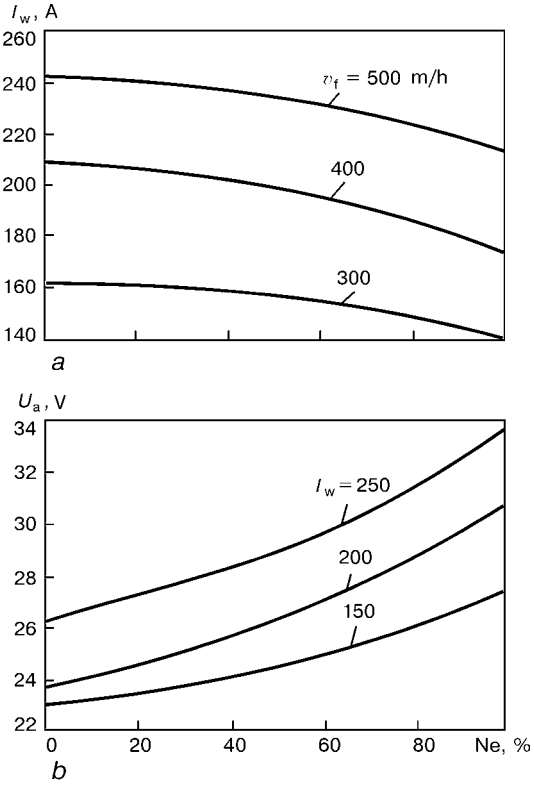

Figure 4. Influence of neon in Ar + Ne mixture on welding current at $U_a \approx 25$ V (*a*) and on arc voltage (*b*) at IA-MIG: *a* — at a constant feed of welding wire; *b* — at direct welding current

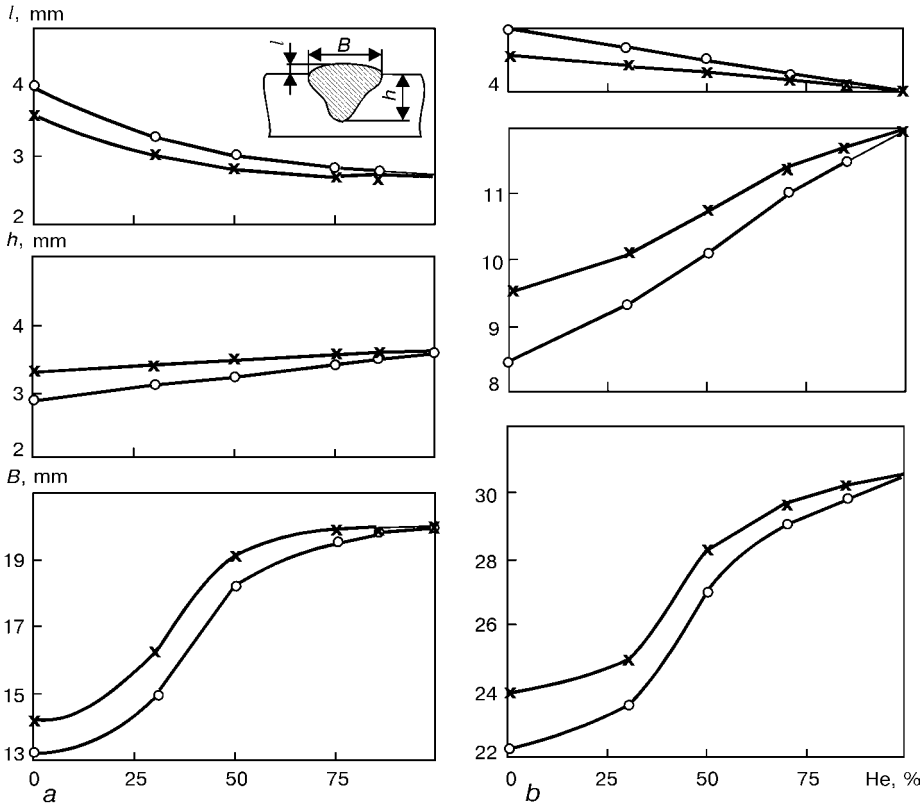

Figure 5. Influence of the composition of He + Ar (○) and He + Ne (×) mixture on geometrical parameters of SA-MIG welds (d_{wire} = = 2.0 mm, $l_a \approx 4 \pm 1$ mm, v_w = 20 m/h) at I_w = 250 (*a*) and 350 (*b*) A

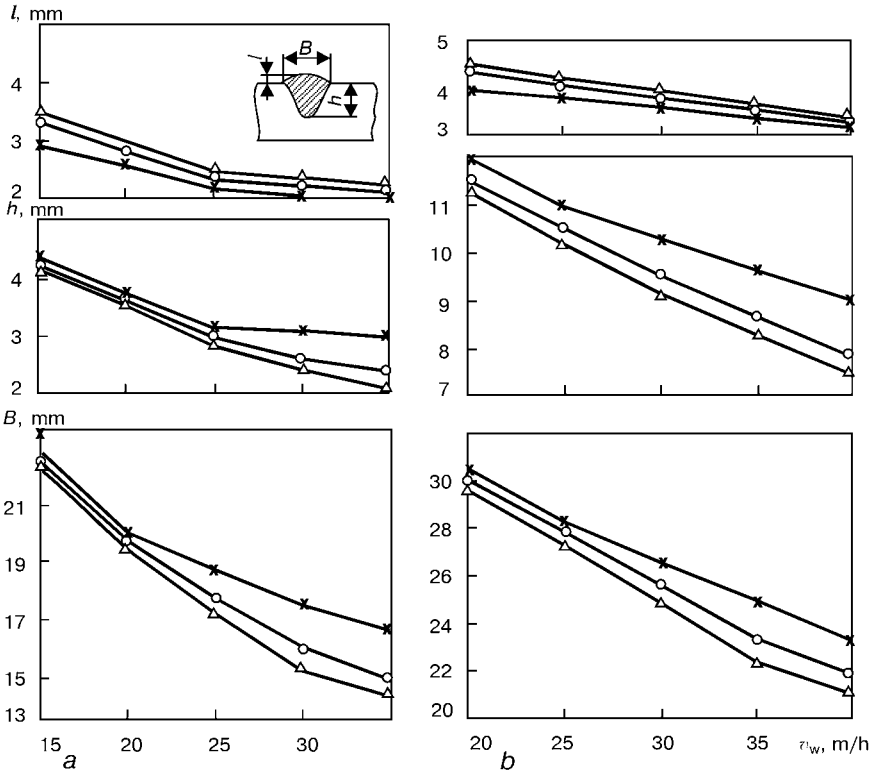

Figure 6. Influence of welding speed and shielding gas composition (× — He; ○ — He (base) + 15 % Ne; Δ — He (base) + 15 % Ar) on the geometrical parameters of welds in SA-MIG (U_a = 36 ± 1 V, d_{wire} = 2.0 mm): *a* — I_w = 250 A, v_f = 275 m/h; *b* — I_w = 350 A, v_f = 470 m/h

Investigation of transverse macrosections showed that porosity in the deposited metal, obtained in neon and He + Ne mixtures, is 1.1–1.6 times smaller than in argon and He + Ar mixtures. This is related to thermophysical properties of neon and smaller content of «harmful» impurities (hydrogen, moisture, hydrocarbons, etc.) in it, compared to argon.

In view of the increase of the volume (weight) of weld pool in welding in neon (see Figure 5), it may be assumed that neon, similar to helium [9, 10], lowers the average temperature of electrode metal drops and increases the average temperature of weld pool. This creates favorable conditions for lowering hydrogen solubility in electrode drops and increasing the rate of its evolution from the weld pool in the form of gas bubbles [6].

Technico-economic calculations show that application of neon alone as the shielding gas it not rational in view of its deficit and high cost (neon is more expensive than helium). At the same time, the cost of 1 m^3 of ready He + Ne mixtures (3–25 % Ne) is practically independent on the amount of neon and is on average 25 % lower than the cost of helium alone. Use of three-component mixtures of inert gases, prepared from the He + Ne mixtures, supplied in bottles, and argon (50–70 % He + 3–23 % Ne + 7–47 % Ar), allows further reduction of the shielding gas cost and of the cost of welding operations, respectively.

It should be noted that replacement of He + Ar mixtures by ready He + Ne mixtures in welding of aluminium alloys leads to a higher arc voltage, greater depth of penetration and weld width, reduction of weld convexity and porosity of the deposited metal.

1. Ishchenko, A.Ya., Lozovskaya, A.V., Poklyatsky, A.G. et al. (2002) Increase of strength of welds in arc welding of alloy 1420 using the Sc-containing fillers. *The Paton Welding J.*, **1**, 10–14.
2. Rabkin, D.M., Ignatiev, V.G., Dovbishchenko, I.V. (1982) *Arc welding of aluminium and its alloys*. Moscow: Mashinostroenie.
3. Mashin, V.S., Pavshuk, V.M., Dovbishchenko, I.V. et al. (1991) Influence of pulsed arc welding conditions of AD0 aluminium on shape and porosity of welds. *Avtomatich. Svarka*, **4**, 57–60.
4. Mashin, V.S., Dovbishchenko. I.V., Tsyplyukhin, A.V. (1991) Nomograms of the modes of consumable electrode helium-argon arc welding of aluminium alloys. *Ibid.*, **10**, 55–56.
5. Dovbishchenko, I.V., Ishchenko, A.Ya., Mashin, V.S. (1993) Peculiarities of consumable electrode helium-argon arc welding of aluminium alloys. *Ibid.*, **6**, 38–43.
6. Dovbishchenko, I.V., Ishchenko, A.Ya., Mashin, V.S. (1997) Use of helium in consumable electrode welding of aluminium alloys. *Ibid.*, **2**, 14–19.
7. Ishchenko, A.Ya., Budnik, V.P., Poklyatsky, A.G. et al. (2000) Effect of composition of shielding gases on technological characteristics of arc during non-consumable electrode welding of aluminium alloys. *The Paton Welding J.*, **2**, 17–20.
8. Finkelshtejn, D.N. (1979) *Inert gases*. Moscow: Nauka.
9. Ishchenko, A.Ya., Mashin, V.S., Dovbishchenko, I.V. et al. (1994) Mean temperature of the metal of electrode drops during inert-gas shielded welding of aluminium alloys. *Avtomatich. Svarka*, **1**, 48–49.
10. Ishchenko, A.Ya., Mashin, V.S., Dovbishchenko, I.V. et al. (1994) Mean temperature of weld pool metal in inert-gas arc welding of aluminium alloys. *Ibid.*, **11**, 15–19.

PREVENTION OF FORMATION OF OXIDE FILMS IN WELDS ON Li-CONTAINING ALUMINIUM ALLOYS

A.G. POKLYATSKY, A.V. LOZOVSKAYA and **A.A. GRINYUK**
The E.O. Paton Electric Welding Institute, NASU, Kyiv, Ukraine

Effect of different technological factors on formation of extended filamentary inclusions of oxide films in TIG welds on Li-containing aluminium alloys is considered. It is suggested that these defects are caused primarily by a higher melting temperature of filler metal, compared with base metal. Recommendations allowing production of quality welded joints on Li-containing aluminium alloys are given.

Key words: *argon-arc welding, lithium-containing aluminium alloys, tungsten electrode, oxide film, filler wire, preheating, asymmetric current, secondary phases*

Advanced Li-containing aluminium alloys are characterised by low specific weight and high strength properties [1]. They find wide application in aircraft and space engineering particularly owing to this combination of properties [2–4]. Designs of individual elements, assemblies and casings of flying vehicles provide for the use of different welding methods, among which the most widespread method is tungsten-electrode argon-arc (TIG) welding. However, a drawback of this method is the risk of formation of defects in the weld metal [4–6], such as pores and oxide films, which lead to deterioration of mechanical properties of welded joints and loss of their tightness.

It is a known fact that aluminium oxide, i.e. Al_2O_3, in the form of a film is always present on the surface of aluminium, its melting point being 2300–2320 °C. Aluminium hydroxide, $Al_2O_3{\cdot}nH_2O$, having a variable composition and structure, is usually formed in a humid atmosphere. Thickness of the oxide film varies over wide ranges (from 2–3 to 20–40 nm) and grows with a heating temperature. It may amount to 200 nm and more on a hot-rolled metal. The oxide film has a substantial adsorption ability with respect to gases and different types of non-metallic inclusions. The presence of additions of alkali and alkali-earth metals in aluminium alloys leads to saturation of the film with oxides of these metals [7, 8].

Available now are some technological recommendations providing the weld metal of a better quality in welding aluminium alloys. They are reduced to removal of oxide films from the surface of welding consumables and improvement of welding parameters and technologies.

In addition to increased requirements for preliminary preparation of weld edges and improved protection of metal from oxidation, it is indicated to use pulsed-arc welding in order to degas the weld pool and produce defect-free welded joints [9–11].

However, meeting the above recommendations does not yet guarantee the quality weld formation in welding Li-containing aluminium alloys. Supposedly, an increased sensitivity of the weld metal to formation of oxide films results from the nature of the above alloys. Laps, microlaminations and stringer-type clusters of phase components get to the penetration zone together with the film located on the base metal surface which is not treated by the arc. However, no films are formed in the weld metal in making joints on Li-containing aluminium alloys by arc welding using no filler wire.

The mechanism and causes of formation of extended inclusions of oxide films, located as a rule in the central part of the welds, have been little studied so far and require further investigations.

Materials and experimental procedure. Butt joints on Li-containing aluminium alloys 1420 (Al–Mg–Li) and 1460 (Al–Cu–Li) 3, 4 and 6 mm thick, were welded to study the effect of different technological factors on the processes of formation of extended inclusions of oxide films in weld metal. Welding wires of pure aluminium and of the Al–Mg, Al–Cu + Sc, Al–Si (Sv-AK5), Al–Cu–Mg and Al–Cu–Si alloying systems, having different diameters (1.2, 1.6, 2.0 and 2.5 mm), were used as filler materials, and plates of alloys 1420, 1460, 1201 (Al–Cu) and AMg63 (Al-6.3Mg) were used as filler materials. Prior to welding the surfaces of the samples were etched by a common technology, and the weld edges were machined to a depth of not less than 0.1 mm.

Stationary and pulsed welding conditions were provided using the ISVU-315, I-126 (Ukraine) and MW-450 (Austria) arc power supplies.

The welds were formed on a backing with different sizes of grooves. Special backings with holes to feed argon were used to ensure extra shielding of the root part of the welds. In addition, an aluminium foil was applied to shield the top and bottom surfaces of some of the joints.

An alternating sinusoidal commercial-frequency current was supplied using the TDM-315 transformer and RB-300 ballast resistor to preheat filler wire 25 mm long. The UTT-5 current transformer was used to measure the current flowing through the filler wire. This was done allowing for the following known formula:

$$cm\Delta T = I^2Rt, \qquad (1)$$

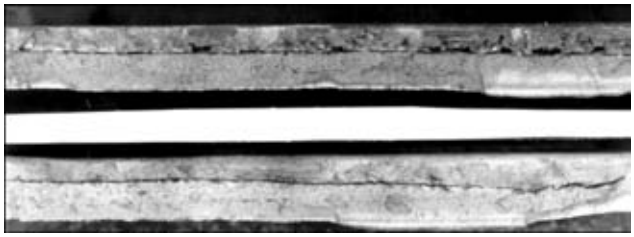

Figure 1. Extended filamentary inclusions of oxide films in fractures of the TIG welds on plates of alloy 1460

where c is the specific heat of the material of a conductor; m is its mass; ΔT is the variation in its temperature; I and R are the current and resistance in the conductor, respectively; and t is the time during which the current flows.

Temperature of preheating of the filler wire was determined from the following expression:

$$\Delta T = 16 \frac{I^2 \rho l}{\pi^2 d^4 v c j}, \qquad (2)$$

where I is the current flowing through the filler wire; ρ is the specific resistance of the filler wire material; l is the length of the region of the filler wire through which the current flows; v is the filler wire feed speed; and j is the specific weight of the filler wire material.

Reinforcement and root parts of the welds were removed by machining after welding, and the longitudinal fractures were made. The quality of the welds made using different technological approaches was assessed on the basis of investigations of the fractures.

Experimental results. No extended inclusions of oxide films were detected in the welds made by conventional stationary-arc TIG welding without a filler wire on Li-containing aluminium alloys 1420 and 1460 both in similar and dissimilar combinations. Extended defects in the central part of the welds were formed in the case where the filler wire was fed to the weld pool, independently of the wire alloying system, diameter and method of preliminary preparation of the wire surface (Figure 1). Even mechanical cleaning of the surface of the wire immediately before welding failed to eliminate the filamentary inclusions, although thinner in this case.

The package of arrangements aimed at ensuring reliable shielding of metal from oxidation in TIG welding failed to provide quality welded joints either. Feeding of argon through the holes in a special backing did not prevent formation of the extended defects. Shielding of a joint from the ambient atmosphere by applying an aluminium foil strip to the top surface or both top and back surfaces of the weld led to formation of fine disoriented defects, in addition to the extended longitudinal films.

All the attempts to affect the character of location of oxide inclusions in the weld metal by changing the shape and size of a forming groove, inclination angle of the torch or the edge preparation shape turned out to be ineffective. Formation of filamentary extended inclusions of oxide films still occurs in the central part of the weld.

The use of the I-126, ISVU-315 and MW-450 arc power supplies with differing dynamic characteristics and wave forms of the welding current failed to exert any substantial effect on formation of the above type of oxide inclusions in the weld metal on Li-containing aluminium alloys. Variations in frequency of alternating the current polarity (f = 50–250 Hz) or using the welding current with a low-frequency pulsation in modulation (f_m = 2–5 Hz) yielded no appreciable results either. Intensive oscillations of molten metal of the weld pool led to periodic changes in its solidification rate, but they did not disturb continuity of the process. Therefore, oxide inclusions in the weld metal are still formed in this case along the entire length of a welded joint, like in the case of stationary-arc welding.

The probability of formation of filamentary inclusions in the weld metal can be reduced by activating the processes of destruction of the oxide film during welding, which is achieved through using the asymmetric current with prevalence of duration of the reverse-polarity pulses. As shown by the results of investigations of longitudinal fractures of the welds, it is necessary to vary the ratio of durations of the straight- to reverse-polarity current pulses to provide the quality weld formation in welding using filler wires of different alloying systems. In the case of welding using the Al–Cu system filler wire the defect-free welds are formed by applying the asymmetric current with a time asymmetry factor of K_{as}^{τ} = 0.35–0.40. In the case of filler wires of the Al–Mg and Al–Cu–Mg alloying systems the value of K_{as}^{τ} should be decreased to 0.25–0.30 to avoid formation of defects. But in welding using filler wires of the Al–Cu–Si and Al–Si alloying systems, oxide inclusions are formed in the weld metal even at $K_{as}^{\tau} \le 0.2$.

Figure 2 shows fracture surfaces of the welds with oxide film inclusions in the TIG welded joints made on the 1460 alloy plates 3 mm thick by using filler wires of different alloying systems. Independently of the filler wire type, the oxide film inclusions had a differing shape and colour, as well as a developed surface with peaks and valleys. A change in colour of the film from bright to black is most probably caused by differences in its thickness. A dendritic structure of the cast metal can be seen under the thin transparent film (Figure 2, *a* and *b*). Black films are dense and contain a large number of cracks (Figure 2, *c* and *d*).

Inclusions of intermetallic phases containing iron, silicon and scandium, as well as a large amount of potassium and calcium, were found to accumulate on the surface of oxide films. As shown by the results of scanning X-ray microanalysis of fracture surfaces of the welds in the oxide film locations and complete fracture surfaces, the content of alloying and impurity elements depends upon chemical composition of the weld metal. Comparing spectra which reflect the quantitative content of elements in regions with and without the film showed no substantial difference. Therefore, the use of filler wires of different alloying

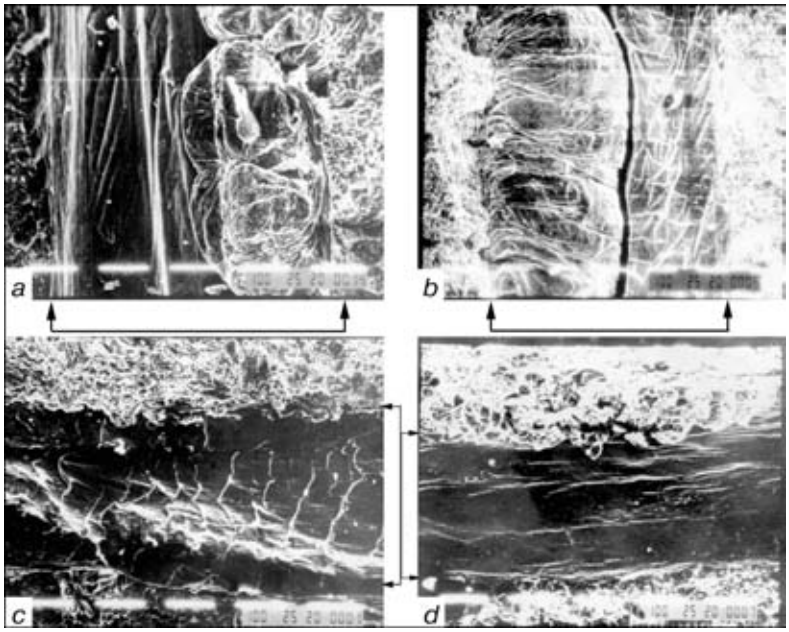

Figure 2. Microstructures of oxide films in fractures of the TIG welds on 1460 alloy plates made by using different types of filler wires (oxide film regions are indicated by arrows): *a* — Sv-AK5; *b* — Sv-AMg63; *c* — 1201Sc; *d* — Sv-1201 (×100)

systems does not exclude formation of oxide films in the weld metal, although it leads to changes in its composition.

As proved by the investigation results, formation of extended filamentary inclusions of oxide films in the central part of the welds made by the TIG method using a filler wire is a characteristic feature of Li-containing aluminium alloys. And if at least one of the butt welded aluminium alloy plates contains lithium, formation of defects is unavoidable. Analysis of fractures of macro- and microstructures of the weld metal definitely evidences that oxide films are located in the centre of the weld at a distance of about 1/3 from its root.

No extended defects were detected in fractures of the welds made by the TIG method at an increased current or in the helium atmosphere. Increase in the temperature of heating of a filler wire favours activation of the processes of cathodic and thermal destruction of the oxide film. It is for this reason that the probability of formation of extended oxide films in the weld metal is reduced in the case of using the asymmetric current with prevalence of the reverse-polarity pulse duration.

However, TIG welding of heat-hardening Li-containing alloys at increased parameters is unacceptable because it leads to overheating of the weld and HAZ metal.

It can be assumed that, since filler wires of the Sv-1201 and Sv-AMg63 types have a higher melting point than base metal, under conditions which ensure its melting a complete cathodic destruction of the oxide film on the filler wire surface will not occur and its non-destroyed fragments will go to the melt. They flow down to the bottom part of the weld pool under gravity, whereas the surface tension forces prevent them from being completely immersed. That is why, oxide inclusions are found in the central part of the weld pool in the majority of cases.

Results of comparative studies of temperature ranges of melting and solidification of welding consumables under non-equilibrium conditions, close to welding conditions, made it possible to establish that base metal has the largest melting temperature range and the lowest solidus temperature. Solidus temperature of alloy 1460 is not higher than 500 °C and varies from 460 to 490 °C. Solidus temperature of filler welding wires is 50–70 °C and liquidus temperature is 20–30 °C higher than those of the base metal.

Occurrence of this mechanism of formation of defects is proved by the fact that they are not formed in the case of making welded joints without a filler wire. If instead of a filler wire continuously fed to the weld pool we place a metal strip of an identical composition between the edges or on the edges, no defects will be formed in longitudinal fractures of the welds. It is likely that heating of the filler results in disappearance of temperature gradient at the interface between the filler wire and base metal melts. As a result, the remaining precipitates in the weld metal disperse in the bulk, rather than concentrate in a certain location. And even if fine particles of the film from the weld edges of base metal or from the applied strip of a filler metal do not destroy and get into the weld pool, they cannot initiate the surrounding accumulation of precipitated disconnected phases. As a result, no extended oxide film inclusions are formed.

To develop a method for prevention of formation of oxide films in the weld metal on Li-containing aluminium alloys, one should bear in mind that the oxide film is formed on the surface of the materials welded instantaneously within $\approx 1 \cdot 10^{-7}$ s [12]. The oxide film features an adsorption ability with respect to gases and moisture. Formulation and structure of the film vary with the heating temperature, and local

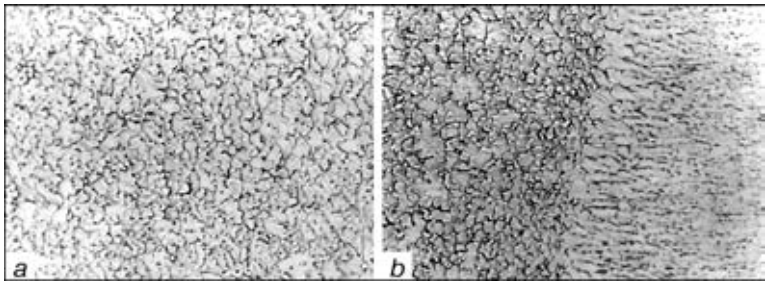

Figure 3. Microstructure of weld metal (*a*) and fusion zone (*b*) of welded joint made on the 1460 alloy plates by the TIG method using a preheated filler wire (×200)

cooling of the melt takes place at the interface between the «cold» filler wire and the weld pool.

Therefore, preheating of the filler wire favours decrease in nH_2O adsorbed by the oxide film and increase or levelling of temperature in the zone of contact of the filler wire and molten metal of the weld pool. The experiments conducted proved expediency of this operation.

In TIG welding of Li-containing aluminium alloys 1420 and 1460 the filler wire was preheated to 50–200 °C by the alternating current flow. Results of investigations of fractures of the welds made with a filler wire preheated to 150 °C showed that no extended defects were formed in the weld metal, independently of the filler wire alloying system.

As evidenced by metallography of macro- and microstructures of welded joints made on alloy 1460 by using a preheated filler wire, the resulting weld metal is characterised by a high quality, i.e. it has a fine-crystalline structure without oxide films or other types of defects (Figure 3).

It was established as a result of the investigations conducted that formation of extended filamentary inclusions of oxide films in welds made by TIG welding of Li-containing aluminium alloys using filler wires of the Sv-1201 and Sv-AMg63 types was caused by local cooling in the zone of contact of the filler wire and molten metal of the weld pool.

To avoid formation of such defects, it is necessary to provide favourable conditions for activation of the processes of destruction of oxide films on the surface of the filler wire being fed and on the weld edges. Therefore, it is recommended to perform welding of Li-containing aluminium alloys by using the asymmetric electric current with prevalence of duration of the reverse-polarity pulses and by preheating the filler wire prior to feeding it to the weld pool.

1. Fridlyander, I.N., Chuistov, K.V., Berezina, A.L. et al. (1992) *Aliminium-lithium alloys. Structure and properties*. Kyiv: Naukova Dumka.
2. Bratukhin, A.G., Redchits, V.I., Lukin, V.I. (1996) Prospects of application of aluminium-lithium alloys for aircraft stamped-welded structures. *Svarochn. Proizvodsvto*, **7**, 18–21.
3. Chien, P. (1998) Welding the space shuttle's Al-Li external tank presents a challenge. *Welding J.*, **6**, 45–48.
4. Ovchinnikov, V.V., Drits, A.M., Krylova, T.V. (1997) Technological peculiarities of production of aircraft welded structures from 1460 aluminium-lithium alloy. *Svarochn. Proizvodstvo*, **12**, 26–29.
5. Ryazantsev, V.I., Fedoseev, V.A., Mantsev, V.N. (1999) Welding of aluminium alloy car body. *Ibid.*, **11**, 36–42.
6. Poklyatsky, A.G. (2001) Peculiarities of formation of macroinclusions of oxide film in weld metal of aluminium alloys (Review). *The Paton Welding J.*, **3**, 36–38.
7. Varakina, P.P., Mironenko, V.V., Polyansky, V.M. (1979) Influence of maturing of 01420 alloy at room temperature on changes in surface layer phase composition. *Tekhnologiya Lyogk. Splavov*, **6**, 10–11.
8. Shiryaeva, N.V., Ovchinnikov, V.V., Gabidullin, R.M. (1987) Formation of pores in welding of aluminium-magnesium-lithium system alloy. *Avtomatich. Svarka*, **3**, 16–18.
9. Ryazantsev, V.I., Fedoseev, V.A., Grishin, V.V. et al. (1982) Influence of methods for preparation of mating surfaces on formation of pores in aluminium-magnesium-lithium alloy. *Ibid.*, **6**, 53–54.
10. Chayun, A.G. (1980) Welding of 01420 aluminium alloy with metallic flexible weld backing. *Ibid.*, **8**, 72–73.
11. Ilyushenko, R.V. (1990) Influence of pulsed argon-arc welding parameters on porosity of 1420 alloy joints. *Ibid.*, **9**, 27–30.
12. Rabkin, D.M. (1986) *Metallurgy of fusion welding of aluminium and its alloys*. Kyiv: Naukova Dumka.

COATED ELECTRODES OF UANA GRADE FOR WELDING AND SURFACING ALUMINIUM AND ITS ALLOYS

N.V. SKORINA and **V.S. MASHIN**
The E.O. Paton Electric Welding Institute, NASU, Kyiv, Ukraine

The paper gives the characteristics and some features of the technology of manufacturing coated electrodes for manual arc welding of aluminium and its alloys, developed at the PWI. The need is shown for completion of chemical reactions, proceeding in preparation of the coating mass to stabilize it during extrusion. The optimal temperature of electrode baking is established, which provides a low susceptibility of coatings to absorption of atmospheric moisture.

Key words: *coated aluminium electrodes, coating mass, heat treatment modes, aluminium alloys, welding modes, mechanical properties*

Over the last years it has been more and more often necessary to restore and repair parts, components and structures of agricultural machinery, cars, pipelines and tanks of cast and wrought aluminium alloys for various purposes. The widely used process of tungsten and consumable electrode argon-arc welding (surfacing) requires a thorough preparation of the edges to be welded and the electrode wire, expensive tungsten electrodes, inert gases, sophisticated welding equipment and highly qualified welding operators.

The simplest and least expensive process of welding and repair of aluminium items is coated-electrode welding, which can be readily applied in the field conditions, and even in small repair shops.

Analysis of published data showed that the electrodes for manual arc welding and surfacing of aluminium and its alloys are ever wider applied in the leading industrially-developed countries. Practically all the known foreign companies, manufacturing electrodes (Oerlikon, ESAB, Castolin, Thyssen, Böhler, Kestra, UTP, etc.) have several grades of aluminium electrodes in their output programs, and their number is rising every year. Ukrainian enterprises also have positive experience of application of electrodes, produced by these companies. However, the high cost of the electrodes limits their application in the required volumes.

In CIS countries mostly coated electrodes of grades OZA-1, OZANA-1 (for welding commercial purity aluminium) and OZA-2, OZANA-2 (for welding silumins), which are manufactured by Company «Spetselektrod», Moscow, are used by industry. They, however, do not meet the modern requirements, because of the low strength and high hygroscopicity of the coating, high metal spatter in welding, poor separability of the slag crust, low quality of welds and need for a high-temperature preheating of the metal being welded.

The E.O. Paton Electric Welding Institute of the NAS of Ukraine developed coated electrodes of UANA grade [1] for arc welding and surfacing of parts and structures of wrought and cast aluminium alloys. The coating base is made up of fluorides and chlorides of alkali and alkali-earth metals. As liquid glass — the traditional binder for coating of electrodes, designed for welding steel, coagulates under the influence of the soluble chlorides and fluorides of alkali and al-

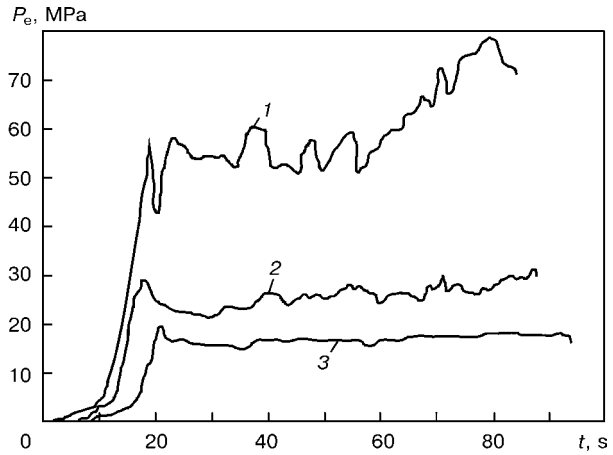

Figure 1. Curves of extrusion of the electrode coating mass P_e of electrodes of UANA series during its stirring t (drawing die of 4×40 mm size at mass consumption $Q = 1$ cm^3/s): *1* — 26; *2* — 35; *3* — 45 min

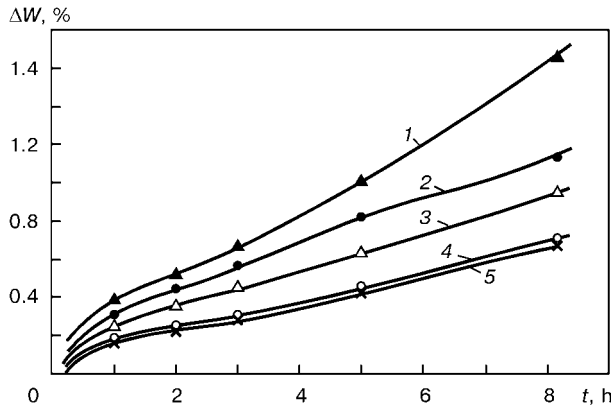

Figure 2. Kinetics of absorption of atmospheric moisture by the coating of electrodes of UANA series, baked at different temperatures: *1* — 100; *2* — 150; *3* — 200; *4* — 250; *5* — 300 °C

Table 1. Main characteristics of coated electrodes for welding aluminium and its alloys

Electrode grade	*Wire grade*	*Wire diameter, mm*	*Alloys being welded*	*Recommended preheating of alloys, °C*
UANA-1	Sv-A5	3.15; 4.0; 5.0; 6.3	AD00; AD0; AD1; AD	200–350
UANA-2	Sv-AK5	3.15; 4.0; 5.0; 6.3	AD31; AD33; AD35; AL2; AL4; AL9, et al	100–300

Table 2. Modes of welding electrodes of UANA series

Parameter	*Electrode diameter, mm*			
	3.15	*4.0*	*5.0*	*6.3*
Recommended* values of current in the following weld position, A:				
downhand	80–110	100–130	130–160	160–180
vertical	80–100	90–130	120–150	150–170
Thickness of metal being welded, mm	3–5	4–10	8–14	12–16
Recommended* preheating temperature, °C	100–200	100–250	100–350	100–350

*For welding butt joints of sheet structures.

kali-earth metals and loses its binding properties, a binder, compatible with strong electrolytes, is used in the new electrodes.

X-ray structural analysis in X-ray diffractometer DRON-2 demonstrated that the process of coating mass preparation is accompanied by chemical reactions, proceeding between the coating components. During interaction, slightly soluble salts are formed and solidification moisture is released. Optimal conditions (mixing duration, method of feeding and dose of the binder) are selected, which enable the running of the reaction and its completion by the end of the stage of coating mass preparation. This eliminates the risk of lumping and provides the required stable in time consistence of the coating mass (Figure 1). Ready coating mass is characterised by a smooth extrusion mode in electrode extrusion (Figure 1, curve *3*), and a sufficient strength of the coating on the electrode.

Hygroscopicity of the electrode coatings was determined by the increase of their weight ΔW as a result of moisture absorption in the hydrostat at constant moisture φ, which was equal to 84 % (saturated solution of potassium bromide at room temperature).

Optimal conditions have been selected for electrode heat treatment. Electrode baking temperature T_b = 250 °C. In this case, a minimal hygroscopicity of the coating is achieved. Further increase of baking temperature does not affect the hygrosorbtion ability of coatings (Figure 2), but leads to an abrupt increase of power consumption for electrode manufacture.

Table 3. *HRB* hardness of the deposited metal in welding alloy AL2 with coated aluminium electrodes

Electrode grade	*HRB at T, °C*	
	20	*200*
UANA-2 (5.8 % Si)	57–60	57–62
2101 Super (8.8 % Si)	59–62	60–62
OK 96.50 (9.1 % Si)	68–70	69–70

Note. Weight fraction of silicon in the base metal is 11.4 %, *HRB* hardness of alloy AL2 at the temperature of 20 °C is 49–50.

Increase of baking temperature up to 250 °C improves the welding-technological properties of electrodes, in particular promotes a spray transfer of electrode metal. Duration of short-circuits, determined by information-measurement system ANP-2 [2] is lowered from 13.7 (T_b = 100 °C) to 12 μs (T_b = 250 °C). The same transfer parameters are found for similar-purpose electrodes of 2101 Super grade of Castolin Company (12 μs), which were tested in parallel.

Main characteristics of aluminium electrodes of UANA series and welding modes are given in Tables 1 and 2. Deposition rate is 6.0–6.8 g/(A·h). Electrode consumption per 1 kg of deposited metal is not more than 2.0–2.2 kg.

It is recommended to preheat metal edges by gas flame or in a furnace prior to welding. Preheating temperature is selected, depending on the alloy grade and thickness of parts being welded (Table 2). It should be noted, that for aluminium alloys the welding modes and preheating temperature may only be given tentatively, as, considering the high heat conductivity of the metal, selection of welding parameters is greatly affected by the configuration and dimensions of items, in addition to the metal thickness and its composition. If at selection of preheating temperature the temperature values for the alloy grade (Table 1) and for the thickness of the metal being welded (Table 2) differ from each other, the value of preheating temperature, recommended for the alloy grade, is selected.

Welding with aluminium electrodes is performed at DCRP. Welding rectifiers of VDU-306 type with a falling volt-ampere characteristic and smooth adjustment of arc voltage are used as power sources. At two-sided welding of metal up to 10 mm thick edge preparation usually is not performed. Slag is removed, using steel brushes and hot water. Mechanical prop-

Table 4. Mechanical properties of aluminium alloy joints, produced by coated-electrode manual arc welding.

Alloy grade	*Electrode grade*	*Preheating temperature, °C*	*Mechanical properties*		
			σ_t, *MPa*	a_n, *J/cm²*	α, *deg*
AD1	UANA-1	20	73.6–77.2 / 75.4	33–40 / 39	160–170 / 165
		200	72.4–78.6 / 75.2	43–45 / 44	180 / 180
AD33	UANA-2	20	188.4–202.2 / 198.4	12–15 / 13	110–126 / 118
		150	192.6–202.2 / 198.4	15–17 / 16	155–165 / 160
	OK 96.50	20	188.4–202.2 / 198.2	11–14 / 12	102–114 / 110
		150	196.8–202.2 / 198.8	14–17 / 16	145–152 / 146
AL9	UANA-2	20	172.4–180.6 / 176.2	1.1–1.3 / 1.2	10–12 / 11
		200	180.2–195.6 / 186.4	1.9–2.2 / 2.0	13–15 / 14
	2101 Super	20	178.2–186.4 / 182.8	1.2–1.4 / 1.3	10–12 / 11
		200	182.6–198.4 / 190.2	2.0–2.4 / 2.2	12–15 / 14

Note. The numerator gives minimum and maximum values, the denominator gives the average values by the results of testing 5 to 9 samples.

erties of the joints, produced by coated-electrode manual arc welding, were studied on sheets of wrought alloys of AD1 and AD33 grade 6 mm thick and cast alloys of grade AL2 and AL9 8 mm thick. Foreign-made aluminium electrodes of OK 96.50 grade of ESAB Company and 2101 Super grade of Castolin Company were also used for comparative evaluation of electrode quality. In all cases electrode wire diameter was $\cong 3.2$ mm. One-sided manual arc welding was performed at room temperature and with base metal preheating to 200 °C. Deposited metal hardness was determined in Rockwell instrument, using a sphere of 1/16 inch diameter at 600 N load.

Investigations showed that base metal hardness of alloy AL2 is by 8 to 10 units lower than that of the deposited metal (Table 3). A somewhat higher hardness of welds, produced with electrode of OK 96.50 and 2101 Super grades, is due to a higher content of silicon in them.

It is also found that preheating of the alloys being welded reduces the total content of voids in the welds and somewhat improves the mechanical properties of the joints (Table 4). The welded joints (with weld convexity from one or two sides) fail in the zone of fusion of the weld with the base metal or in the base metal (alloy AD33). After removal of the convexity (from both sides), the samples fail in the weld.

UANA electrodes provide a sufficient stability of arcing, good weld formation, also in the vertical position, easy separation of the slag crust and high values of mechanical properties of the weld metal. Electrode coating is characterized by a low hygroscopicity and high mechanical strength.

Electrodes are supplied in a moisture-proof packing. Prior to welding the electrodes are baked at the temperature of 150–200 °C for 1.0–1.5 h. Baked electrodes should be stored in a moisture-proof packing. The time between baking and welding should not exceed 24 h. Experimental production of small batches of new electrodes (of up to 200 kg) has been mastered at the E.O. Paton Electric Welding Institute of the NAS of Ukraine, and the industrial technology of manufacturing electrodes UANA-1 and UANA-2 has been introduced in Company «Spetselektrod», Russia.

1. Skorina, N.V., Mashin, V.S. (2000) Coated electrodes for manual arc welding of aluminium and its alloys. *Svarshchik*, **2**, 26, 32.
2. Pokhodnya, I.K., Zaruba, I.I., Andreev, V.V. et al. (1985) Application of ANP-2 system for measurement of electric and time parameters of welding circuit. In: *SMEA Inform. Mat.*, Issue 2.

COMBINED METHOD FOR PLASMA AND ARC WELDING USING DIFFERENT-POLARITY CURRENT PULSES (HIDRA-PROCESS)

N.M. VOROPAJ and **V.A. MISHENKOV**
The E.O. Paton Electric Welding Institute, NASU, Kyiv, Ukraine

The process of combined plasma and arc welding of aluminium alloys 10–30 mm thick was developed. The process provides for feeding pulses of current (reverse polarity) to the first and third tungsten electrodes as welding progresses, and, in the intervals between them, pulses of current (straight polarity) to the central plasmatron. Design of the device for realisation of the process and its technological capabilities are given.

Key words: *arc welding, plasma welding, aluminium alloys, combined method, metal penetration, weld shape, properties of welded joints*

The term «Hidra» which was first introduced into welding terminology in 2001 [1–3], means utilisation of several welding heat sources (plasma + arc, laser + arc), forming either common or separate weld pools. The plasma-arc process «Hidra» realised by the German Company «Münchengladbach», involving two or three TIG torches and one plasmatron, used for high-speed longitudinal welding of stainless steel pipes 0.8–3.5 mm thick is described in [4]. Ingenious designs of a one-piece unit of torches and plasmatron, electromagnetic and gas stabilisation of the arcs, and microprocessor systems for control of the technological cycle made it possible to achieve a welding speed of up to 800 m/h at an excellent quality of the pipes and continuity of operation of the equipment.

The E.O. Paton Electric Welding Institute developed the «Hidra» welding process (Figure 1) for single-pass welding of light metals and alloys of increased thickness (10–30 mm), involving two tungsten electrodes *1* and *3* and plasmatron *2* located between them. The process provides for feeding of pulses of the reverse-polarity (RP) current to the tungsten electrodes and, in the intervals between them, pulses of the straight-polarity (SP) current to the plasmatron. The role of the arc of the first tungsten electrode *1* is reduced to cathode cleaning of surfaces of weld edges and filler wire from oxides, melting down of the filler wire and preliminary heating of the base metal. Plasmatron *2* supplied with relatively high-power pulses of the SP current provides deep penetration of the metal welded. The arc of electrode *3* serves for the improved weld formation, elimination of end undercuts and ensuring the smooth weld to base metal transition.

Specialised power supply (Figure 2) was developed to realise the «Hidra» welding process. The power supply comprises two welding transformers *1* and *2*, the secondary windings of which are connected with their beginnings via diodes *3–6* to electrodes *7* and *9* and to plasmatron *8*, and with their ends via regulated active resistors *10* and *11* and high-frequency choke *12* to workpiece *13*. The power supply circuit includes starting arc exciter *14* connected to each of the electrodes, and two units *15* and *16* serving to maintain the stable arc between the electrodes and the workpiece. The starting exciter is switched off after igniting both arcs, and their further repeated ignition is done at the beginning of each positive half-

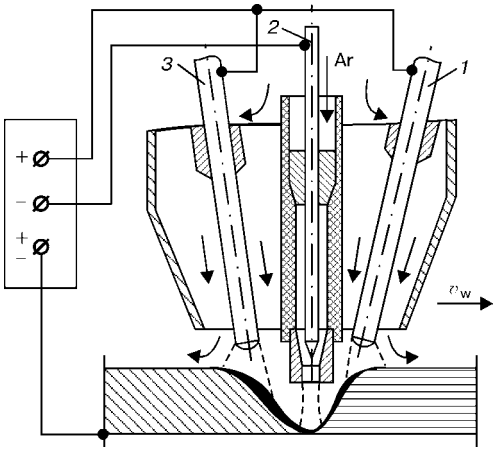

Figure 1. Schematic of the plasma-arc welding process «Hidra» (see designations in the text)

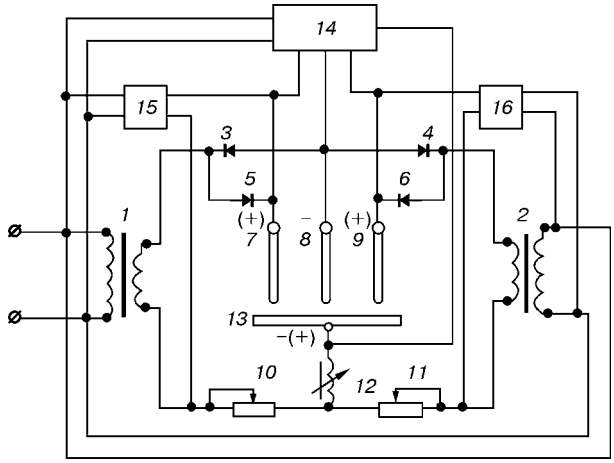

Figure 2. Block diagram of the plasma-arc welding device (see designations in the text)

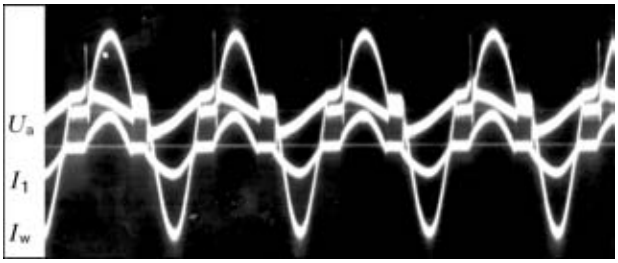

Figure 3. Oscillograms of welding current I_w, current in the primary winding of the transformer, I_1, and voltage in the arc gap, U_a, at $I_{SP}/I_{RP} = 2/1$

period between electrodes *7* and *9* and workpiece *13* using units *15* and *16*. Choke *12* is used to protect welding circuits from high-frequency currents.

The described power supply and one-piece unit of torches and plasmatron provide the stable welding process at an asymmetric different-polarity current with almost no magnetisation of secondary windings of the welding transformers (Figure 3). Increase in the current asymmetry factor leads to redistribution of power of heat sources in the anode and cathode parts of a period to increase heat released in the base metal and decrease heat consumed for heating of tungsten electrode [5].

Technology tests of the «Hidra» welding process were conducted by making single-pass butt joints in Al-6.2Mg alloy (AMg6). For metal 25 mm thick the first (as welding progresses) tungsten electrode 6 mm in diameter was supplied with positive current pulses (I_{ef} = 150 A) relative to the workpiece. The second tungsten electrode was supplied with the same current pulses. In the intervals between them the SP current pulses (I_{ef} = 300 A) were fed to the plasmatron. The welding speed was 12 m/h, the filler wire diameter was 3 mm, and the total shielding and plasma gas (argon) flow rate was 30 l/min. Macrosections of the resulting welded joints are characterised by a favourable weld shape (Figure 4). The weld width is commensurable with thickness of the metal welded. Mechanical properties of the welded joint metal are at a level of those of the base metal after annealing. After extra tests, the plasma-arc welding process «Hidra» can be recommended for the manufacture of rocket casings, aluminium tanks used in transport and chemical engineering, hovership hydrofoils and other parts of aluminium alloys. Of practical interest is to study technological capabilities of the developed process for welding carbon and alloyed steels, as well as other non-ferrous metals and alloys.

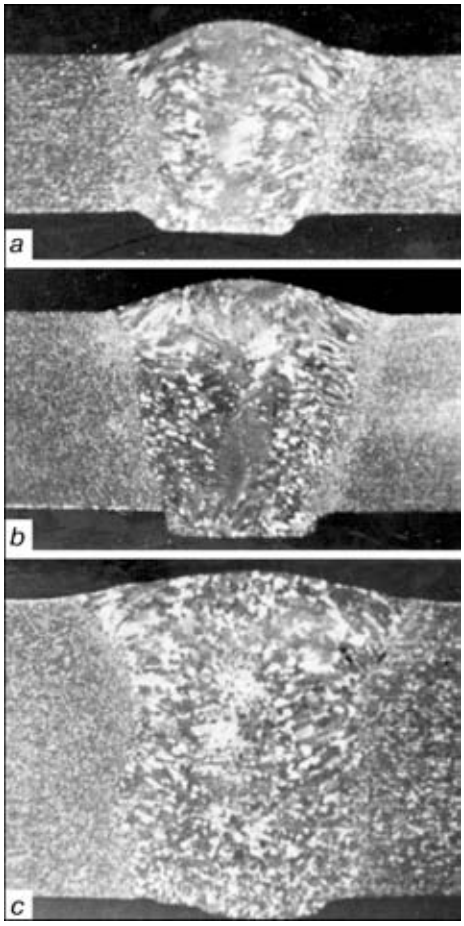

Figure 4. Macrosections of the AMg6 alloy welds 10 (*a*), 14 (*b*) and 25 (*c*) mm thick

1. Wieschemann, A. (2001) *Entwicklung des Hybrid- und Hidra-Schweiβverfahrens am Beispiel des Schiffbaus*. Aachen.
2. Dilthey, V., Wieschemann, A., Keller, H. (2001) CO_2-Laser-MSG-Hybrid- und Hidra-Schweiβen. Innovative Fügeprozesse für den Schiffbau. *Laser Opto*, **2**, 56–63.
3. Dilthey, V., Keller, H. (2001) Einsatz der Hybrid- und Hidra-Schweiβverfahren zur Wirtschaftlichkeitssteigerung im Schiffbau. *Vorträge der Gleichnamigen Groβen Schweiβtechnischen Tagung*, Essen, Sept. 11–13, 2001. Düsseldorf: DVS.
4. Czuyack, A. (2001) Stand und Entwicklungstendenzen bei der Herstellung Längsnahthgeschweister Qualität — Edelstahlrohre. *Ibid*.
5. Rabkin, D.M., Voropaj, N.M., Mishenkov, V.A. (1978) Energy characteristics of the welding process with asymmetric different-polarity current. *Avtomatich. Svarka*, **4**, 5–10.

METHOD OF DETERMINATION OF CORRECTIVE ACTIONS IN STATISTICAL CONTROL OF WELDING PROCESSES

I.A. TARARYCHKIN
East-Ukrainian National University, Lugansk, Ukraine

Procedure of a simultaneous construction of charts of control of condition and relative accuracy for defining corrective actions directed to the recovery of a disturbed accuracy of the technological process is offered. Procedure capabilities are shown on example of making a circumferential weld using technology of narrow-gap arc welding.

Key words: *narrow-gap welding, statistical control, quality of products, process accuracy, procedure, corrective actions, control charts, criteria of accuracy*

Statistical control of welding technological processes is one of the effective means of quality assurance of products [1, 2]. Selection of a definite method of control is realized depending on conditions of production and nature of quality characteristic being controlled. For control characteristics having a quantitative nature in the conditions of large-scale and mass production, the processes are controlled using control charts of arithmetic mean values, root-mean-square deviations and ranges [3].

At single-piece and small-scale production the statistical control of process should be made using charts of condition control which allow timely detection of accuracy disturbance of the process being controlled [4]. However, the direct use of condition control charts does not answer the question about the proper selection of a corrective action for the recovery of the disturbed accuracy.

The method described in the present publication makes it possible to define the nature of necessary corrective actions directed to the recovery of the disturbed accuracy of the controlling process, if the statistical control is made using the condition control charts. The designations used by us correspond to those given in the present [4].

Let us consider the specifics of proceeding three different technological processes given in Figure 1 (schemes *1–3*). It should be noted that the use of an integrated criterion of accuracy $g_S = \theta + \eta$ for construction of condition control charts in accordance with the procedure given in work [4], provide the same system of broken lines for moments of time t_1, t_2, ... t_5 in description of condition of the mentioned processes (Figure 2, *a*). The accuracy of all these processes at the moment of time t_5 is occurred to be disturbed by different means, however, the direct use of criterion g_S cannot reveal the cause of disturbances.

To formulate the quantitative criterion which can characterize the condition of process controlled near the boundary of limiting condition AB (see Figure 1), it is necessary first of all to define the terminology used. Thus, the characteristics of process accuracy θ and η will be further considered commensurable, if their values are differed by not more than twice. Then the region E_2 of commensurable values θ and η in plane $\theta 0 \eta$ will be located between two rays described by equations $\theta = 0.5\eta$ and $\theta = 2\eta$.

Position of arbitrary point Z_i characterizing the current condition of the process with respect to regions E_1, E_2, E_3, can be defined using criterion of a relative accuracy of process g_E:

$$g_E = \frac{\theta}{\eta} = \frac{\sqrt{2}\,|\,\bar{x} - W_0\,|}{S\,\Phi^{-1}(P)}.$$

For region E_1 the condition $g_E \geq 2$ is fulfilled. Transition of process into this region should be considered as a result of preferential scattering of the controlling characteristic of quality.

For region E_3 the condition $g_E \geq 0.5$ is fulfilled. Transition of process into this region should be considered as a result of preferential shifting of a center of scattering of the controlling characteristic of quality.

In fulfillment of condition $0.5 < g_E < 2$ (region E_2 of values θ and η) a commensurable increase in values of coefficients of shifting setting and scattering leading to the disturbance of the process accuracy takes place.

Defined approaches make it possible to formulate the following procedure of determination of nature

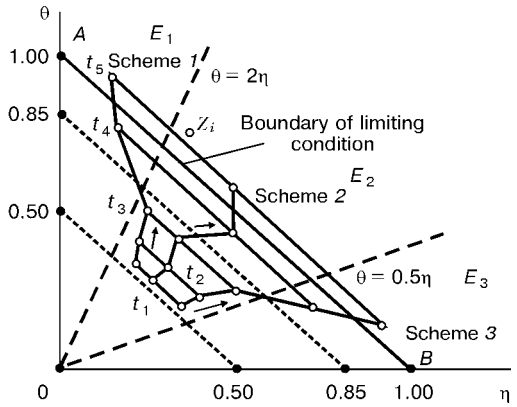

Figure 1. Different schemes of proceeding of technological processes presented in system of coordinates $\theta 0 \eta$

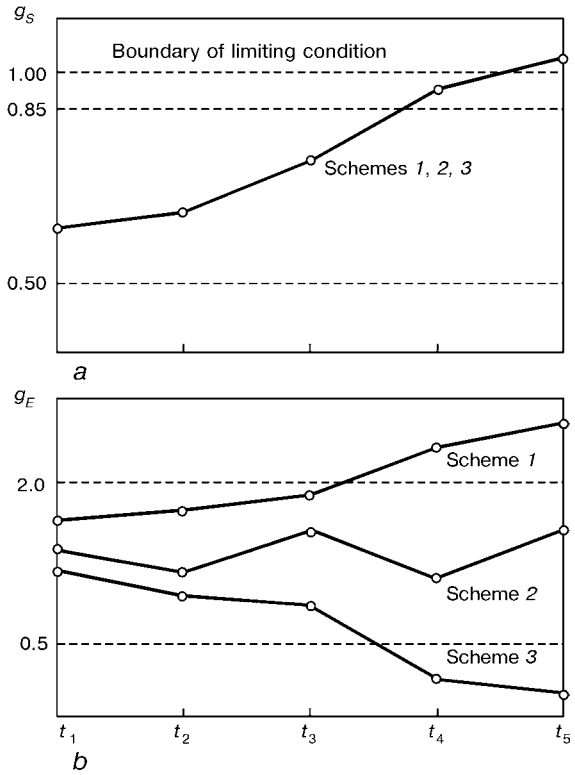

Figure 2. Control charts of condition (*a*) and relative accuracy (*b*) of processes proceeding by different schemes

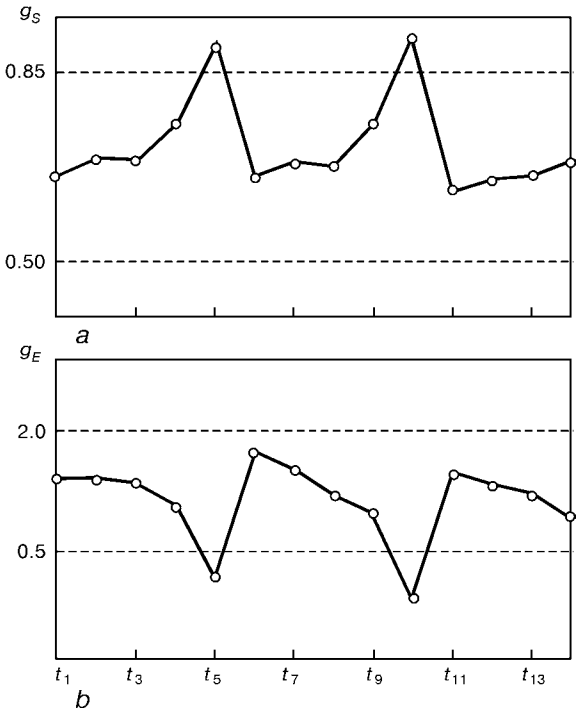

Figure 3. Control charts of condition (*a*) and relative accuracy (*b*) of multidimensional process of narrow-gap welding with a control by welding speed

of control actions at statistical control of technological processes:

- condition of process is evaluated periodically for set moments of time t_i with a construction of control chart of condition in the form of a system of lengths, joining points $g_S(t_i)$ successively [4];
- for the same moments of time t_i a simultaneous construction of chart of control of a relative accuracy of the process in the form of lengths joining points $g_E(t_i)$ successively is fulfilled;
- in case, if the condition $g_S(t_j) > 0.85$ is fulfilled from the moment of time t_j, then to recover the process accuracy it is necessary to make corrective actions whose nature is determined by appearance of the chart of control of a relative accuracy (if $g_E(t_j) \geq 2$, then these actions should be oriented mainly to the decrease in scattering of values of controlling characteristic of quality; if $g_E(t_j) \leq 0.5$, then these actions should be oriented mainly to the decrease in shifting of X value relative to a center of a design field of tolerance; if $0.5 < g_E(t_j) < 2$, then the taken measures should be directed to a simultaneous decrease both in value X scattering and also for recovery of its position relative to the middle of tolerance field).

Combined form of control charts of relative accuracy $g_E(t_j)$ for processes proceeding by schemes *1–3*, is given in Figure 2, *b*. It is seen that the nature of corrective actions directed to the recovery of disturbed accuracy for each of processes considered, is different and set in accordance with the described procedure.

The offered method of a combined construction of control charts of condition and relative accuracy promotes the increase in efficiency of statistical control of welding technological processes in the conditions of single- and small-scale production, that can be explained by a definite example.

To provide the quality formation of a multilayer circumferential weld in a narrow-gap welding of shell of 1 m inside diameter and 75 mm wall thickness is possible only in the conditions of a continuous control of condition of the multidimensional process [4]. Here, the maintenance of condition parameters in a preset range is an important condition of providing quality and prevention of formation of shape defects (undercuts and lack of fusion).

Change in values of condition parameters in the welding process can be stipulated both by factors of a random nature and also by systematic causes. Studying the process of a continuous filling the groove, it should noted that the change in values of welding speed v_w can be connected not only with variations in angular speed of a rotation drive and non-coincidence of rotation axis with the axis of a cylindrical shell, but also with a gradual vertical shifting of the torch. This shifting in groove filling can lead to the increase in v_w by 15 % with respect to the rated value.

In accordance with requirements of the technology the deviation of welding speed from a rated value by absolute value should not exceed 6 %. By this reason, the parameter $X = v_w$ should be controlled in the process of welding, making, when necessary, the corrective action.

Charts of control of condition and relative accuracy of the process are presented in Figure 3. As is follows from the Figure the process approaching to the limiting condition boundary was recorded at the moments of time t_5 and t_{10}. The control actions in both cases were due to the recovery of the process

accuracy by an appropriate decrease in angular speed of drive of the shell rotation. In addition, the condition of its satisfactory proceeding with an accuracy control by the welding speed was not disturbed during the whole period of the groove filling.

The above-given example demonstrates clearly those additional possibilities which appear in a combined use of formulated statistics g_S and g_E in documentation, evaluation of condition and prediction of the process progress. However, the effective use of criteria g_S and g_E is occurred to be possible in those cases when there are no requirements to documentation of the process progress, as their current values cannot be used in the solution of problems of in-process control and control of welding processes in a real time.

1. Volchenko, V.N., Gurvich, A.K., Majorov, A.N. et al. (1975) *Welding quality control*. Moscow: Mashinostroenie.
2. Goncharov, E.N., Kozlov, V.V., Kruglova, E.D. (1987) *Quality control of products*. Moscow: Standart.
3. Houler, L., Howell, J., Gold, B. et al. (1984) *Statistical methods of quality control of products*. Moscow: Standart.
4. Tararychkin, I.A. (2001) Statistical regulation of welding technological processes using the method of construction of charts of condition control. *The Paton Welding J.*, **10**, 28–31.

DISPERSION-STRENGTHENED HEAT-RESISTANT SOLDER

V.F. KHORUNOV, O.M. SABADASH, S.V. MAKSIMOVA and **B.V. STEFANIV**
The E.O. Paton Electric Welding Institute, NASU, Kyiv, Ukraine

Methods for production, properties and microstructure of dispersion-strengthened solder Sn-39Pb were studied. Short-time strength of soldered joints made by using the dispersion-strengthened solder, depending upon the content of the strengthening phase, was evaluated.

Key words: *soldering, soldered joints, short-time strength, dispersion-strengthening phase, microstructure, composite solder, copper*

Modern electronic devices should reliably operate under high thermal loads, i.e. up to 120–150 °C. This requires that a certain structure be formed in the joining zone to ensure strength at a working temperature. For this the solder should not have an excessive melting point to provide good formation of soldered joints.

High-temperature strength of soldered joints can be increased by different methods: by treating the joints at an increased temperature to provide the «diluted» seam [1], by using solders containing components-depressants which are partially evaporated during soldering [2], and ensuring conditions under which the depressants could combine to form stable chemical compounds [3] to increase soldering temperature of a joint.

The required high-temperature strength of soldered joints can be achieved also by using new soldering consumables which consist, unlike the available solders, of a metal matrix (the solder proper) and strengthening particles (finely dispersed particles of metals, non-metals or chemical compounds).

Adding 1, 3, 5, 10 and 15 % nickel with a purity of 99.94 % in the form of powder to solders of the Sn–Pb system with a tin content of 40, 63 and 90 wt.% was found [4] to cause an increase of 1.5 times (45 MPa) in shear strength of the joints made by using the Sn–27Pb–10Ni solder, compared with the joints made by using Ni-free solders. A marked increase in strength of the soldered joints at normal temperature was seen in adding more than 5 % Ni to the Sn–Pb solder.

The strengthened soldered joints were made by using the eutectic solder Sn–39Pb, which was achieved due to an application of flux containing 20–80 % copper powder in the form of fine particles less than 44 μm in size [5]. The flux was applied prior to soldering on the mating surfaces of workpieces. After melting the solder melt spread and wetted particles of the strengthening phase to form a composite soldered joint. Fracture of the joints made by using solder with 66 % copper powder occurred under an assigned load (5 MPa) after 4000 hours, whereas the joints made by using the Sn–50Pb solder and subjected to the same load fractured after 1500 hours.

Therefore, an addition of components (particles) having a gradient of chemical potential relative to the matrix alloy makes it possible to solve a set of special problems: improve electrical conductivity, increase strength, achieve required corrosion or radiation resistance, etc.

Strengthening is provided by addition of finely dispersed particles of a certain chemical nature to the matrix alloy. Besides, one should take into account that the amount of the strengthening phase particles should be relatively small to maintain technological properties of the solder. Two strengthening mechanisms were offered to increase high-temperature strength of the eutectic Sn-39Pb solder: age-hardening and dispersion-strengthening. In the second case the

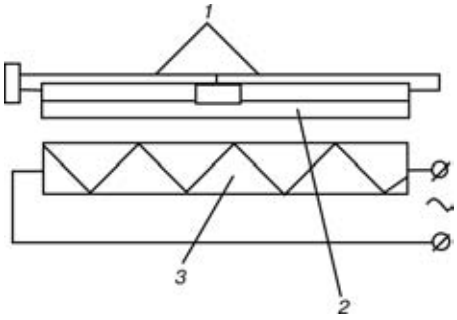

Figure 1. Schematic of the device used for soldering samples: *1* — butt samples made from copper; *2* — aluminium plate; *3* — heater

potentialities of using individual elements and intermetallic compounds to form finely dispersed phases in the matrix alloy are substantially widened. Shape, degree of dispersion and relative location of the strengthening phase depend upon many factors associated with chemical composition of the melt and solidification conditions.

In accordance with the chosen area of investigations, it is necessary to identify methods for metallurgical dissolution and distribution of strengthening particles of intermetallic Ni_3Sn_4 in the metal matrix of the eutectic solder (Sn–39Pb), as well as determine the short-time strength characteristics of the copper joints at room and increased (120 °C) temperatures made by using the developed solders.

Two melting processes using the high-frequency unit VChG1/0.066 with a power of 60 kV·A and working frequency of 66 kHz (under a layer of the PV209 flux) were tried out to identify the optimal method for adding strengthening particles to the matrix of the eutectic solders:

- addition of solid strengthening particles less than 10 μm in size to the matrix melt within a temperature range of 600 to 750 °C during melting of the melt in a graphite crucible, involving electromagnetic stirring (the solid strengthening particles–eutectic solder melt system);
- addition of strengthening particles by joining two liquid melts at a temperature above the liquidus temperature of materials of the strengthening particles (the molten strengthening particles–eutectic solder melt system).

Samples of solders were cut by a mechanical method. The samples were cleaned and polished using abrasive pastes, washed in acetone and ethyl alcohol, dried and etched to reveal a fine structure.

Metallographic examinations of initial alloys of the Sn–Pb system were carried out using optical scanning electron microscopy (optical microscope «Neophot-8» and scanning electron microscope ISM-840).

Butt soldered samples of copper MI (99.9 % Cu) with a diameter of 1.8 mm and 80 mm long, made by using wire PETV-2 and covered with the double layer of a heat-resistant lacquer, were used. Soldering of the butt copper samples was carried out using a special device (Figure 1). Copper billets for simultaneous soldering of three samples were located on a heated plate of appropriate dimensions, made from a material

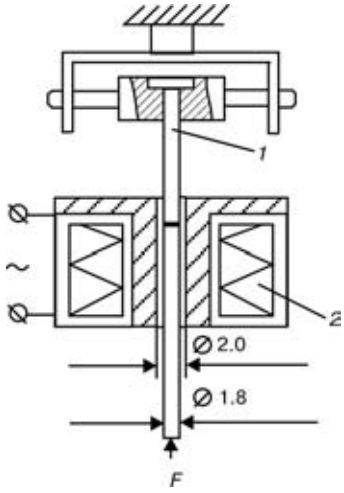

Figure 2. Schematic of loading of soldered joints: *1* — butt joint samples; *2* — heater

with a high heat capacity and diffusivity, i.e. aluminium, which could not be wetted with the solder at the soldering temperature. The temperature to which the plate was heated was maintained at a constant level, i.e. (230 ± 3) °C. The time of heating of the samples to the soldering temperature, i.e. 60 s, was found experimentally. The flux (orthophosphoric acid) was deposited on the solder billets by dipping, and then the solder was manually introduced into the soldering gap 0.1–0.3 mm in size. The time of soldering from the moment of filling the soldering gap with the solder was not more than 5 s. Then the samples in the soldering zones were cooled with an aqueous-alcohol solution.

After visual examination the soldered samples were subjected to tensile tests (Figure 2) using the testing machine RMU-0.05 (maximum tensile load — 500 N). The rate at which the load was applied with all the testing methods was equal to 1 mm/min. Tensile strength of the soldered joints was determined from the results of testing six samples. The test temperature for the Sn–Pb solders was 120 °C.

X-ray microanalysis revealed that microstructure of the matrix alloy Sn–Pb was the Sn- and Pb-base solid solution.

The first method of melting alloys, where the solid finely dispersed particles were added to the liquid melt, failed to achieve the purpose. The particles were

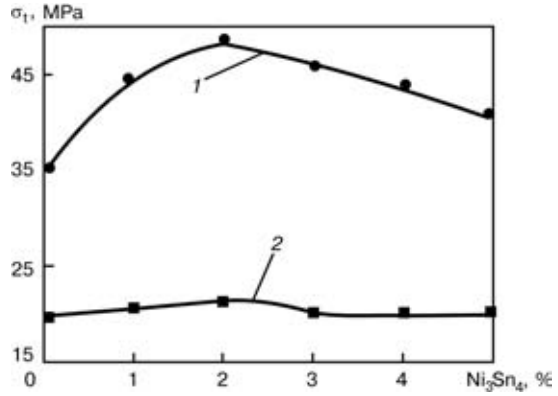

Figure 3. Short-time strength σ_t of soldered joints at different test temperatures: *1* — 120; *2* — 20 °C

distributed non-uniformly and formed coarse conglomerates. The second method managed to provide a uniform distribution of the strengthening phase, i.e. dispersed particles of intermetallic Ni_3Sn_4.

Results of comparative tests to short-time strength of the copper joints made by using the POS-61 (wt.%: St — 59.0–61.0; Sb — ≤ 0.8; Pb — balance) and experimental solders are shown in Figure 3. It can be concluded on the basis of the results obtained that the developed composite solder made it possible not only to provide the required strength of the soldered joints at a temperature of 120 °C, but also to increase this strength at room temperature. The maximum increase in strength at 120 °C was noted in the joints made with the solders containing 2 % strengthening particles of intermetallic Ni_3Sn_4. Further increase in the content of the intermetallic strengthening particles is undesirable, as this leads to a marked decrease in strength of the soldered joints.

CONCLUSIONS

1. A promising method for producing composite solders with a sufficiently uniform distribution of the finely dispersed intermetallic phase in the matrix was identified.

2. The use of the composite solder Sn–39Pb containing 2 % strengthening intermetallic particles was found to provide the required strength of the soldered joints at 120 °C.

1. Schweward, G.E., Adam, R. (1972) Research on re-melt temperature in any system of filler metals utilized in industry. In: *Proc. of 1st Int. Conf. on Brazing and Soldering*. London: Brit. Assoc. Braz. and Sold.
2. Breds, H. (1964) Development of the partially volatile brazing filler metals. *Welding J.*, **2**, 63–65.
3. Kawakatsu, I. (1973) Development of brazing filler metals and technology. *Kinzoku*, **5**, 60–64.
4. Lashko, S.V., Lashko, N.F. (1988) *Brazing of metals*. Moscow: Mashinostroenie.
5. Raynes, B., Pike, P., Pescatrice, M. *Reinforced soft solder joints*. Pat. 3488071 USA. Publ. 06.01.70.

INDEX OF ARTICLES FOR TPWJ'2002, No. 1–12

Activators

A-TIG welding of structural steels for power engineering applications (Bajic D.R., Savitsky M.M., Melnichuk G.M. and Lupan A.F.) 9

Press welding of pipes using activating materials (Pismenny A.S. and Prokofiev A.S.) 7

Procedure and parameters of A-TIG welding of structural steels (Bajic D.R., Melnichuk G.M., Lupan A.F. and Savi-tsky M.M.) 10

Alloying

Features of pulsed-plasma alloying of the surface of iron-base alloys (Tyurin Yu.N., Zhadkevich M.L., Gubenko B.G. and Kolisnichenko O.V.) 3

Alloys

Aluminium alloys

Coated electrodes of UANA grade for welding and surfacing aluminium and its alloys (Skorina N.V. and Mashin V.S.) 12

Combined method for plasma and arc welding using different-polarity current pulses (Hidra-process) (Voropaj N.M. and Mishenkov V.A.) 12

Deposition of oxide coatings on surfaces of products of aluminium-based alloys (Tyurin Yu.N., Zhadkevich M.L., Golovenko S.I. and Chigrinova N.M.) 2

Development of methods for arc welding of aluminium and its alloys (Dovbishchenko I.V. and Steblovsky B.A.) 12

Features of consumable-electrode arc welding of aluminium alloys in neon and its mixtures with helium and argon (Ishchenko A.Ya., Dovbishchenko I.V., Mashin V.S. and Pashulya M.P.) 12

Friction stir welding of aluminium alloys (Review) (Tretyak N.G.) 7

Improvement of weldability of high-strength aluminium alloys in explosion cladding (Markashova L.I., Dobrushin L.D. and Arsenyuk V.V.) 12

Investigation and development of the technology of light alloy welding at the PWI (Ishchenko A.Ya.) 12

Non-consumable electrode argon-arc welding of aluminium alloys with arc oscillations (Poklyatsky A.G., Ishchenko A.Ya., Grinuyk A.A., Chajka A.A. and Fedorchuk V.E.) 2

Prevention of formation of oxide films in welds on Li-containing aluminium alloys (Poklyatsky A.G., Lozovskaya A.V. and Grinyuk A.A.) 12

Simulation of thermal and solidification processes in laser welding of aluminium plates (Karkhin V.A., Ploshikhin V.V. and Bergman Kh.V.) 8

Copper alloys

Vacuum brazing of dispersion-strengthened copper alloy Glidcop Al-25 (Maksimova S.V., Khorunov V.F., Shonin V.A., Zvolinsky I.V., Voronov V.V. and Kostin V.A.) 10

Fe–C alloys

Peculiarities of carbon oxidation in welding with ilmenite-covered electrodes (Kalin N.A. and Efimenko N.G.) 4

Molybdenum alloys

Formation of crystallographic texture in the metal of welded joints on molybdenum alloys (Zadery B.A., Kotenko S.S., Marinchenko A.E., Polishchuk E.P. and Yushchenko K.A.) 11

Nickel alloys

Method for investigation of longitudinal residual stresses in bead on nickel alloy plate welding (Chervyakov N.O. and Yushchenko K.A.) 8

Structure and properties of nickel-based alloy deposited by laser-powder method (Skripka N.N.) 6

Niobium alloys

Erection assembly-welding of tubular structures of niobium alloys in the jig (Blashchuk V.E.) 2

Titanium alloys

Narrow-gap arc welding of titanium alloys (Review) (Belous V.Yu.) 9

Barrier inserts

Fusion welding of titanium to steel (Review) (Kireev L.S. and Zamkov V.N.) 8

Bimetal joints

Mechanism of bimetal joints formation in friction welding (Kuchuk-Yatsenko S.I. and Zyakhor I.V.) 7

Brazing

Express-method for development and verification of pressure brazing technologies (Pismenny A.S., Polukhin V.V., Prokofiev A.S., Bondarev V.A. and Pismenny A.A.) 1

Vacuum brazing of dispersion-strengthened copper alloy Glidcop Al-25 (Maksimova S.V., Khorunov V.F., Shonin V.A., Zvolinsky I.V., Voronov V.V. and Kostin V.A.) 10

Calculations

Allowance for effect of cycle asymmetry on fatigue resistance of welded joints (Kovalchuk V.S.) 4

Calculation of penetration depth of workpieces in CO_2 welding (Varukha E.N. and Morozov A.A.) 8

Estimation of stressed state of the wall of coiled vertical cylindrical tanks in welding-in of insert plates (Makhnenko V.I., Barvinko A.Yu., Barvinko Yu.P. and Tsiarkovsky P.) 5

Method of calculation of voltage drop in electrode stickout length with allowance for non-linearity of thermophysical parameters (Pentegov I.V. and Petrienko O.I.) 4

Cladding

Improvement of weldability of high-strength aluminium alloys in explosion cladding (Markashova L.I., Dobrushin L.D. and Arsenyuk V.V.) 12

Laser cladding of hypoeutectoid complexly-alloyed steels (Khaskin V.Yu. and Garashchuk V.P.) 3

Plasma-powder cladding of internal combustion engine valves (Pereplyotchikov E.F.) 1

Coatings

Bioceramic coatings

Investigation of bioceramic coatings produced by microplasma spraying (Borisov Yu.S., Vojnarovich S.G., Ulianchich N.V., Jensen J. and Wolke J.) 9

Composite vanadium carbide coatings

Tribological characteristics of composite carbide coatings (Borisov Yu.S., Sychev V.S., Shavlovsky E.N., Labunets V.F. and Zolotareva E.P.) 2

Electrode coatings

Slime of water-conditioning units of thermal power engineering as raw material for electrode coatings (Lazebnov P.P. and Pulina N.N.) 9

Fe–C–Cr–Al system coatings

Phase composition of Fe–C–Cr–Al system coatings produced by the method of electric arc metallizing (Pokhmursky V.I., Student M.M., Sidorak I.I., Ryabtsev I.A. and Kuskov Yu.M.) 10

Magnetron coatings

Properties of magnetron coatings on the Fe–Cr–Ni base with amorphous structure (Lukina G.N., Bolshakov M.V. and Pidgajchuk S.Ya.) 4

Oxide coatings

Deposition of oxide coatings on surfaces of products of aluminium-based alloys (Tyurin Yu.N., Zhadkevich M.L., Golovenko S.I. and Chigrinova N.M.) 2

Steel–bronze composite coatings

Physical-mechanical characteristics of steel–bronze coatings produced using laser surfacing (Shatrava A.P.) 5

Thermal coatings

Thermal coatings containing dry lubricants for operation under conditions of dry friction and elevated temperatures (Tunik A.Yu.) 8

Wear-resistance coatings

Flux-cored wires of FeCrB + Al and FeCr + Al + C systems for electric arc metallizing (Pokhmursky V.I., Student M.M., Dovgunyk V.M. and Sidorak I.I.) 3

Composite materials

Development of composite materials for zirconium-based active elements of plasmatron electrodes (Shapoval A.N.) 10

Dispersion-strengthened heat-resistant solder (Khorunov V.F., Sabadash O.M., Maksimova S.V. and Stefaniv B.V.) 12
Effect of alloying elements on structure of composite alloy based on tungsten carbides (Bely A.I., Zhudra A.P. and Dzykovich V.I.) 11
Fusion welding of dispersion-strengthened aulminium-based composite materials, containing silicon carbide particles (Review) (Cherepivskaya E.V. and Ryabov V.R.) 4
Peculiarities of deoxidation of the weld pool metal in plasma surfacing with composite materials (Bely A.I., Zhudra A.P. and Dzykovich V.I.) 10

Control systems
Mathematical model of technological adaptation of the robot to the gap in arc welding (Korinets I.F. and Ji Cheng Chung) 9

Cracks
Peculiarities of cold cracking in welding of high-strength low-alloy steels (Shvachko V.I. and Stepanyuk S.N.) 5
Resistance of the HAZ metal of steeL M76 to cold cracking after surfacing using ferritic grade wires (Chernyak Ya.P., Bursky G.V. and Kalensky V.K.) 11
Role of mathematical modelling in solving problems of welding dissimilar steels (Review) (Makhnenko V.I. and Saprykina G.Yu.) 3

Crystallographic texture
Formation of crystallographic texture in the metal of welded joints on molybdenum alloys (Zadery B.A., Kotenko S.S., Marinchenko A.E., Polishchuk E.P. and Yushchenko K.A.) 11

Cycle asymmetry
Allowance for effect of cycle asymmetry on fatigue resistance of welded joints (Kovalchuk V.S.) 4

Deformational treatment
Investigation of effect of deformational treatment on resi-dual stresses in circumferential welds (Zubchenko A.S., Koloskov M.M., Amelianchik A.V., Levitan L.M. and Shirolapova T.B.) 1

Dissimilar joints
Effect of process parameters and braking dynamics in friction welding on structure and properties of joints between copper and aluminium (Kuchuk-Yatsenko S.I., Zyakhor I.V. and Gordan G.N.) 6
Fusion welding of titanium to steel (Review) (Kireev L.S. and Zamkov V.N.) 8
Mass transfer processes in pressure joining of dissimilar metals (Markashova L.I., Arsenyuk V.V., Grigorenko G.M. and Berdnikova E.N.) 7
Peculiarities of phase formation in pressure welding of dissimilar metals under conditions of high-rate deforming (Markashova L.I., Arsenyuk V.V., Grigorenko G.M. and Berdnikova E.N.) 9
Peculiarities of plastic deformation of dissimilar materials in pressure joining (Markashova L.I., Arsenyuk V.V. and Grigorenko G.M.) 5
Solid-state joining of titanium to steel (Review) (Kireev L.S. and Zamkov V.N.) 7
Vacuum percussion welding of aluminium to copper (Kharchenko G.K., Falchenko Yu.V., Arsenyuk V.V. and Polovetsky E.V.) 9

Electric field fluctuations
About effect of electric field fluctuations in arc column on arc welding process stability (Tsybulkin G.A.) 6

Electrode metal droplet
Effect of an electrode metal droplet on arc voltage in gas-shielded welding (Ponomaryov V., da Costa A.V. and Scotti A.) 4

Electrohydropulse pressing-in
Electrohydropulse permanent joining of hollow pieces using exploding elements (Boroznyak A.I.) 5

Electron beam diagnostics
System of diagnostics of electron beam in installations for electron beam welding (Akopiants K.S., Nazarenko O.K., Gumovsky V.V. and Chernyakin V.P.) 10

Electromagnetic field
Distribution of induction of control longitudinal magnetic field in welding T-joints (Sidorenko S.M., Razmyshlyaev A.D. and Maevsky V.R.) 9
Effect of welding speed on welding current magnetic field (Shchetinina V.I., Shchetinin S.V., Chapni N.I., Shcherbina A.V., Melnikov A.E. and Golubkov S.P.) 2

Exploding elements
Electrohydropulse permanent joining of hollow pieces using exploding elements (Boroznyak A.I.) 5

Explosion treatment
Improvement of weldability of high-strength aluminium alloys in explosion cladding (Markashova L.I., Dobrushin L.D. and Arsenyuk V.V.) 12
Limiting thickness of welded joints to be explosion treated (Petushkov V.G., Titov V.A. and Bryzgalin A.G.) 1
Technology for explosion hardening of support surfaces of axle boxes (Dragobetsky V.V.) 4

Fatigue resistance
Allowance for effect of cycle asymmetry on fatigue resistance of welded joints (Kovalchuk V.S.) 4

Field conditions
Field welding of large-size spherical isothermal tanks for storage of cryogenic products (Yushchenko K.A., Monko G.G., Starushchenko T.M., Belorusets B.O. and Naumov A.S.) 9
Mechanized equipment for welding, hardfacing and cutting in the field conditions (Lebedev V.A. and Pichak V.G.) 6

Floating welded megastructures
Floating welded megastructures (Review) (Bernadsky V.N., Maksimov S.Yu. and Netrebsky M.A.) 4

Fluxes
Classification of arc welding fluxes by the method of their application, manufacture, composition and type of metal being welded (Sidoruk V.S. and Galinich V.I.) 5
Classification of fluxes for arc welding by metallurgical and technological properties (Sidoruk V.S. and Galinich V.I.) 6
Selection of the composition of welding fluxes, allowing for the structural characteristics of their melts (Kuzmenko V.G., Tokarev V.S., Galinich V.I., Sokolsky V.E. and Ka-zimirov V.P.) 10

Foam materials
Mathematical modelling of heat processes in welding foam materials (Makhnenko V.I., Velikoivanenko E.A., Rozynka G.F., Pivtorak N.I., Seyffarth P. and Jasnau U.) 10

Fracture resistance
Problems in application of new steels of increased and high strength in welded structures (Kirian V.I. and Mikhoduj L.M.) 3
Some peculiarities of delayed fracture of HAZ metal in steel M76 after cladding using austenitic wire (Chernyak Ya.P., Bursky G.V. and Kalensky V.K.) 8

Fuel elements
Experience of using guns with plasma cathodes for electron beam welding of nuclear power station fuel elements (Vasilkov V.I., Kislitsky A.A., Onuchin N.V., Pchelkin R.D., Rozhkov V.V., Ushakov A.V., Strukov A.V., Rempe N.G. and Osipov I.V.) 6
On the causes for formation of defects in welds of E110 alloy made by electron beam welding and methods of controlling them (Vasilkov V.I., Kislitsky A.A., Onuchin N.V., Rozhkov V.V., Strukov A.V., Chizhov V.B. and Lavrenyuk P.I.) 5
Unit for resistance welding of nuclear reactor fuel elements (Sidorov I.N., Gradovich A.A., Kislitsky A.A., Rozhkov V.V., Strukov A.V., Chapaev I.G. and Lavrenyuk P.I.) 3

Gas turbine blades
Technology of restoration of gas turbine blades (Zhadkevich M.L., Bondarev A.A., Zelenin V.I., Teplyuk V.M., Sidorenko S.I., Mokhort V.A., Nesterenko Yu.V. and Zelenin O.V.) 2

Hardfacing
Optimisation of inductor parameters for uniform heating of discs across the width of the hardfacing zone, allowing for screening (Shably O.M., Pulka Ch.V. and Pismenny A.S.) 11
Properties of the metal deposited by electroslag process using chips of tool steel 5KhNM as filler material (Kuzmenko O.G. and Ryabtsev I.A.) 11

Heat treatment
High-frequency power transformers for induction units (Pismenny A.S., Shinlov M.E. and Yukhimenko R.V.) 9
Increase in strength of welds in arc welding of alloy 1420 using the Sc-containing fillers (Ishchenko A.Ya., Lozovskaya A.V., Poklyatsky A.G., Sklabinskaya I.E., Mashin V.S. and Yavorskaya M.R.) 1

Heterogeneity
Effect of deformation on electrochemical heterogeneity of pipeline welded joints (Radkevich A.I.) 4
Heterogeneity of pipe steel joints made by flash butt welding (Kuchuk-Yatsenko S.I., Kharchenko G.K., Grigorenko G.M., Falchenko Yu.V., Taranova T.G., Gritskiv Ya.P., Zagadarchuk V.F. and Grigorenko S.G.) 2

High technologies

Floating welded megastructures (Review) (Bernadsky V.N., Maksimov S.Yu. and Netrebsky M.A.) 4

Japan determines its priorities in the field of welding for XXI century (Bernadsky V.N.) 3

Holographic interferograms

Automatic computer analysis of holographic interferograms in nondestructive quality control of materials and elements of structures (Lobanov L.M., Pivtorak V.A., Savitsky V.V. and Olejnik E.M.) 10

Hydrogen concentration

Effect of microstructural transformations on redistribution of hydrogen in fusion welding of structural steels (Makhnenko V.I., Korolyova T.V. and Lavrinets I.G.) 2

Laser technologies

Development of laser technologies for materials treatment at the Institute for Problems of Laser and Information Technologies (Panchenko V.Ya. and Golubev V.S.) 4

Local thermal effect

Experimental investigations of fields of residual stresses in welded and rolled I-beams (Golodnov A.I. and Khvortova M.Yu.) 3

Metal transfer

Effect of an electrode metal droplet on arc voltage in gas-shielded welding (Ponomaryov V., da Costa A.V. and Scotti A.) 4

Microstructural transformations

Effect of microstructural transformations on redistribution of hydrogen in fusion welding of structural steels (Makhnenko V.I., Korolyova T.V. and Lavrinets I.G.) 2

Military tank construction

Works of the E.O. Paton Electric Welding Institute of the NAS of Ukraine in the field of military tank construction (Paton B.E. and Gordonny V.G.) 2

Mirror systems

Improvement of efficiency of laser treatment using off-axis beams focused by mirror systems (Paton B.E., Bulatsev A.R., Gavrish S.S., Zagrebelny A.A., Pavlova S.V. and Shulym V.F.) 11

Modelling

Calculation of penetration depth of workpieces in CO_2 welding (Varukha E.N. and Morozov A.A.) 8

Computer program «Welding of tubes to tube sheets of heat exchangers» (Makhnenko V.I., Velikoivanenko E.A., Makhnenko O.V., Rozynka G.F., Pivtorak N.I., Seyffarth P. and Bautzmann K.) 8

Effect of gap on sizes of butt weld in consumable electrode arc welding in Ar + 25 % CO_2 mixture (Korinets I.F. and Ji Cheng Chung) 8

Energy dosing in ultrasonic welding of rigid polymers (Lugovoj Z.P. and Nesterenko N.P.) 5

Effect of microstructural transformations on redistribution of hydrogen in fusion welding of structural steels (Makhnenko V.I., Korolyova T.V. and Lavrinets I.G.) 2

International Conference «Mathematical Modelling and Information Technologies in Welding and Related Processes» 11

Improvement of efficiency of laser treatment using off-axis beams focused by mirror systems (Paton B.E., Bulatsev A.R., Gavrish S.S., Zagrebelny A.A., Pavlova S.V. and Shulym V.F.) 11

Mathematical model of technological adaptation of the robot to the gap in arc welding (Korinets I.F. and Ji Cheng Chung) 9

Mathematical modelling of heat processes in welding foam materials (Makhnenko V.I., Velikoivanenko E.A., Rozynka G.F., Pivtorak N.I., Seyffarth P. and Jasnau U.) 10

Numerical modelling of the process of formation of a molten metal drop at the tip of a consumable electrode (Tarasov N.M., Gorlov A.K. and Lashko S.N.) 6

On construction of the model of weld pool in consumable-electrode arc welding (Gulakov S.V. and Nosovsky B.I.) 9

Peculiarities of cold cracking in welding of high-strength low-alloy steels (Shvachko V.I. and Stepanyuk S.N.) 5

Role of mathematical modelling in solving problems of welding dissimilar steels (Review) (Makhnenko V.I. and Saprykina G.Yu.) 3

To the question of GMAW stability (Tsybulkin G.A.) 5

Simulation of thermal and solidification processes in laser welding of aluminium plates (Karkhin V.A., Ploshikhin V.V. and Bergman Kh.V.) 8

6th International Seminar «Numerical analysis of weldabi-lity» 2

Neural networks

Adaptive algorithm of quality control of resistance spot welding using neural networks (Podola N.V., Rudenko P.M. and Gavrish V.S.) 1

Selection of input variables and structure of neural network to evaluate the quality of resistance spot welding (Podola N.V., Gavrish V.S. and Rudenko P.M.) 4

News

Extraordinary and Plenipotentiary Ambassador of the USA to Ukraine is Introduced to the activity of STC «E.O. Paton Electric Welding Institute» 2

International Conference «Mathematical Modelling and Information Technologies in Welding and Related Processes» 11

International Exhibition «Welding — Ukraine'2002» 6

Lebedev V.K. is 80 6

Professor Detlef von Hofe is 60 2

6th International Seminar «Numerical analysis of weldability» 2

U.S. Congressman visits the E.O. Paton Electric Welding Institute of the National Academy of Sciences of Ukraine 4

Visit by the Extraordinary and Plenipotentiary Ambassador of the Russian Federation in Ukraine to the STC «E.O. Paton Electric Welding Institute» of the NAS of Ukraine 3

Visit of the Minister of Foreign Affairs of the Republic of India to the E.O. Paton Electric Welding Institute of the NAS of Ukraine 2

Visit to the E.O. Paton Electric Welding Institute by Dr. Wayne Thomas, the laureate of the Evgeny Paton Prize of the International Institute of Welding 11

Welding in surgery — a new direction in welding technology 4

Nickel

Peculiarities of microstructure of explosion welded joints in nickel (Markashova L.I., Arsenyuk V.V., Petushkov V.G. and Grigorenko G.M.) 11

Open honeycomb metal structures

A system for mechanized microplasma welding of honeycomb aluminium metal structures (Paton V.E., Voropaj N.M. and Gvozdetsky V.S.) 3

Oxide films

Prevention of formation of oxide films in welds on Li-containing aluminium alloys (Poklyatsky A.G., Lozovskaya A.V. and Grinyuk A.A.) 12

Perforated interlayer

Vacuum diffusion bonding of chromium to copper (Kharchenko G.K., Falchenko Yu.V., Novomlinets O.A. and Gorban V.F.) 7

Pore formation

On the causes for formation of defects in welds of E110 alloy made by electron beam welding and methods of controlling them (Vasilkov V.I., Kislitsky A.A., Onuchin N.V., Rozhkov V.V., Strukov A.V., Chizhov V.B. and Lavrenyuk P.I.) 5

Quality control

Adaptive algorithm of quality control of resistance spot welding using neural networks (Podola N.V., Rudenko P.M. and Gavrish V.S.) 1

Automatic computer analysis of holographic interferograms in nondestructive quality control of materials and elements of structures (Lobanov L.M., Pivtorak V.A., Savitsky V.V. and Olejnik E.M.) 10

Improvement of quality of welding electrodes on the basis of standards ISO of series 9000:2000 (Marchenko A.E.) 11

Method of determination of corrective actions in statistical control of welding processes (Tararychkin I.A.) 12

Selection of input variables and structure of neural network to evaluate the quality of resistance spot welding (Podola N.V., Gavrish V.S. and Rudenko P.M.) 4

System of in-process quality control of welding equipment during its manufacturing (Paton B.E., Korotynsky A.E., Skopyuk M.I., Yumatova V.I., Kopilenko E.A., Pavlenko G.V., Pavlenko G.L. and Chmykhov N.V.) 5

Rare-earth metals

Modifying, refining and alloying with yttrium in welding of steels (Efimenko N.G.) 6

Soldering

Dispersion-strengthened heat-resistant solder (Khorunov V.F., Sabadash O.M., Maksimova S.V. and Stefaniv B.V.) 12

Space experiments

Results of experiments on manual EBW in a manned space simulation test chamber (Mikhajlovskaya E.S., Shulym V.F. and Zagrebelny A.A.) 2

Welding technologies under extreme conditions. Part 1. Analysis of multifactortial potential risk (Paton B.E., Bulatsev A.R., Gavrish S.S., Zagrebelny A.A., Pavlova S.V. and Shulym V.F.) 11

Welding technologies under extreme conditions. Part 2. Degree of risk and possibilities for risk mitigation (Paton B.E., Bulatsev A.R., Gavrish S.S., Zagrebelny A.A., Pavlova S.V. and Shulym V.F.) 12

Spraying

Investigation of bioceramic coatings produced by microplasma spraying (Borisov Yu.S., Vojnarovich S.G., Ulianchich N.V., Jensen J. and Wolke J.) 9

Microplasma spraying using wire materials (Borisov Yu.S. and Kislitsa A.N.) 3

Thermal coatings containing dry lubricants for operation under conditions of dry friction and elevated temperatures (Tunik A.Yu.) 8

Steels

Armoured steels

Works of the E.O. Paton Electric Welding Institute of the NAS of Ukraine in the field of military tank construction (Paton B.E. and Gordonny V.G.) 2

Austenitic steels

Welded joints of austenitic steel 25Cr–20Ni–2Si in augmented turbopiston engines (Pinchuk N.I., Ryazanstev N.K. and Rovensky I.L.) 6

Complexly-alloyed steels

Laser cladding of hypoeutectoid complexly-alloyed steels (Khaskin V.Yu. and Garashchuk V.P.) 3

Low-alloyed steels

Magnetically-impelled arc butt welding of thick-walled pipes (Kuchuk-Yatsenko S.I., Kachinsky V.S. and Ignatenko V.Yu.) 7

Pipe steel

Heterogeneity of pipe steel joints made by flash butt welding (Kuchuk-Yatsenko S.I., Kharchenko G.K., Grigorenko G.M., Falchenko Yu.V., Taranova T.G., Gritskiv Ya.P., Zagadarchuk V.F. and Grigorenko S.G.) 2

Rail steels

Resistance of the HAZ metal of steeL M76 to cold cracking after surfacing using ferritic grade wires (Chernyak Ya.P., Bursky G.V. and Kalensky V.K.) 11

Sparsely-alloyed structural steels

Problems in application of new steels of increased and high strength in welded structures (Kirian V.I. and Mikhoduj L.M.) 3

Stable-austenitic steels

Field welding of large-size spherical isothermal tanks for storage of cryogenic products (Yushchenko K.A., Monko G.G., Starushchenko T.M., Belorusets B.O. and Naumov A.S.) 9

Structural steels

A-TIG welding of structural steels for power engineering applications (Bajic D.R., Savitsky M.M., Melnichuk G.M. and Lupan A.F.) 9

Procedure and parameters of A-TIG welding of structural steels (Bajic D.R., Melnichuk G.M., Lupan A.F. and Savitsky M.M.) 10

Stresses and deformations

Effect of deformation on electrochemical heterogeneity of pipeline welded joints (Radkevich A.I.) 4

Estimation of stressed state of the wall of coiled vertical cylindrical tanks in welding-in of insert plates (Makhnenko V.I., Barvinko A.Yu., Barvinko Yu.P. and Tsiarkovsky P.) 5

Experimental investigations of fields of residual stresses in welded and rolled I-beams (Golodnov A.I. and Khvortova M.Yu.) 3

Investigation of effect of deformational treatment on resi-dual stresses in circumferential welds (Zubchenko A.S., Koloskov M.M., Amelianchik A.V., Levitan L.M. and Shirolapova T.B.) 1

Limiting thickness of welded joints to be explosion treated (Petushkov V.G., Titov V.A. and Bryzgalin A.G.) 1

Mass transfer processes in pressure joining of dissimilar metals (Markashova L.I., Arsenyuk V.V., Grigorenko G.M. and Berdnikova E.N.) 7

Method for investigation of longitudinal residual stresses in bead on nickel alloy plate welding (Chervyakov N.O. and Yushchenko K.A.) 8

Peculiarities of cold cracking in welding of high-strength low-alloy steels (Shvachko V.I. and Stepanyuk S.N.) 5

Peculiarities of phase formation in pressure welding of dissimilar metals under conditions of high-rate deforming (Markashova L.I., Arsenyuk V.V., Grigorenko G.M. and Berdnikova E.N.) 9

Peculiarities of plastic deformation of dissimilar materials in pressure joining (Markashova L.I., Arsenyuk V.V. and Grigorenko G.M.) 5

Role of mathematical modelling in solving problems of welding dissimilar steels (Review) (Makhnenko V.I. and Saprykina G.Yu.) 3

Surfacing

Control of penetration depth in surfacing of copper tracks (Royanov V.A. and Psaras G.G.) 5

Effect of alloying elements on structure of composite alloy based on tungsten carbides (Bely A.I., Zhudra A.P. and Dzykovich V.I.) 11

Flux-cored wires of FeCrB + Al and FeCr + Al + C systems for electric arc metallizing (Pokhmursky V.I., Student M.M., Dovgunyk V.M. and Sidorak I.I.) 3

Peculiarities of deoxidation of the weld pool metal in plasma surfacing with composite materials (Bely A.I., Zhudra A.P. and Dzykovich V.I.) 10

Peculiarities of melting and solidification of 20KhGS type deposited metal alloyed with phosphorus (Kuskov Yu.M., Ryabtsev I.I., Doroshenko L.K. and Vasiliev V.G.) 8

Physical-mechanical characteristics of steel–bronze coatings produced using laser surfacing (Shatrava A.P.) 5

Resistance of the HAZ metal of steeL M76 to cold cracking after surfacing using ferritic grade wires (Chernyak Ya.P., Bursky G.V. and Kalensky V.K.) 11

Structure and properties of nickel-based alloy deposited by laser-powder method (Skripka N.N.) 6

Surfacing with nitrogen alloys (Kalianov V.N.) 10

Technology of restoration of gas turbine blades (Zhadkevich M.L., Bondarev A.A., Zelenin V.I., Teplyuk V.M., Sidorenko S.I., Mokhort V.A., Nesterenko Yu.V. and Zelenin O.V.) 2

Thermal power plant slime

Slime of water-conditioning units of thermal power engineering as raw material for electrode coatings (Lazebnov P.P. and Pulina N.N.) 9

Vacuum diffusion bonding

Vacuum diffusion bonding of chromium to copper (Kharchenko G.K., Falchenko Yu.V., Novomlinets O.A. and Gorban V.F.) 7

Wear resistance

Laser cladding of hypoeutectoid complexly-alloyed steels (Khaskin V.Yu. and Garashchuk V.P.) 3

Wear resistance of deposited metal of Fe–C–Cr–Ti–Mo alloying system (Ryabtsev I.A., Kondratiev I.A., Vasiliev V.G. and Doroshenko L.K.) 4

Welded hopper cars

Integrated mechanisation and automation of manufacture of welded hopper cars (Tsygan B.G., Pirogov L.I., Donchenko A.V. and Trubachev Yu.A.) 8

Welding

Japan determines its priorities in the field of welding for XXI century (Bernadsky V.N.) 3

Welding and allied technologies at the Essen Fair 1

Welding in surgery — a new direction in welding technology 4

A-TIG welding

A-TIG welding of structural steels for power engineering applications (Bajic D.R., Savitsky M.M., Melnichuk G.M. and Lupan A.F.) 9

Procedure and parameters of A-TIG welding of structural steels (Bajic D.R., Melnichuk G.M., Lupan A.F. and Savitsky M.M.) 10

EBW

Electron beam welding of 60 mm thick steels using longitudinal oscillations of beam (Akopiants K.S., Nesterenkov V.M. and Nazarenko O.K.) 9

Experience of using guns with plasma cathodes for electron beam welding of nuclear power station fuel elements (Vasilkov V.I., Kislitsky A.A., Onuchin N.V., Pchelkin R.D., Rozhkov V.V., Ushakov A.V., Strukov A.V., Rempe N.G. and Osipov I.V.) 6

On the causes for formation of defects in welds of E110 alloy made by electron beam welding and methods of controlling them (Vasilkov V.I., Kislitsky A.A., Onuchin N.V., Rozhkov V.V., Strukov A.V., Chizhov V.B. and Lavrenyuk P.I.) 5

System of diagnostics of electron beam in installations for electron beam welding (Akopiants K.S., Nazarenko O.K., Gumovsky V.V. and Chernyakin V.P.) 10

Results of experiments on manual EBW in a manned space simulation test chamber (Mikhajlovskaya E.S., Shulym V.F. and Zagrebelny A.A.) 2

Welding technologies under extreme conditions. Part 1. Analysis of multifactortial potential risk (Paton B.E., Bulatsev A.R., Gavrish S.S., Zagrebelny A.A., Pavlova S.V. and Shulym V.F.) 11

Welding technologies under extreme conditions. Part 2. Degree of risk and possibilities for risk mitigation (Paton B.E., Bulatsev A.R., Gavrish S.S., Zagrebelny A.A., Pavlova S.V. and Shulym V.F.) 12

Erection assembly-welding

Erection assembly-welding of tubular structures of niobium alloys in the jig (Blashchuk V.E.) 2

Explosion welding

Peculiarities of microstructure of explosion welded joints in nickel (Markashova L.I., Arsenyuk V.V., Petushkov V.G. and Grigorenko G.M.) 11

Special conditions for formation of joints in shock wave welding of metals (Dobrushin L.D., Fadeenko Yu.I. and Petushkov V.G.) 2

Friction stir welding

Friction stir welding of aluminium alloys (Review) (Tretyak N.G.) 7

Friction welding

Effect of process parameters and braking dynamics in friction welding on structure and properties of joints between copper and aluminium (Kuchuk-Yatsenko S.I., Zyakhor I.V. and Gordan G.N.) 6

Mechanism of bimetal joints formation in friction welding (Kuchuk-Yatsenko S.I. and Zyakhor I.V.) 7

Fusion welding

Fusion welding of dispersion-strengthened aulminium-based composite materials, containing silicon carbide particles (Review) (Cherepivskaya E.V. and Ryabov V.R.) 4

Fusion welding of titanium to steel (Review) (Kireev L.S. and Zamkov V.N.) 8

Hybrid welding

Combined method for plasma and arc welding using different-polarity current pulses (Hidra-process) (Voropaj N.M. and Mishenkov V.A.) 12

Hybrid CO_2-laser and CO_2 consumable-arc welding (Shelyagin V.D., Khaskin V.Yu., Garashchuk V.P., Siora A.V., Bernatsky A.V. and Sakharnov A.V.) 10

Hybrid laser-microplasma welding of thin sections of metals (Paton B.E., Gvozdetsky V.S., Krivtsun I.V., Zagrebelny A.A., Shulym V.F. and Dzheppa V.L.) 3

Tendencies in development of laser-arc welding (Review) (Shelyagin V.D. and Khaskin V.Yu.) 6

Laser welding

Simulation of thermal and solidification processes in laser welding of aluminium plates (Karkhin V.A., Ploshikhin V.V. and Bergman Kh.V.) 8

Magnetically-impelled arc butt welding

Magnetically-impelled arc butt welding of thick-walled pipes (Kuchuk-Yatsenko S.I., Kachinsky V.S. and Ignatenko V.Yu.) 7

Microplasma welding

A system for mechanized microplasma welding of honeycomb aluminium metal structures (Paton V.E., Voropaj N.M. and Gvozdetsky V.S.) 3

MIG/MAG welding

About effect of electric field fluctuations in arc column on arc welding process stability (Tsybulkin G.A.) 6

Calculation of penetration depth of workpieces in CO_2 welding (Varukha E.N. and Morozov A.A.) 8

Effect of an electrode metal droplet on arc voltage in gas-shielded welding (Ponomaryov V., da Costa A.V. and Scotti A.) 4

Effect of gap on sizes of butt weld in consumable electrode arc welding in Ar + 25 % CO_2 mixture (Korinets I.F. and Ji Cheng Chung) 8

Effect of welding speed on welding current magnetic field (Shchetinina V.I., Shchetinin S.V., Chapni N.I., Shcherbina A.V., Melnikov A.E. and Golubkov S.P.) 2

Features of consumable-electrode arc welding of aluminium alloys in neon and its mixtures with helium and argon (Ishchenko A.Ya., Dovbishchenko I.V., Mashin V.S. and Pashulya M.P.) 12

Method of calculation of voltage drop in electrode stickout length with allowance for non-linearity of thermophysical parameters (Pentegov I.V. and Petrienko O.I.) 4

Method of determination of corrective actions in statistical control of welding processes (Tararychkin I.A.) 12

On construction of the model of weld pool in consumable-electrode arc welding (Gulakov S.V. and Nosovsky B.I.) 9

Selection of the composition of welding fluxes, allowing for the structural characteristics of their melts (Kuzmenko V.G., Tokarev V.S., Galinich V.I., Sokolsky V.E. and Ka-zimirov V.P.) 10

To the question of GMAW stability (Tsybulkin G.A.) 5

Multistation welding

About design of electronic controllers of welding current for multistation welding systems (Korotynsky A.E., Makhlin N.M. and Bogdanovsky V.A.) 12

Narrow-gap welding

Narrow-gap arc welding of titanium alloys (Review) (Belous V.Yu.) 9

Repairing defects in thick metal using the technology of narrow-gap arc welding (Tararychkin I.A. and Tkachenko A.N.) 4

Pressure welding

Peculiarities of phase formation in pressure welding of dissimilar metals under conditions of high-rate deforming (Markashova L.I., Arsenyuk V.V., Grigorenko G.M. and Berdnikova E.N.) 9

Resistance welding

Adaptive algorithm of quality control of resistance spot welding using neural networks (Podola N.V., Rudenko P.M. and Gavrish V.S.) 1

Selection of input variables and structure of neural network to evaluate the quality of resistance spot welding (Podola N.V., Gavrish V.S. and Rudenko P.M.) 4

Unit for resistance welding of nuclear reactor fuel elements (Sidorov I.N., Gradovich A.A., Kislitsky A.A., Rozhkov V.V., Strukov A.V., Chapaev I.G. and Lavrenyuk P.I.) 3

SAW

Development of methods for arc welding of aluminium and its alloys (Dovbishchenko I.V. and Steblovsky B.A.) 12

Distribution of induction of control longitudinal magnetic field in welding T-joints (Sidorenko S.M., Razmyshlyaev A.D. and Maevsky V.R.) 9

Works of the E.O. Paton Electric Welding Institute of the NAS of Ukraine in the field of military tank construction (Paton B.E. and Gordonny V.G.) 2

Shock wave welding

Special conditions for formation of joints in shock wave welding of metals (Dobrushin L.D., Fadeenko Yu.I. and Petushkov V.G.) 2

Solid-state joining

Solid-state joining of titanium to steel (Review) (Kireev L.S. and Zamkov V.N.) 7

TIG welding

Non-consumable electrode argon-arc welding of aluminium alloys with arc oscillations (Poklyatsky A.G., Ishchenko A.Ya., Grinuyk A.A., Chajka A.A. and Fedorchuk V.E.) 2

Prevention of formation of oxide films in welds on Li-containing aluminium alloys (Poklyatsky A.G., Lozovskaya A.V. and Grinyuk A.A.) 12

Ultrasonic welding

Energy dosing in ultrasonic welding of rigid polymers (Lugovoj Z.P. and Nesterenko N.P.) 5

Optimization of characteristics of electroacoustic transducers for ultrasonic welding of thermoplastic composite materials (Nesterenko N.P.) 2

Using ultrasonic welding for joining varnish-insulated wire in electric engineering applications (Herold H., Martinek I. and Grechuk V.) 1

Vacuum percussion welding

Vacuum percussion welding of aluminium to copper (Kharchenko G.K., Falchenko Yu.V., Arsenyuk V.V. and Polovetsky E.V.) 9

Underwater welding

Floating welded megastructures (Review) (Bernadsky V.N., Maksimov S.Yu. and Netrebsky M.A.) 4

Welding-in of insert plates

Estimation of stressed state of the wall of coiled vertical cylindrical tanks in welding-in of insert plates (Makhnenko V.I., Barvinko A.Yu., Barvinko Yu.P. and Tsiarkovsky P.) 5

Welding arc

About effect of electric field fluctuations in arc column on arc welding process stability (Tsybulkin G.A.) 6

Distribution of rate and pressure of plasma flows in welding arcs (Voropaj N.M.) 12

Non-consumable electrode argon-arc welding of aluminium alloys with arc oscillations (Poklyatsky A.G., Ishchenko A.Ya., Grinuyk A.A., Chajka A.A. and Fedorchuk V.E.) 2

Welding consumables

Improvement of quality of welding electrodes on the basis of standards ISO of series 9000:2000 (Marchenko A.E.) 11

State of the art in production of welding consumables and their quality (Ignatchenko P.V.) 11

Electrodes

Coated electrodes of UANA grade for welding and surfacing aluminium and its alloys (Skorina N.V. and Mashin V.S.) 12

Peculiarities of carbon oxidation in welding with ilmenite-covered electrodes (Kalin N.A. and Efimenko N.G.) 4

Fillers

Increase in strength of welds in arc welding of alloy 1420 using the Sc-containing fillers (Ishchenko A.Ya., Lozovskaya A.V., Poklyatsky A.G., Sklabinskaya I.E., Mashin V.S. and Yavorskaya M.R.) 1

Properties of the metal deposited by electroslag process using chips of tool steel 5KhNM as filler material (Kuzmenko O.G. and Ryabtsev I.A.) 11

Wires

Flux-cored wires of FeCrB + Al and FeCr + Al + C systems for electric arc metallizing (Pokhmursky V.I., Student M.M., Dovgunyk V.M. and Sidorak I.I.) 3

Phase composition of Fe–C–Cr–Al system coatings produced by the method of electric arc metallizing (Pokhmursky V.I., Student M.M., Sidorak I.I., Ryabtsev I.A. and Kuskov Yu.M.) 10

Wear resistance of deposited metal of Fe–C–Cr–Ti–Mo alloying system (Ryabtsev I.A., Kondratiev I.A., Vasiliev V.G. and Doroshenko L.K.) 4

Welding equipment

About design of electronic controllers of welding current for multistation welding systems (Korotynsky A.E., Makhlin N.M. and Bogdanovsky V.A.) 12

High-frequency power transformers for induction units (Pismenny A.S., Shinlov M.E. and Yukhimenko R.V.) 9

Main tendencies of development of welding equipment manufacture in «SELMA-ITS» Association and its application in Russia and CIS countries (Karasev M.V., Kopilenko E.A., Pavlenko G.V., Rabotinsky D.N., Soroka V.L., So-lyanik V.V. and Karasev E.V.) 5

Mechanized equipment for welding, hardfacing and cutting in the field conditions (Lebedev V.A. and Pichak V.G.) 6

Methods of design of welding inductors (Review) (Yukhimenko R.V.) 5

New machine for electroslag welding of large parts at JSC «NKMBF» (Nevidomsky V.A., Krasilnikov S.G., Panin A.D., Gulida V.P. and Lychko I.I.) 2

On welding properties of thyristor rectifiers (Postolaty N.I., Glushchenko A.D., Dukh S.V. and Gritsenko L.S.) 10

Optimization of characteristics of electroacoustic transducers for ultrasonic welding of thermoplastic composite materials (Nesterenko N.P.) 2

Optimisation of inductor parameters for uniform heating of discs across the width of the hardfacing zone, allowing for screening (Shably O.M., Pulka Ch.V. and Pismenny A.S.) 11

RDK-300 resonance welding power source with a combined external characteristic 11

State-of-the-art, tendencies and prospects of development of high-frequency welding converters (Review) (Korotynsky A.E.) 7

Unit for resistance welding of nuclear reactor fuel elements (Sidorov I.N., Gradovich A.A., Kislitsky A.A., Rozhkov V.V., Strukov A.V., Chapaev I.G. and Lavrenyuk P.I.) 3

Using ultrasonic welding for joining varnish-insulated wire in electric engineering applications (Herold H., Martinek I. and Grechuk V.) 1

Welding three-phase transformers with improved technical-economical characteristics (Pentegov I.V., Rymar S.V., Lavrenyuk A.V. and Petrienko O.I.) 5

Plasmatrons

A system for mechanized microplasma welding of honeycomb aluminium metal structures (Paton V.E., Voropaj N.M. and Gvozdetsky V.S.) 3

Development of composite materials for zirconium-based active elements of plasmatron electrodes (Shapoval A.N.) 10

Hybrid laser-microplasma welding of thin sections of metals (Paton B.E., Gvozdetsky V.S., Krivtsun I.V., Zagrebelny A.A., Shulym V.F. and Dzheppa V.L.) 3

Welding robot

Mathematical model of technological adaptation of the robot to the gap in arc welding (Korinets I.F. and Ji Cheng Chung) 9

Advertising **3, 6, 10, 11**

Index of articles for TPWJ'2001 **12**

List of authors **12**